10-24-2013

Formation of Polycyclic Aromatic Hydrocarbons and Nitrogen Containing Polcyclic Aromatic Compounds in Titan's Atmosphere, the Interstellar Medium and Combustion

Alexander Landera
Florida International University, compchemist726@gmail.com

FLORIDA INTERNATIONAL UNIVERSITY

Miami, Florida

FORMATION OF POLYCYCLIC AROMATIC HYDROCARBONS AND NITROGEN CONTAINING POLYCYCLIC AROMATIC COMPOUNDS IN TITAN'S ATMOSPHERE, THE INTERSTELLAR MEDIUM AND COMBUSTION

A dissertation submitted in partial fulfillment of

the requirements for the degree of

DOCTOR OF PHILOSPHY

in

CHEMISTRY

by

Alexander Landera

2013

To: Dean Kenneth G. Furton
College of Arts and Sciences

This dissertation, written by Alexander Landera, and entitled Formation of Polycyclic Aromatic Hydrocarbons and Nitrogen Containing Polycyclic Aromatic Compounds in Titan's atmosphere, the Interstellar Medium and Combustion, having been approved in respect to style and intellectual content, is referred to you for judgment.

We have read this dissertation and recommend that it be approved.

_____
Jeffrey Joens

_____
David C. Chatfield

_____
Xuewen Wang

_____
Piero R. Gardinali

_____
Alexander M. Mebel, Major Professor

Date of Defense: October 24, 2013

The dissertation of Alexander Landera is approved.

_____
Dean Kenneth G. Furton
College of Arts and Sciences

_____
Dean Lakshmi N. Reddi
University Graduate School

Florida International University, 2013

DEDICATION

This dissertation is dedicated to M. L. Z. Without her love and support, this would not have been possible. For this I am forever grateful.

ACKNOWLEDGMENTS

I would like to thank my parents (obviously), for without their constant support and guidance, I would (clearly) not be in the position I am today. Although, they have no clue what it is I do for a living, they have still supported me throughout the entirety of my graduate career.

My friends also deserve to be acknowledged, for although they do not know it, they have helped me as much (if not more) as I have helped them. Without them, my graduate experience would be a factor of 5 lower than it currently is. They have played a critical role in my success as a graduate school, and while they deserve to be mentioned all individually, this acknowledgments section cannot drag on forever.

I need to also thank my advisor Alexander M. Mebel. The vast majority of what I have learned, I have learned from him, and without his constant help, I would (very clearly), not be the research scientist I am today. His open door policy is much appreciated, as I can always walk into his office and ask questions.

ABSTRACT OF THE DISSERTATION

FORMATION OF POLYCYCLIC AROMATIC HYDROCARBONS AND NITROGEN CONTAINING POLYCYCLIC AROMATIC COMPOUNDS IN TITAN'S ATMOSPHERE, THE INTERSTELLAR MEDIUM AND COMBUSTION

by

Alexander Landera

Florida International University, 2013

Miami, Florida

Professor Alexander M. Mebel, Major Professor

Several different mechanisms leading to the formation of (substituted) naphthalene and azanaphthalenes were examined using theoretical quantum chemical calculations. As a result, a series of novel synthetic routes to Polycyclic Aromatic Hydrocarbons (PAHs) and Nitrogen Containing Polycyclic Aromatic Compounds (N-PACs) have been proposed. On Earth, these aromatic compounds originate from incomplete combustion and are released into our environment, where they are known to be major pollutants, often with carcinogenic properties. In the atmosphere of a Saturn's moon Titan, these PAH and N-PACs are believed to play a critical role in organic haze formation, as well as acting as chemical precursors to biologically relevant molecules. The theoretical calculations were performed by employing the ab initio G3(MP2,CC)/B3LYP/6-311G** method to effectively probe the Potential Energy Surfaces (PES) relevant to the PAH and N-PAC formation. Following the construction of the PES, Rice-Ramsperger-Kassel-Markus (RRKM) theory was used to evaluate all unimolecular rate constants as a function of collision energy under single-collision conditions. Branching ratios were then

evaluated by solving phenomenological rate expressions for the various product concentrations. The most viable pathways to PAH and N-PAC formation were found to be those where the initial attack by the ethynyl (C_2H) or cyano (CN) radical toward a unsaturated hydrocarbon molecule led to the formation of an intermediate which could not effectively lose a hydrogen atom. It is not until ring cyclization has occurred, that hydrogen elimination leads to a closed shell product. By quenching the possibility of the initial hydrogen atom elimination, one of the most competitive processes preventing the PAH or N-PAC formation was avoided, and the PAH or N-PAC formation was allowed to proceed. It is concluded that these considerations should be taken into account when attempting to explore any other potential routes towards aromatic compounds in cold environments, such as on Titan or in the interstellar medium.

TABLE OF CONTENTS

LIST OF FIGURES

ABBREVIATIONS AND ACRONYMS

1,4-Diethynylphthalazine	1,4-DPZ
1-Buta-1,3-Diynyl-2-Vinyl-Benzene	BDVB
Complete Active Space Second Order Perturbation	CASPT2
Coupled Cluster Single Doubles with Perturbed Triples	CCSD(T)
Cis-PhenylVinylAcetylene	c-PVA
Density Functional Theory	DFT
Moller Plesset Second Order Perturbation	MP2
Nitrogen-containing Polycyclic Aromatic Compounds	N-PACS
Polycyclic Aromatic Hydrocarbons	PAHs
Potential Energy Surface	PES
Rice-Ramsperger-Kassel-Markus	RRKM
Rice-Ramsperger-Kassel-Markus Master Equation	RRKM-ME
Single Point	SP
Trans-1-Hexene-3,5-diynyl-Benzene	THDB
Trans-PhenylVinylAcetylene	t-PVA

Chapter 1: Introduction

Gas phase chemical reactions are ubiquitous. They occur everywhere, from our own planet's atmosphere, to far and distant galaxies where they govern the formation of small molecules and their growth leading to more complex species[1-4]. They can happen under frigid temperatures, bordering on the coldest temperatures science is known to reach, to the sweltering hot conditions that occur just above a hot lava flow. And, yes, pressures can reach from thousands of atmospheres, to near vacuum. Gas phase reactions govern nearly every aspect of our lives yet surprisingly; we still know little about them.

This dissertation is designed to elucidate some of the pathways which lead to the formation of Polycyclic Aromatic Hydrocarbons (PAH) in combustion and the cold temperatures of Titan (one of Saturn's moons). PAHs produced in combustion processes are important contributors to pollution. They have been identified as both carcinogenic and mutagenic, and if left unchecked, can also lead to respiratory distress[5]. Although found in nature, PAHs in the environment are largely formed through anthropogenic processes such as occur in internal combustion engines. Typical combustion temperatures are in the range of 500 to 2500 K, and at these temperatures, PAHs are formed through the incomplete combustion of fossil fuels[6]. Minimizing the production of PAHs formed in combustion engines can lead to an overall healthier environment, while also increasing fuel efficiency. On the other hand, studying the formation of PAHs on Titan, can also be important. For one, it can give us insight in to how larger and more complicated molecules formed from the basic gaseous constituents found in Titan's atmosphere (N_2 and methane)[7]. Because of the similarities Titan has become a model of our own Pre-

biotic Earth, and the studies of Titan's atmospheric processes can give us a better idea of how these molecules formed early on in the evolution of our own Earth from a non-hospitable to hospitable planet. Furthermore, this information can also yield insights into how biologically (macromolecular) relevant molecules were formed.

One of the best ways science has to understand gas phase reactions is to simulate them in laboratories. This can, in some instances, give us valuable information, such as the final product distributions, and even (in some cases) a time profile of the evolution of products. Sometimes however, this is not the case. The norm, as it were, is that experiments are very costly to perform. Moreover, they often suffer from several deficiencies, which can lead to an incorrect understanding of the results, or results which are erroneous. Some of the issues which can plague experiments include problems with detection, products reacting with other reactants (secondary reactions), and difficulties with obtaining measurements at the appropriate conditions. Moreover, to unravel the maze of reaction mechanisms governing a particular process may require carrying out hundreds, if not thousands, of reactions. This, in and of itself, is not possible, both on a cost and man power basis.

Another tool valuable to gas phase communities is modeling. In this context, one would gather up all the thousands of reactions which make up the process being studied, and attempt to find rate constants for each individual reaction. If the rate constants are accurate enough, then the time evolution can be modeled mathematically. Unfortunately, as it were, rate constants obtained this way are often not reliable[8]. Rate constants are routinely "guessed," by association with other closely related reactions, or are

extrapolated from previous sets of experiments. By and large, modeling suffers from the same 'throughput' problems as experiment. There are simply too many rate constants that need to be measured, and not enough people willing to provide them.

Theoretical chemistry offers a framework to obtain rate constants accurately and reliably at nearly any pressure and temperature. As advances in computers, mathematics, and program design have advanced in the last couple of decades, so too has the speed and reliability of theoretical chemistry to provide these much needed rate constants. Nowadays, with the calculation of a few molecular parameters (energy of reactant, relative energy of transition state, moment of inertia, harmonic frequencies, and available energy), unimolecular rate constants can be computed in mere minutes.

This dissertation brings to bear the weight of theoretical chemistry onto two particular processes, atmospheric chemistry and combustion chemistry. More specifically, we consider the formation of Polycyclic Aromatic Hydrocarbons (PAHs) in these environments. In combustion flames, PAHs represent a class of molecules which have been shown to be both carcinogenic and mutagenic. They are formed in virtually any combustion process known to man, and their insertion into the environment is dominated by anthropogenic means. Lifetimes of PAHs in our environment range from a couple of hours to a couple of days, meaning that once in the atmosphere, there is no clean and efficient removal mechanism[9]. In fact, their only major removal mechanism is through rain processes. It is clear that the minimization of the PAHs yield into our environment is advantageous to our overall health.

A good model of engine combustion often contains hundreds, if not thousands of individual reactions. Due to practical considerations, experiments are not capable of obtaining rate constants for each reaction. Furthermore, rate constants are dependent on pressure and temperature, and these often lead to practical difficulties with regards to experimentation. Theoretical physics offers a way around this, by providing a platform through which rate constants can be computed accurately, and more efficiently.

Though a large number of PAHs exist, only about 17 PAHs are considered to have a profound effect on human health[5]. These are: acenaphthene, acenaphthylene, anthracence, benz[a]anthracene, benzo[a]pyrene, benzo[k]fluoranthene, chrysene, dibenz[a,h]anthracence, fluoranthene, fluorene, indeno[1,2,3-cd]pyrene, phenanthrene, and pyrene[5]. The structures of these molecules are given in reference 5. In a 1981 study using hamsters exposed to 46.5 mg/m^3 of benzo[a]pyrene for 60 straight weeks, the authors noted a decrease in their survival over the course of 109 weeks. They noted that this was primarily due to an inability to consume food due to the development of tumors in the throat region[10]. In another relevant study, Gupta et. al. monitored the health of 667 workers working in a rubber factory[11]. Firstly, they showed that there was a negative correlation between the health of employees, and the length of employment. Generally speaking, those employees who were employed by the factory the longest, had the poorest health[11]. Interestingly, health was also correlated to which places in the factory employees worked. They found that factory employees who worked in areas with smaller concentrations of benzo[a]pyrene, had better health than those who worked in areas with larger concentrations of the PAH[11]. In 1994 a study found that serum

immunoglobin levels were decreased in workers that were exposed to PAHs[12]. These workers were coke oven workers, who were exposed to various harmful PAHs including fluoranthene, perylene, pyrene, benzo[a]pyrene and chrysene[12]. Additionally, there is also evidence that suggests the formation of PAH-DNA adducts. These may interrupt cellular processes, and eventually lead to cancer[12].

So, having established the health impact of PAHs, we turn our attention towards the primary molecules (intermediate or otherwise) formed in combustion. While an understanding of the type of molecules formed during combustion is somewhat achieved, quantification of these species remains an ongoing task for the combustion community[13]. The problem lies in the fact that temperature varies depending on where a chemical reaction occurs in a flame. As one starts moving away from a burner, the temperature starts to increase until a certain distance is reached, and then it flattens out. A schematic of this is shown in Fig. 1[13]. In combustion, the temperature a reaction takes place at is very important, because it determines if a particular reaction has enough energy to occur. Certain reactions will occur only at high enough temperatures, while others will occur, unabated, even at the lowest combustion temperatures. This means that final product distributions of incomplete combustion products will be largely influenced by temperature. Depicted in Fig. 2 are graphs showing the mole fractions of certain flame products as a function of height from the burner[13].

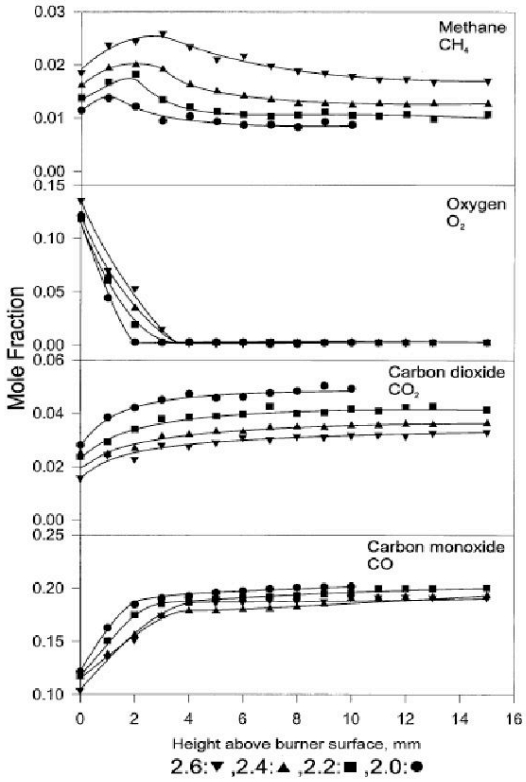
Methane
CH_4
Oxygen
O_2
Carbon dioxide
CO_2
Carbon monoxide
CO
Mole Fraction
Height above burner surface, mm
2.6:▼,2.4:▲,2.2:■,2.0:●

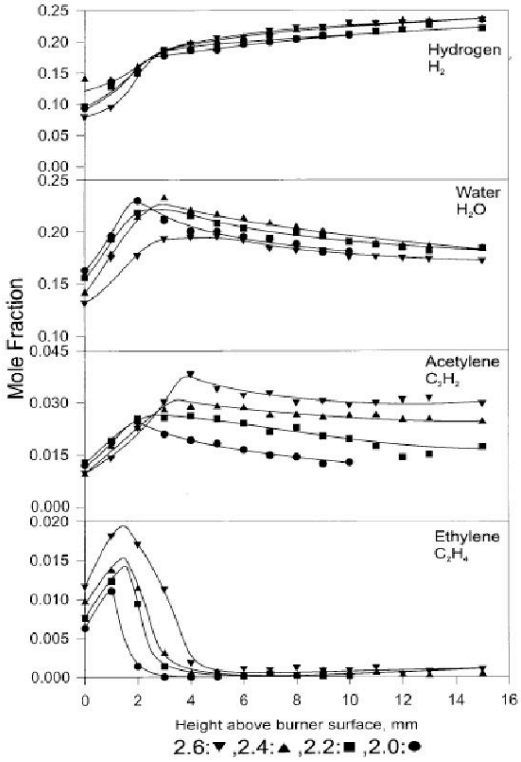
Hydrogen
H_2
Water
H_2O
Acetylene
C_2H_2
Ethylene
C_2H_4
Mole Fraction
Height above burner surface, mm
2.6:▼,2.4:▲,2.2:■,2.0:●

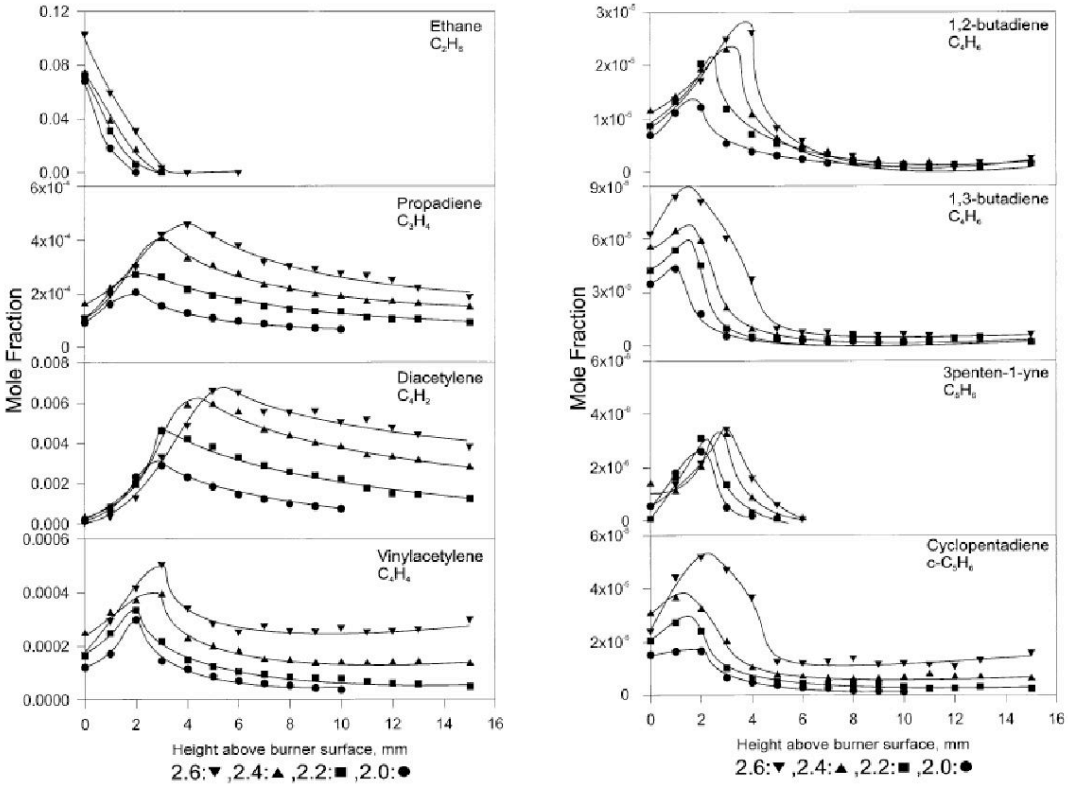

Figure 1: Depiction of various combustion intermediate mole fractions as a function of burner height

Although this is only a small portion of the molecules that are present in flames, these figures show that the concentration of various species is very strongly temperature dependent. Also, while one may assume that the initial fossil fuel used to burn makes a difference, in reality it only makes a modest difference in mole fractions observed. The reason for this is that numerous chemical reactions occur in combustion, and they occur so quickly, that shortly after the ignition, the reaction mixture looks nothing like the original starting fuel source. A depiction of concentration profiles in an ethane flame is given in Fig. 2.

Aside from some fairly common (non aromatic) compounds, is there any evidence that aromatic compounds exist in flames? Measurements taken from an ethane flame (Fig. 2) show that indeed aromatics are also formed in flame combustion. It should be

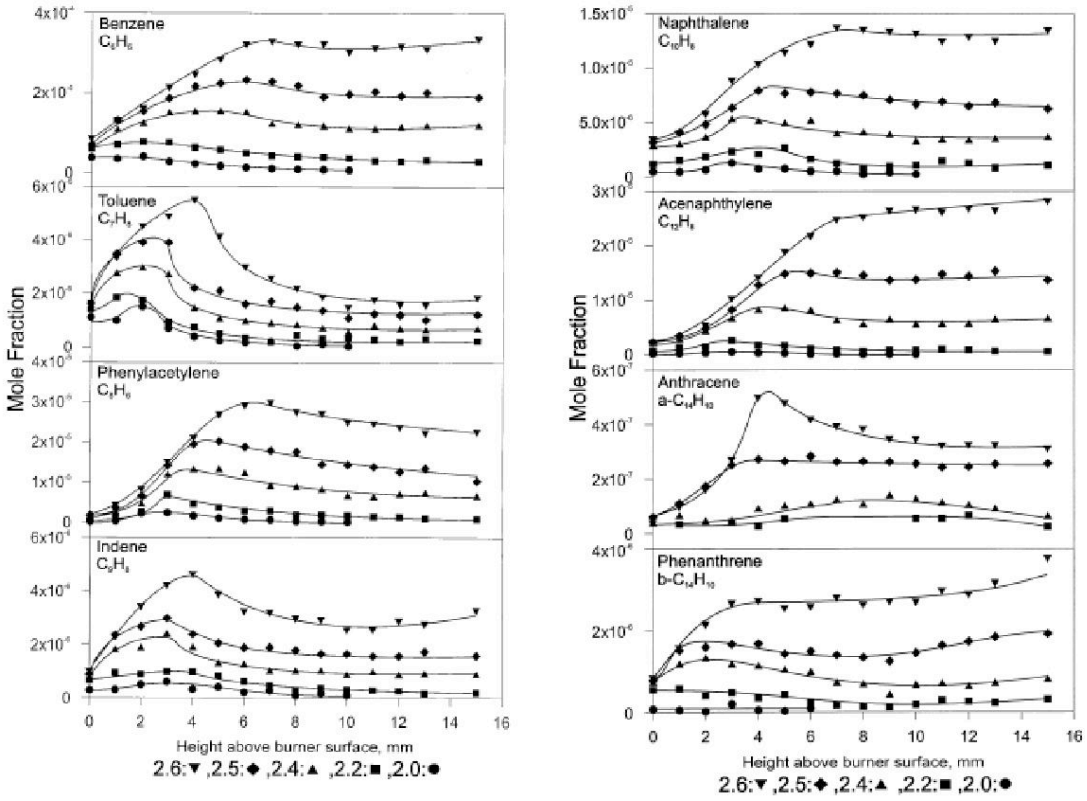

Figure 2: Depiction of various aromatic compund mole fractions as a function of burner height

noted that this figure represents only a small fraction of the aromatic compounds detected in flames. One should note (also) that there appears to be an optimal distance above the burner at which aromatic ring formation is most favorable. This is due to a delicate balance between temperature and pressure. Recently, recently, while pyrolysizing n-decane, a group was able to measure the existence of 24 unsubstituted PAHs, and 43

alkylated PAHs. These determinations were made through the aid of 2-D High Pressure Liquid Chromatography (HPLC) in conjunction with UV-vis and Mass Spectrometeric techniques[14]. In another study, the shock wave compression of the pyrolysis of naphthalene produced various methylated, naphthylated and dehydrogenated variants of naphthalene, a clear indication that naphthalene can serve as one of the building blocks for further PAH growth[15].

The present estimates place the percentage of carbon in our galaxy involved in polycyclic aromatic hydrocarbon (PAH) at between 2 and 30 percent.[16] The existence of PAH in the interstellar media (ISM) was suggested early on by the spectroscopic analysis of IR emission bands by Allamandola and coworkers in 1989.[17] Recently, a more detailed analysis of characteristic spectral bands between 15 and 20 μm by Peeters has revealed the presence of CCC out-of-plane bending vibrations likely due to PAHs.[18] Moreover, based on the IR spectra from the interacting galaxy UGC 10214 (the Tadpole galaxy), it has also been suggested that extranuclear star formation is accompanied by PAH formation, further establishing the importance of PAHs in astrochemistry.[19] In our own Solar System, PAHs represent an important class of molecules and their production and growth processes deserve careful consideration. Although they have not been observed directly in planetary atmospheres, PAHs have been identified in laboratory experiments simulating Jupiter's atmosphere and also the atmospheric chemistry of Saturn's moon Titan.[20] It is strongly believed that PAHs are primarily responsible for the famous orange/reddish haze layers found on Titan. Early laboratory simulations by Khare, Sagan and others suggested a possible existence of substituted PAHs in Titan's

tholins.[21] Tholins are the solid materials produced in laboratory simulations of Titan's atmosphere, and can be useful in determining the constituents that are formed and then subsequently deposited onto Titan's surface. In 1993, again by utilizing laboratory simulated Titan atmospheres, Khare et al. have detected several two to four ring PAH's by using a two step laser desorption mass spectrometry method, but no definite chemical identification could be made.[22] In 2002, Khare et al. studied the nature of laboratory simulated Titan's haze layers and ascertained, by time dependent IR and GCMS techniques, that aromatics are formed within the first few seconds of simulation.[23] PAH precursors are also postulated to exist in Titan's atmosphere. For instance, Coustenis and coworkers in 2003 reported the first spectroscopic identification of benzene at 674 cm^{-1}.[24] Hard evidence for benzene on Titan was finally achieved in 2007 by using the Composite Infrared Spectrometer (CIRS) instrument on board of Cassini (Coustenis, Icarus, 2007).[25] Naphthalene, the simplest PAH, has been also postulated to exist on Titan. For instance, naphthalene was detected in 2006 as one of the tholin pyrolysis products using a two dimensional GC/MS technique (McGuigan, Journal of Chromatography A, 2006).[26]

Until recently, the kinetic models of the PAH formation and growth in low temperature environments such as on Titan or in the interstellar medium relied upon the models of PAH and soot formation in combustion processes and assumed that similar mechanisms are important both at combustion temperatures (1000 – 2500 K) and in the extraterrestrial, low temperature environments (10 – 150 K).[27-30] Wilson et al.[31] suggested, for instance, that once the first aromatic ring is available, the further growth of PAHs proceeds by the hydrogen-abstraction-acetylene-addition (HACA) mechanism,[30,32] which is believed to be the most important PAH formation mechanism in combustion

flames.[27] However, an apparent flaw of these models is that both hydrogen abstraction and acetylene addition reactions exhibit significant barriers and as a result are very slow at low temperatures relevant to the atmospheric conditions on Titan or in the Interstellar Medium (ISM). As a low-temperature alternative to HACA, our group has recently proposed a new ethynyl addition mechanism (EAM) of PAH growth.[33] Within EAM, an addition of the ethynyl radical C_2H to benzene, produces phenylacetylene $C_6H_5C_2H$ after H loss from the initial adduct. Next, a second C_2H addition to the *ortho* carbon atom of phenylacetylene gives a reaction intermediate, which then rapidly loses a hydrogen atom forming 1,2-diethynylbenzene. The latter can react with a third ethynyl molecule via addition to a carbon atom of one of the ethynyl side chains and a consecutive ring closure of the intermediate leads to an ethynyl-substituted naphthalene core. Under single collision conditions of the ISM, this core loses a hydrogen atom to form ethynyl-substituted 1,2-didehydronapthalene, but under higher pressures of Titan's atmosphere, three-body reactions can lead to a stabilization of this naphthalene-core intermediate. The reactions of C_2H, and C_2H like molecules, with a variety of unsaturated and aromatic hydrocarbons have been shown to be fast, with rate constants in the order of 10^{-10} cm^3 $molecule^{-1}$ s^{-1}, both experimentally and theoretically[34-36] even at temperatures down to 15 K and hence, the viability of EAM would depend on the abundance of the reactant species.[34, 37-38] On Titan, the ethynyl radical can be produced easily by the photolysis of acetylene.[39-42] However, a drawback of the EAM involving benzene is that it can only produce dehydro naphthalene derivatives and H (or a hydrocarbon radical) additions followed by collisional or radiative stabilization are required to form closed-shell PAH molecules.

The main hypothesis of this work is that PAH and nitrogen-containing polycyclic aromatic compound (NPAC) molecules can grow in size via consecutive additions of the ethynyl radical, C_2H, cyano radical, CN, as well as phenyl radical, C_6H_5, leading to the formation of an additional aromatic ring. Based on the experimental and theoretical data available in the literature, the addition reactions are hypothesized to be barrierless and thus should be sufficiently fast even in very cold astrochemical environments. The ubiquitous presence of acetylene, C_2H_2, and cyanic acid, HCN, in planetary atmospheres and the interstellar medium makes possible the production of the ethynyl and cyano radicals via photodissociation of C_2H_2 and HCN, respectively, if the sun light (or UV irradiation from a nearest star) is available. Alternatively, the phenyl radical can be formed via photodissociation of benzene, C_6H_6, and its subsequent addition reaction may drive the growth of larger PAH. Another hypothesis is that the reaction mechanisms for the PAH and NPAC in cold and very-low-pressure astrochemical environments can and should be different than those governing the same processes in combustion flames.

These hypotheses determine the goals of this work to unravel various mechanisms for the formation of polycyclic aromatic compounds at different temperatures and pressures, especially in cold astrochemical conditions. We also look for mechanisms that lead to nitrogen atom insertion into one of the aromatic rings and thus result in the formation of nitrogen-containing polycyclic aromatic compounds. These goals will be achieved through the careful and judicious choice of starting reagents, coupled with accurate quantum mechanical methods to obtain energies at the optimized structures of reagents, intermediates and products. Statistical methods will then be used to obtain branching ratios either as a function of temperature, pressure or energy.

Chapter 2: Theory of Unimolecular and Recombination Reactions

All of the information presented in this chapter came from my readings of the first four chapters of "Theory of Unimolecular and Recombination Reactions", written by Robert G. Gilbert and Sean C. Smith[43], a good text on the intricacies of RRKM theory. Rather than continue to give credit over and over again throughout this chapter, I give them full credit in the very first sentence of this chapter.

In chemical reactions, one is often confronted with the idea of a phase space. A phase space can be thought of as the space in which the reaction "lives." It consists of a space of all 3N position (q) coordinates, and all 3N momenta (p) coordinates. If one wished to evaluate the rate constant for a particular reaction, one could (in principle) take every single unique starting position (and momenta), and trace out the natural trajectory which arises from solving Hamilton's equations. One can then imagine a dividing surface, which divides the reactant region from the product region. The rate coefficient will then be the "flux" of trajectories going through the dividing surface divided by the total number of trajectories (N).

$$H(P_1, P_2, \ldots P_{3N}; q_1, q_2, \ldots q_{3N}) = \sum_i \frac{P_i^2}{2m} + V(q_1, q_2, \ldots q_{3N}) \qquad 2.1$$

Sampling the entire phase space sufficiently would require studying an enormous number of trajectories and is not achievable in practice.

One way around this, as Transition State Theory explains, is to change coordinates. This change of coordinates involves the creation of a special coordinate called the reaction

coordinate (s). The reaction coordinate connects the reactant to the product, and, generally speaking, is the minimum energy path. All other coordinates are orthogonal to s, and represent a departure (either vibration or rotation) away from the reaction coordinate.

To help understand the reaction coordinate better, one might envision starting from the bottom of a valley. To either side of the valley are sheer rock faces which go nearly vertically upwards. Since you are at the bottom of a valley, any direction you move, will lead you to a higher elevation (energy), but as long as you stay along the valley, your energy increase is only gradual (again remember that there are sheer rock faces to either side of you). So, you travel along the valley, and eventually you reach the peak of the valley. This is called the transition state, and beyond it is the product valley. The reaction coordinate, as we will see shortly, plays a central role in TST theory.

Derivation of the TST expression for the rate constant at the high pressure limit:

Before we plunge head long into this derivation, we should ask ourselves, what is so special about the high pressure limit? I think the best explanation comes from the following process:

$$A + M \rightarrow A^* + M$$

$$A^* \rightarrow B + C$$

In the above process, a molecule, A, is collisionally activated by a collision with a bath gas molecule , M. Then A^*, the activated molecule, dissociates into product molecules

B and C. Typically, the activation process occurs every about 10^{-13} s, while the lifetime of A^* is about 10^{-9} s. At these conditions, because the collision process occurs nearly instantaneously, we can neglect it, and assume that all of our molecules are collisionally activated. While this severely simplifies the process, these conditions are only valid at the highest pressures and temperatures available. It is, for the simplicity of it all, that we start with the high pressure limit derivation of the rate constant.

To begin this derivation, we may ask ourselves the following question: What is the probability of finding a trajectory in the hypersurface defined by a small change in the μ coordinate momentum, p_μ, a small change in the μcoordinate itself, μ, a small change in the s coordinate momentum, p_s and a small change in the s coordinate, s,? Because we are at high pressure, this is simply given by Boltzmann's distribution. Then, the number of trajectories residing in this space is given by the following expression.

$$\frac{N\exp(-H/kbT)dP\mu d\mu dPsds}{\iiint_{allspace}\exp(-H/kbT)dP\mu d\mu dPsds} \qquad 2.2$$

This makes sense, as N is simply the total number of trajectories and the Boltzmann distribution is simply the probability for finding a trajectory in this space. The denominator is simply a normalization factor, and, in this context, is equal to unity. Now, imagine having a dividing surface placed in the product region , s_{prod} ,. We now want to find out the flux (number of trajectories moving through s_{prod} per unit time). From the kinetic theory of gasses, we know that this can be calculated as

$$Vddxdydz$$

where V is the velocity of molecules and d is the number density of gas molecules per unit volume. In physics, we encounter problems dealing with flux on a fairly routine basis, and this equation is simply the flux of molecules through a unit volume of dimensions dx, dy and dz. In our case, the number density , d , is simply the result of equation and $V = \frac{Ps}{m}$. All written out, this means that the flux, or the number of trajectories going through the hypersurface $dP\mu d\mu d\mu dPsds$ is equal to

$$\frac{N}{P}\iiint_{allspace}\frac{Ps}{m}\exp(\frac{-H}{kbT})dP\mu d\mu d\mu dPs \qquad 2.3$$

However, it is not fair to call this result the rate coefficient. What we are really interested in is the number of trajectories that originate from the reactant valley, cross over (through the dividing surface S_{prod}) to the product valley, and stay in the product valley. Traditionally speaking, it is appropriate to include a Heaviside function (Θ), which is equal to unity when a trajectory has enough momentum in the s coordinate (P_s) to pass through S_{prod}, and zero if it does not. Also, the introduction of (χ), which is unity if the trajectory originates from the reactant region, and zero if not, allows for the correction of the rate coefficient resulting from TST theory. This leads to one of the assumptions inherent in TST theory, and that is that once trajectories pass through S_{prod}, they will never 'turn around,' and pass back to the reactant region. This assumption is often referred to as the 'no re-crossing' assumption. In general, this is true, and more so true for low energy trajectories, but need not be strictly true. After the addition of these two parameters, the equation becomes

$$\frac{N}{P}\iiint_{allspace}\frac{Ps}{m}\exp(\frac{-H}{kbT})\chi(P\mu,\mu,Ps,s=sprod)\Theta(Ps)dP\mu d\mu dPs \qquad 2.4$$

It can also be shown that the partition function (Q) is related to P in the following way:

$$Q=\frac{1}{h^n}\iiint_{allspace}\exp(\frac{-H}{k_bT})dpdq \text{ i.e.}$$

$$P=h^2Q \qquad 2.5$$

Finally, this means that

$$k_{uni}^{\infty}=\frac{h^{-n}}{Q}\int_0^{\infty}\frac{p_s}{m}\exp\left(\frac{-p_s^2}{2\pi mk_bT}\right)dp_s\iint\exp\left(\frac{-1}{k_bT}\left(\frac{p_\mu^2}{2m}+V(s=0,\mu\right)\right)dp_\mu d\mu \qquad 2.6$$

which is equal to

$$\frac{k_bT}{h}\frac{Q^{\neq}}{Q} \qquad 2.7$$

So, where should we place the dividing surface? Is there a specific place it should be, or can its location be (more or less) arbitrary? To answer this, let us look at how the line integral changes in response to the position of the dividing surface. To do this, look at the diagram in Figure 3. Here is a depiction of a section of the PES bounded by 4 lines (S_{prod}, S', S'' and S_0). Two of the boundaries (S' and S'') are chosen so as to be so far away from S_{prod}, that no trajectories ever pass through them. That is, their surface integral is null, and can be neglected.

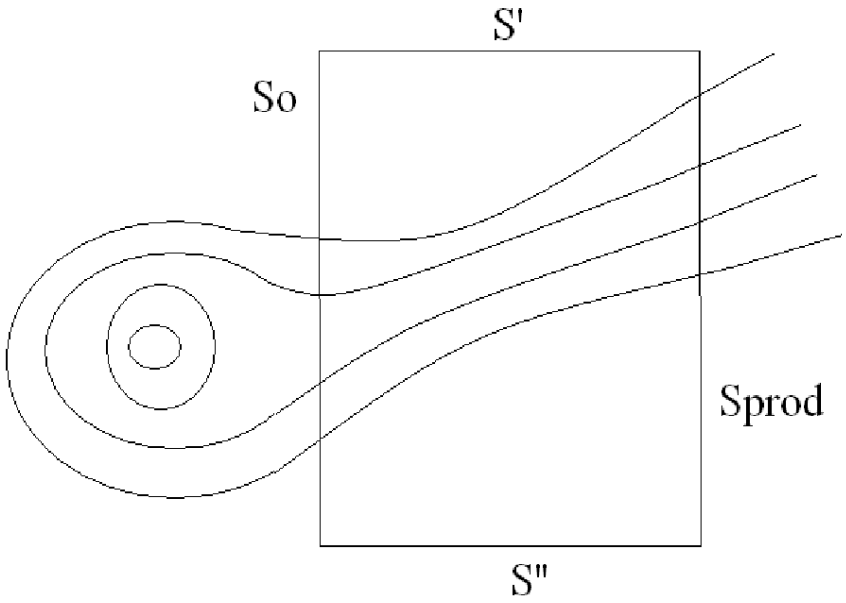

Figure 3: Depiction of a phase space bounded by 4 lines S_0, S', S_{prod}, S''.

The proof relies on conserving the momentum along the s coordinate. At the boundary of S_{prod}, Ps is pointing towards the product valley. Now as we move along the contour and reach the boundary S_0, Ps is pointing towards the reactant side. This means that trajectories will be moving out towards the reactant side. These trajectories are exactly the ones we wish to not count. To compensate for this, we note that the flux should be zero therefore, if trajectories are moving towards the product side in S_{prod}, trajectories should also be moving towards the product valley in S_0. To do this, we simply have to realize that momentum must be conserved along the s coordinate and change the sign of Ps at the S_0 boundary so that it is pointing towards the product valley. Finally, this means

that the two surface integrals (one for S_{prod} boundary, and the other for S_0 boundary) are equal hence the position of the dividing surface is invariant.

Therefore, one could, in principle, move the dividing surface farther into the product valley. This would alleviate the problem of re-crossing, however, you will, at the same time, increase the frequency of trajectories which originate from the product valley, and cross the dividing surface. Clearly, these types of trajectories should not be included in the calculation of flux. A fine line needs to then be struck, which minimizes the amount of re-crossing, while also minimizing contributions from trajectories originating from the product valley. In practice, this fine line is achieved by setting the dividing surface to be at the centrifugal maximum. In the event that there is no barrier to reaction, there are other methods which involve obtaining a multitude of transition state candidates, calculating the rate constant for each candidate and choosing, as the transition state, that candidate which minimizes the reaction flux.

Derivation of RRKM equation for unimolecular rate constants:

Before going into the details of RRKM theory, we should remind ourselves of why we need this type of rate constant expression. Remembering back to the previous section, we can remember that the rate expression obtained was specifically for the high pressure limit. At the high pressure limit, we were able to make the assumption that the rate constant is unaffected by the collision process. Essentially, this was proven to be true, because at the high pressure limit, molecules are constantly being bombarded by gas bath molecules. This leaves reactant molecules in a state of constant excitement, making the overall process of dissociation from the excited state to products the dominant contributor

to the rate constant expression. This allowed us to assume a Boltzmann distribution for the population distribution, which in turn greatly simplified the problem from a conceptual and mathematical perspective.

However, at lower pressures, this constant bombardment of bath gas molecules does not happen. Purely speaking, we can no longer separate the collision process from the dissociation of the activated complex to product. This requires (as seen below) a more careful and detailed examination of the problem.

The basic idea of RRKM theory can be visualized as follows: Consider a molecule undergoing a collision with the surrounding bath gas. The energy it acquires from this collision is randomly interspersed between all degrees of freedom. As energy accumulates at and dissipates from a particular degree of freedom (for example a bond), there is the possibility that larger and larger amounts of energy start to become localized onto this bond. When this happens, the bond starts to become weaker and weaker, until a sufficient amount of energy has been "trapped" in it that the bond breaks. The rate constant can be identified as the inverse of the amount of time it takes for that bond to break. The assumption that energy is randomized is called the ergodic theory, and coupled to it the idea of using a microcanonical ensemble (N, V and E is conserved) along with the TST theory assumption we can derive the RRKM rate expression.

The RRKM rate expression is given below:

$$k(E) = \frac{\int_0^{E-E_0} \rho^{\neq}(E_+) dE_+}{h\rho(E)} \qquad 2.8$$

In this equation, E is the energy stored away in active degrees of freedom, E_0 is the critical energy, $\rho^{\neq}(E_+)$is the density of states for the transition state, $\rho(E)$ is the density of states of the reactant, and h is Plank's constant. The density of states is described as the number of states contained in one interval unit of energy. To obtain the number of states, one would simply integrate from some relative energy to an energy upper bound by the excess energy $E - E_0$.

$$W^{\neq} = \int_0^{E-E_0} \rho(E) dE \qquad 2.9$$

This transforms the above equation into its more conventional notation

$$k(E) = \frac{W^{\neq}}{h\rho(E)} \qquad 2.10$$

From a purely classical trajectory perspective, the exact unimolecular rate constant expression is given as follows:

$$k(E,t) = \frac{\int \ldots \int d\Gamma f(\Gamma) \delta[H - E] \delta[T(\Gamma) - t]}{\int \ldots \int d\Gamma f(\Gamma) \delta[H - E] S[T(\Gamma) - t]} \qquad 2.11$$

where Γ is the distribution of trajectories, $f(\Gamma)$ is how the distribution changes over time, $\delta(H - E)$"picks out" only those trajectories which have energy equal to E, $T(\Gamma)$ is the lifetime for a trajectory to crossover the dividing surface, $\delta[T(\Gamma) - t]$ ensures that only trajectories with lifetimes equal to t are counted and $S[T(\Gamma) - t]$ is a step function

designed to not count those trajectories which have already crossed the dividing surface once.

So, when starting this derivation, what initial distribution, Γ_0, of points (p and q) should we use? One can imagine various scenarios where one, or a limited number, of starting points would carry significantly more weight than others. This may lead one to believe that the starting distribution of points should play a critical role in the outcome of the eventual rate constant, and should therefore be chosen wisely. After all, if a certain process requires extreme localization of energy onto one specific bond, one may correctly reason that it would indeed take forever to achieve that distribution if calculations were started from a completely randomized set of points. Here, the ideas of statistical thermodynamics save RRKM theory from a catastrophe. The saving grace is that the initial distribution of points does not matter. All of these points will trace out individual trajectories that within a short period of time will mix and become sufficiently randomized. This is the idea of ergodicity, and assumes that energy, even if it is initially highly localized, will diffuse through to other bonds sufficiently fast enough, that it very quickly becomes randomized. The ideas of ergodicity, allow us to use any initial distribution of points. In this setting, we chose to use a microcanonical ensemble (conserved N, V and E) which will allow us to model a system as each point having equal weighting.

At this point, because we have specified to give equal weighting to all configurations in phase space, $f(\Gamma)$ is no longer dependent on p and q, and therefore can move out of the integral and cancel out. It is also at this point that we change coordinates to our

curvilinear system of coordinates as we have previously performed. Doing both of these operations leads us to the following result:

$$k(E,t) = \frac{\int\ldots\int dp_{\mu} d\mu \int dp_s \frac{p_s}{m} \int ds\, \delta(s - s_T)\delta(H - E) S(p_s)\chi(\Gamma, t)}{\int\ldots\int d\Gamma\, \delta[H - E] S[T(\Gamma) - t]} \qquad 2.12$$

This is analogous to watching trajectories pass by while "seated" on the dividing surface. If however, one thinks about it further, one would notice that in actuality, the rate constant is independent of time. In essence, because of the randomness of trajectories, one can always stop a set of trajectories in mid run, reset the time to zero, and then continue the simulations. These trajectories will behave similarly to the initial set of chosen trajectories. This is due to the ergodic theorem, which states that the trajectories will be random.

Now, we will do two following things, firstly, assume that the dividing surface is at the reaction barrier (ie. $s = s_T$), and invoke the transition state assumption from the previous section (i.e. $\chi = 1$). This then turns the above equation into

$$k(E) = \frac{\int_{-\infty}^{+\infty} dp_{\mu} \int_{-\infty}^{+\infty} d\mu \int_{0}^{\infty} dp_s \frac{p_s}{m} \delta[H(p_{\mu}, \mu, p_s, s = s_T) - E]}{\int\ldots\int d\Gamma\, \delta[H - E]} \qquad 2.13$$

We will now turn our attention to the nature of the Hamiltonian (H) at the transition state. H can be expressed in the following way:

$$H(p_\mu, \mu, p_s, s) = \frac{p_s^2}{2m} + V(s, \mu = 0) + T(\mu, p_\mu) + V'(\mu; s) \qquad 2.14$$

Within this expression, the potential V, has been separated into one component along $\mu = 0$, and the other component comprising of the remainder. At the transition state, this can be re-expressed in the following form:

$$H(p_\mu, \mu, p_s, s) = \frac{p_s^2}{2m} + E_0 + H_\mu(s_T) \qquad 2.15$$

where

$E_0 = V(s, \mu = 0)$at the transition state, and

$T(\mu, p_\mu) + V'(\mu; s) = H_\mu$

Solving for H_u, and using that to re-express the argument of the delta function in the numerator, we can re-express the rate expression as :

$$k(E) = \frac{\int_0^{E-E_0} dE_0 \left\{ \int dp_\mu \int d\mu \delta\left[H_\mu - (E - E_0 - E_s)\right] \right\}}{\int \ldots \int d\Gamma \delta[H - E]} \qquad 2.16$$

It can be shown that, in the classical limit, the density of states can be expressed in the following way:

$$\rho(E) = \frac{1}{h^n} \int \cdots \int dpdq\delta(E - H) \qquad 2.17$$

where n is the dimensionality.

So, to calculate unimolecular rate constants, it appears relatively simple. The bulk of the computation relies on calculating the sum and density of states. We are now going to talk about how to calculate these two quantities. To do this, we need access to frequencies for intermediates and transition states. Take the first frequency, λ_1, there is a state every λ_1 energy from the energy of the molecule's Zero Point Energy (ZPE), to the maximum energy desired. This means that if the first frequency is 100 cm^{-1}, there will be a state located at 100, 200, 300, 400… cm^{-1} above the energy of the reactant, until you reach the maximum energy desired. Then, take the second frequency λ_2, and repeat the process, until you have calculated the total number of states between the intermediate's energy and the maximum energy desired. Add to this the rotational density of states, and you have the density and sum of states useful in the RRKM rate equation. This methodology assumes the harmonic approximation is correct. The truth is, even if there is anharmonic contributions, it can be shown that each state is simply shifted up or down by some small amount of energy. In this case, the density of states, and the sum of states should be little affected.

Chapter 3: Potential Energy Surfaces, Harmonic frequencies, Moments of Inertia and Total Molecular Energies

As noted in the previous chapter, energies of intermediates, transition states and products are necessary in order to compute accurate rate constants. In this chapter, we will provide some information on Potential Energy Surfaces (PES), and how energies are calculated. It is crucial, as it will serve as a basis for the understanding of the "flow" of energy from reactant to intermediates, and ultimately to final products.

The number of degrees of freedom a molecule may have been shown to be 3N – 6 and 3N – 5 for a non-linear and linear molecule, respectively. This means that a molecule may possess either 3N – 6 or 3N – 5 vibrational modes[44]. In theoretical chemistry, we ascribe each one of these vibrational modes a dimension, and create a PES. A PES is simply a coordinate system which allows one to visualize how the potential of a molecule changes when one (or more) of its vibrational modes are activated. The simplest PESes are those for diatomics in which case, there exists only one possible vibration. This type of PES is shown in Fig. 4.

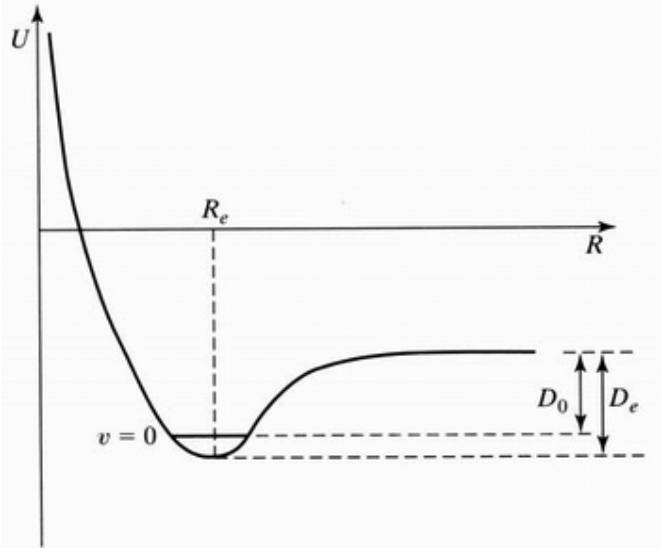

Figure 4: Depiction of a typical PES for a diatomic molecule

Starting from really far distances, as the two atoms start to come closer to each other, the potential of the two atoms still does not change. This is because their individual potentials have yet to influence each other. At some point, as they are drawn closer and closer to each other the potential energy starts to drop until some minimum potential is observed. This is typically denoted as Re, and is called the equilibrium bond distance. From this point on, squeezing the two molecules further together elicits a repulsive effect, as seen by the steeply increasing potential as the function asymptotically reaches a bond distance of zero. One can view a polyatomic molecule as having 3N – 6 or 3N -5 harmonic oscillators each with its own "diatomic" PES.

A consequence of using a PES is that local minimums are required to have all real frequencies, and transition states are required to have exactly one imaginary frequency. I like to think of this in the following way. Imagine that part of your PES is contained within the volume of a cup. At the bottom of that cup is a minimum corresponding to

some intermediate. This is true, because no matter which direction (or dimension) along the side of the cup you are traveling, you are always gaining in altitude (or energy). An intermediate is a point on the PES through which there is no immediate further way to lower yourself in energy. You must at least climb upwards to some barrier before you can drop into another (possibly deeper) intermediate. On the other hand, a transition state can be viewed as a cup with a small hole on the bottom side of it. In this case, there is only one direction along the side of the cup which can lead to an immediate lowering of your potential (the direction with the hole in it). The direction this hole leads to is directly tied to the vector arising from the imaginary frequency (negative force constant). This vector points in the direction one needs to travel in order to reach a minimum. Many computational chemistry programs take advantage of this vector, when trying to find the minimum directly associated with a transition state. They will use this vector as a search direction, and search along this direction (using gradients) until a local minimum has been reached. It has come to be a valuable tool in the arsenal of computational chemists.

The calculation of frequencies has been shown to be pivotal to accurately determining densities of states, and from that, rate constants. So, how are frequencies calculated? We must start with the construction of the hessian[45-46]. The hessian, is a square matrix of 3N dimensions, which consists of the second partial of the potential, with respect to nuclear coordinates. Each entry in the matrix is a force constant, and it essentially describes the ease (or difficulty) with which one atom can move in the x, y or z direction with respect to a second atom. After conversion to mass weighted coordinates, the hessian can then

be diagonalized, yielding 3N eigenvectors (normal modes), and 3N eigenfunctions (fundamental frequencies). This hessian however is contaminated in a way. It includes 3 translational modes, and 3 rotational modes (2 if linear), that need to be eliminated from the hessian. To do this, we must change our hessian from mass weighted coordinates, to internal coordinates. From the mass weighted coordinates, we cannot tell which normal modes correspond to the translational and rotational modes. However, a conversion from mass weighted coordinates to internal coordinates will cause the frequency associated with these modes to become zero. In this way, we will be easily able to distinguish the translational and rotational modes from everything else.

In order to start this conversion process, we will need to build up a transformation matrix (D), which will transform our hessian from mass weighted coordinates to internal coordinates. To aid this construction, moments of inertia need to be calculated. They can be calculated in a straightforward manner, by diagonlizing the following symmetric matrix.

$$\begin{matrix} I_{xx} & I_{xy} & I_{xz} \\ I_{xy} & I_{yy} & I_{zy} \\ I_{xz} & I_{zy} & I_{zz} \end{matrix}$$

The eigenfunctions of this diagonalized matrix are the moments of inertia, while the corresponding eigenvectors will be used to generate the three vectors corresponding to rotations.

$$D_{4j,i} = \frac{\left(\left(P_y\right)_i X_{j,3} - \left(P_z\right)_i X_{j,2}\right)}{\sqrt{m_i}}$$

$$D_{5j,i} = \frac{\left(\left(P_z\right)_i X_{j,1} - \left(P_x\right)_i X_{j,3}\right)}{\sqrt{m_i}} \qquad 2.18$$

$$D_{6j,i} = \frac{\left(\left(P_x\right)_i X_{j,2} - \left(P_y\right)_i X_{j,1}\right)}{\sqrt{m_i}}$$

Additionally, the three vectors for translational modes can be deduced by taking the corresponding coordinate axis (from moments of inertia), and multiplying it through by $\sqrt{m_i}$. Next, the scalar product of each vector with itself is taken, and if it is equal to zero, this vector is excluded as a normal mode (ie the length of the vector is zero). If it is not equal to zero, than it is normalized by multiplying through by the reciprocal of the square root of the scalar product. For linear systems, one of these vectors should be excluded. Through a Schmidt orthogonalization routine, the remaining 3N-6 or 3N-5 vectors are formed, and the transformation matrix D is finally created.

$$f_{\text{int}} = D^{\not\in} f_{mwc} D \qquad 2.19$$

The transformation is shown above, after which diagonalization reveals the harmonic frequencies.

Lastly, I will go over how to obtain accurate energies for intermediates, and transition states. Firstly, structures need to be optimized. This is done using Density Functional Theory (DFT), using the 6-311G** basis set. A variety of methods exist, whose aim is to optimize geometries. They will not be discussed here, except but to say that they all rely (in some way) on the minimization of the gradient. The displacements of atoms from one iteration to another also needs to be small. The geometry, optimized at the DFT level,

does not have the accuracy in energy that we require. To improve upon this, we perform single point (SP) calculations on the optimized structure. SP simply means that no geometry optimization is performed, only an evaluation of the energy is done. Our method is a composite one, in that it requires the addition and subtraction of several SP energies. The composite method is called the G3(MP2,CC) modification[47] of the original Gaussian (G3) scheme[48], and is calculated as follows:

$$G3(MP2) = ECCSD(T)/6\text{-}311G^{**} + (EMP2/G3Large - EMP2/6\text{-}311G^{**}) + ZPE$$

The aim of the G3(MP2,CC) method is to approximate the energy of CCSD(T) at the G3Large basis set. The MP2 calculations can be considered as a correction factor for the lower basis set of the coupled cluster calculation. Energy and frequency calculations were performed using Gaussian 98 [49], Molpro 2002 [50], Gaussian 09 [51] and later on using NW Chem [52].

Up to this point, in this dissertation, the RRKM expression has been derived (both high pressure and microcanonical), and it has been shown that harmonic frequencies, moments of inertia and accurate molecular energies are needed to obtain accurate rate constants. Further, it has also been shown how to obtain moments of inertia, harmonic frequencies, and total molecular energies. I must stress, that these are the only molecular parameters necessary for the accurate determination of rate constants. Because only a handful of parameters are needed, RRKM theory is an attractive route towards the calculation of unimolecular rate constants.

The next several chapters of this thesis are devoted towards the elucidation of our ideas behind the formation of naphthalene, the first benzenoid PAH possible, in Titan's conditions. It includes our thought processes for pursuing certain types of reactions, as well as what we learned along the way.

Chapter 4: Addition of C_2H to Styrene and its Resulting Products: The Formation of Substituted Naphthalene Derivatives

One of the first reactions we considered was the reaction of C_2H with styrene. It accesses the C_8H_9 PES, and with subsequent loss of a hydrogen atom, can lead to the formation of naphthalene. The following gives an outline of the PESes studied, along with some discussion. The numbering of carbons around styrene is given in Fig. 5.

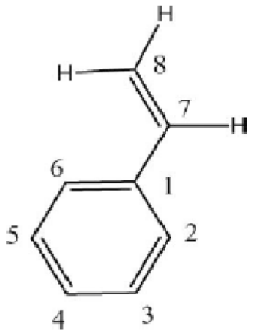

Figure 5: Depiction of the numbering system used for carbon atoms in styrene

The reaction of C_2H radical with styrene at the 8 position occurs without a barrier, and forms **i1** and **i2**, with exothermicity of 63.9 and 63.2 kcal mol^{-1}, respectively. As seen in Figure 6, **i1** and **i2** are conformational isomers produced in the entrance channels and should be able to easily interconvert to each other by rotation around a single C-C bond, which is expected to have a low barrier. **i1** is capable of pursuing three distinct reaction

paths. The first involves loss of a hydrogen atom from the tetrahedral carbon center 8 and leads to trans-phenylvinylacetylene (**t-PVA**) lying 28.4 kcal mol^{-1} lower in energy than the initial reactant species. The reaction has an activation barrier of 39.2 kcal mol^{-1}. Alternatively, **i1** can migrate a hydrogen atom, again from its tetrahedral carbon center, to an adjacent hydrogen-free carbon with an energy barrier of 49.8 kcal $mol^{-1}$to create **i9**. Rotation around a side-chain double bond in **i9** produces another isomer **i12**, via a barrier of 50.2 kcal mol^{-1}. Next, **i12** can readily cyclize with a barrier of ~5 kcal mol^{-1}, proceeding to **i13**, 9-H-naphthyl radical. **i13** can promptly lose a hydrogen atom, via a 14 kcal mol^{-1} barrier, forming naphthalene as the final product. The highest in energy transition state on the C_2H + styrene **→i1→i9 →i12 →i13 →** naphthalene + H pathways is TS9-12 residing 7.1 kcal mol^{-1} below the initial reactants. However, TS9-12 is 17.6 kcal mol^{-1} higher in energy than TS1-H, the transition state for the direct H loss from **i1**. The third alternative channel from **i1** proceeds to the bicyclic compound **i3**, which lies at a relative energy of -42.5 kcal mol^{-1}. Ring opening in **i3** via a 18.4 kcal mol^{-1} barrier forms **i5** with a relative energy of -74.5 kcal mol^{-1}. 1,2-Hydrogen migration from the terminal CH_2 group in **i5** can lead to **i12**, which then can isomerize to naphthalene, but the corresponding barrier is high, nearly 60 kcal mol^{-1}. **i5** is however more likely to rearrange to **i6** through a simple single bond rotation. Next, a ring closure may occur via a ~40 kcal mol^{-1} barrier to form **i10**, which in turn can interconvert to **i13** by hydrogen migration via a 37.5 kcal mol^{-1} barrier. **i13** can then readily form naphthalene. Otherwise, a direct hydrogen loss from **i6**, which proceeds via a barrier of 56.2 kcal mol^{-1}, can lead to phenylbutatriene.

Now we turn our attention to the second initial intermediate **i2**.A direct hydrogen loss from **i2** can form cis-phenylvinylacetylene (**c-PVA**). To do so, **i2** needs to overcome an energy barrier of 38.4 kcal mol^{-1}. On the other hand, **i2** may cyclize via a barrier of 37.5 kcal mol^{-1} to form **i4**, which has a relative energy of -47.5 kcal mol^{-1}. Hydrogen migration from the CH_2 group in the newly formed second ring of **i4** can lead to **i13**, with an activation energy of 38.7 kcal mol^{-1}, which can then directly proceed to naphthalene. 1,2-H migration may also occur from the carbon atom of the C-C bond common for the two rings in **i4** producing **i7**. However, in this case the barrier is much higher, ~53 kcal mol^{-1}, with the corresponding transition state lying 4.5 kcal mol^{-1} above the initial reactants. Next, two different hydrogen shifts (from two CH_2 groups in **i7** to the adjacent hydrogen-less carbon atom between them) can produce **i8** and **i11**. We were able to locate transition states for **i7→i8** and **i7→i11** at the B3LYP level and the calculations show that the corresponding barriers were very low. Single-point G3(MP2,CC) calculations gave energies of these TSs slightly lower than that of **i7**. This result indicates that **i7,** if it exists, can represent only a metastable local minimum; once the H migration via TS4-7 is completed, both **i8** and **i11** can be immediately produced. **i8** and **i11** reside in very deep potential wells and can be described as 2-hydro- and 1-hydronaphthyl radicals, respectively. H elimination from the CH_2 groups in **i8** and **i11** finally lead to naphthalene via barriers of 27.9 and 31.8 kcal mol^{-1}.

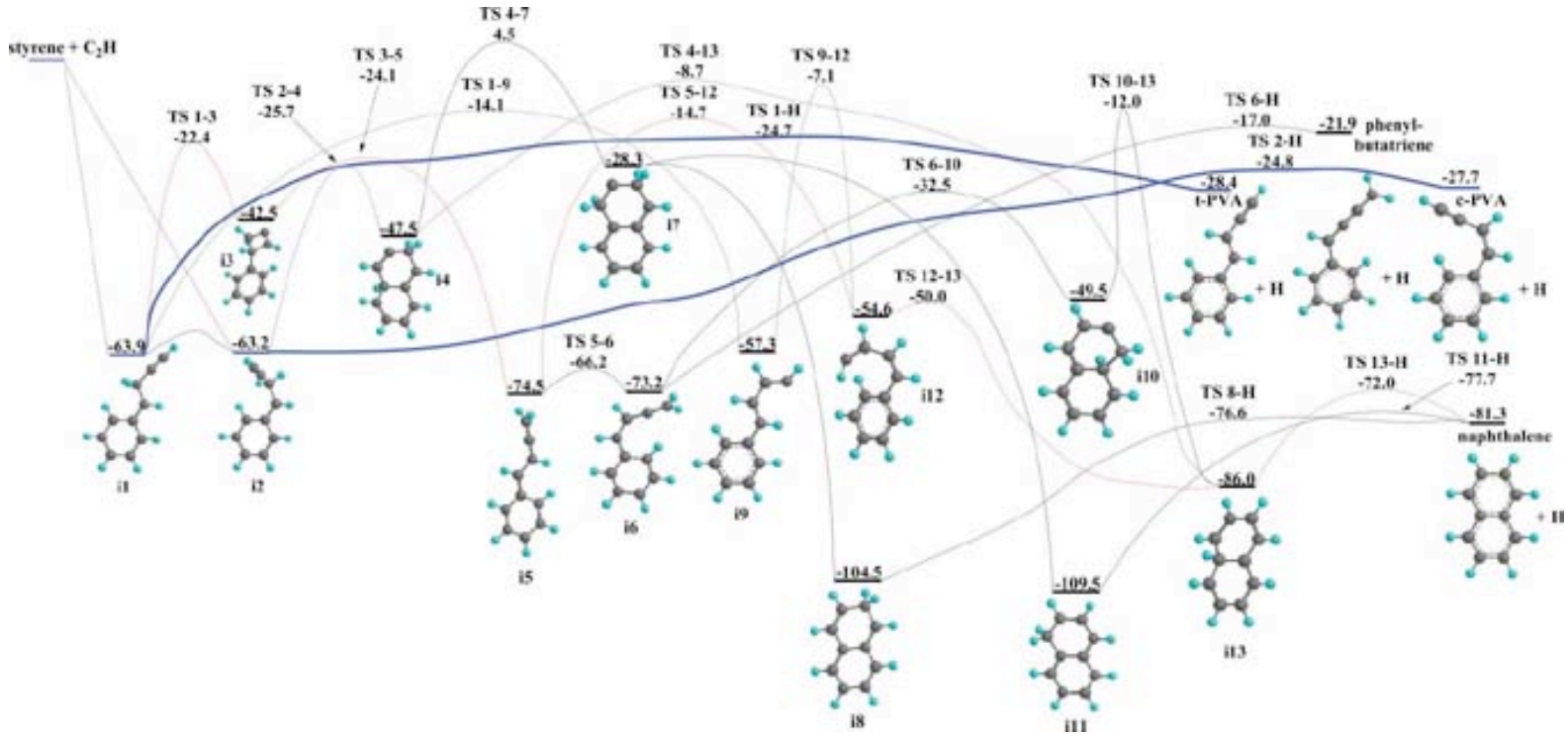

Fig. 6: PES illustrating the addition of C_2H to CH_2 end of Styrene computed at the G3(MP2,CC) level of theory.

When RRKM theory is employed to obtain branching ratios at collision energies of 0 to 5 kcal mol^{-1}, **c-PVA** and **t-PVA** are the exclusive products formed. This can be rationalized by the looseness of their respective transition states (ie. very low frequencies), and their overall greater entropic effect relative to other competing pathways. Further, the barriers for these H eliminations are about 39 kcal mol^{-1}. When compared to the highest barriers encountered through competing pathways, they turn out to be about 10 kcal mol^{-1} lower in energy. Rate constants confirm this, as the H elimination pathways are on the order of 10^4 s^{-1}, while rate constants for competing pathways are at least one order in magnitude lower.

Another possible entrance channel for the styrene + C_2H reaction is the ethynyl attack in position 6 (see Figure 7). This produces the initial adduct **i14** exothermic by 46.7 kcal/mol. At the next step, a loss of the hydrogen atom from the attacked C^6 carbon occurs via a barrier of 28.5 kcal mol^{-1} and leads to the formation of cis-o-ethynylstyrene, which lies 26.5 kcal mol^{-1} lower in energy than styrene + C_2H. Alternatively, **i14** can be subjected to a ring closure involving a barrier of 29.5 kcal mol^{-1} to form **i15**, which is close in energy to **i14**. At this point, **i15** may undergo H loss from two different positions, the CH_2 group and the C atom in the C-C bond shared by the rings. However, both final H elimination products **P1** and **P2** are high in energy, 4.5 and 22.4 kcal mol^{-1} above the initial reactants, respectively, and hence are not likely to be formed to any appreciable extent. On the other hand, instead of the H loss, **i15** may experience an H shift to the hydrogen-less carbon atom leading to 2-hydronaphthyl radical **i8** via a barrier

of 39.9 kcal mol^{-1}.We already considered above that **i8** can eliminate a CH_2 hydrogen atom to produces naphthalene.

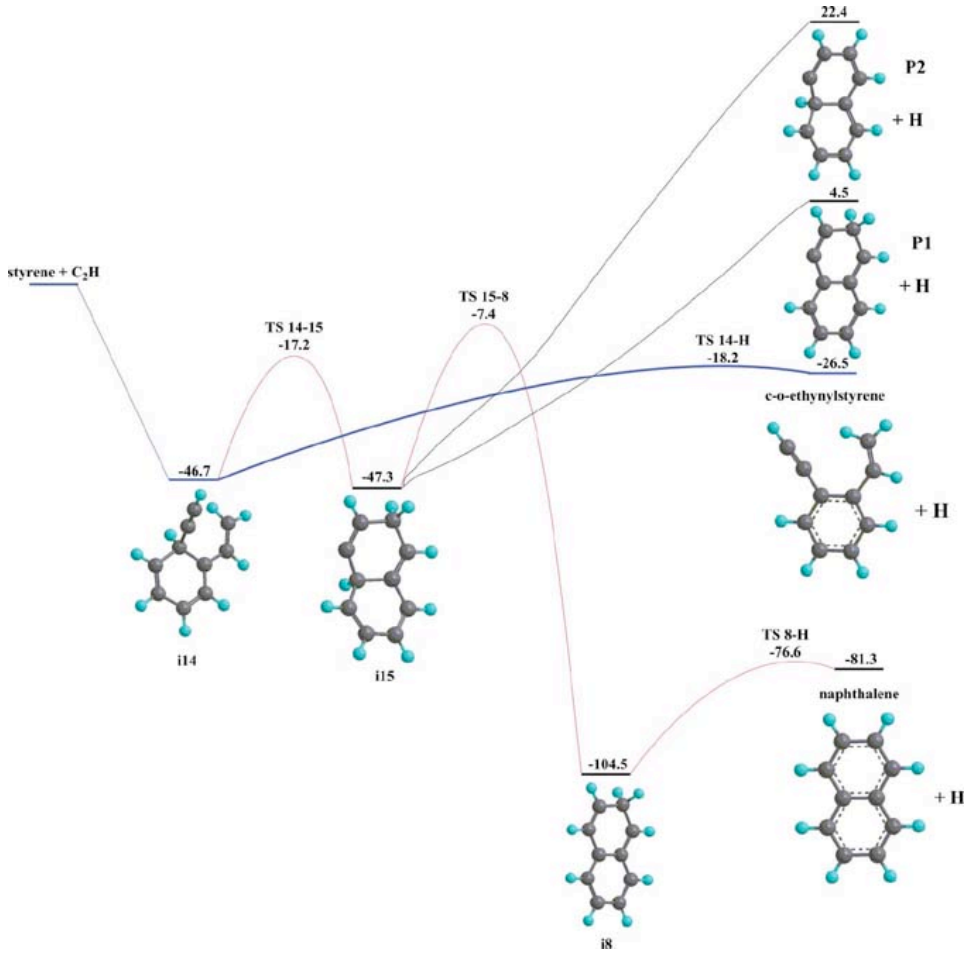

Fig. 7: PES illustrating the addition of C_2H to the ortho position of Styrene computed at the G3(MP2,CC) level of theory.

When C_2H adds to position 6 and **i14** serves as the initial adduct (Fig. 7), the only observable product is expected to be o-ethynlstyrene. The largest barrier on the competing pathway, **i14→i15→i8→naphthalene + H**, is about 10 kcal mol^{-1} higher than the H elimination pathway producing o-ethynylstyrene + H. The other H elimination pathways are endothermic, and so cannot compete. If we look at rate constant date, we find that H loss from **i14** is expected to be between 27.5 and 29.1 times faster than the competing ring cyclization pathway. By analogy, we can expect that C_2H addition to position 2 will produce a trans conformation of o-ethynylstyrene (t-o-ethynylstyrene). No other C_2H additions to carbon atoms on styrene were considered. The reason for this is that they will not produce naphthalene. One of the requirements for naphthalene production is that C_2H additions occur to the side chain, or to an adjacent carbon atom. In lieu of these considerations, we can conclude that the C_2H + styrene reaction would not produce naphthalene.

Nevertheless, our calculations show the formation of several unsaturated hydrocarbons with an aromatic ring and side chains. One of them, o-ethynylstyrene or 1-ethenyl-2-ethynyl-benzene is particularly interesting. In 2005, Zwier et al. investigated the isomerization energetics of o-ethynylstyrene and noted that the *cis* form is 2 kcal mol^{-1} less stable then its *trans* conformer. The authors suggested that if *cis*-ethynylstyrene can be formed, a cyclization process in combustion flames should be most facile from the *cis* conformer. It is worth noting that their spectroscopic measurements were only able to identify the *trans* conformer. It is therefore interesting that our electronic structure calculations show a direct route for the formation of the *cis* conformation of o-

ethynylstyrene.[53] Meanwhile, C_2H addition to position 2 in styrene is expected to produce the *trans* conformation. Recent electronic structure calculations by Hopf and coworkers showed that the ring closure of *cis* o-ethynylstyrene occurs through an activation barrier of 32.1 kcal mol^{-1} at the BLYP/6-31G* level of theory and subsequent H migrations may then lead to naphthalene.[54] In addition, through shocktube studies, Hofmann demonstrated that PVA can isomerize to naphthalene.[55] The processes discussed above occur at high temperatures and are not likely to be relevant to Titan's atmospheric chemistry. Although no PAHs were formed in this round of C_2H additions, we were curious to know what might happen if we added a second C_2H unit to the products formed from the first addition of C_2H to styrene.

Here, we consider C_2H reactions with the most probable primary products of the styrene + C_2H reaction described above, including *trans* and *cis*-phenylvinylacetylenes and *cis*-o-ethynylstyrene. It should be noted that these molecules contain several double, triple, and aromatic C-C bonds, and all of them can be subjected to a barrierless C_2H addition forming a great variety of initial adducts. However, in the present work we investigate only those channels, which can potentially lead to a second ring closure and formation of a PAH species.

An attack by the ethynyl radical toward the *ortho* ring carbon in **t-PVA**produces the initial adduct **i16**, which is stabilized by about 45 kcal mol^{-1} relative to the initial reactants. At this point, **i16** can isomerize to **i17** via a 44.5 kcal mol^{-1} barrier corresponding to a 1,2-H shift from the ring to the C_2H side chain. Alternatively, a hydrogen atom can be lost from the attacked ring C atom in **i16** giving rise to the

$C_6H_4(C_2H)(CHCHC_2H)$ product **P3**. This step proceeds through a 34.9 kcal mol^{-1} barrier and the overall exothermicity of the **t-PVA** + C_2H →**P3** + H reaction is 23.9 kcal mol^{-1}. Lastly, **i16** can undergo ring closure producing the bicyclic intermediate **i18** via a 34.5 kcal mol^{-1} activation barrier. Next, a hydrogen migration in **i18** leads to **i19**, which lies in a deep potential well, 98.1 kcal mol^{-1} below the reactants. A loss of the C_2H group from **i19** can then produce naphthalene as the final product. This dissociation process occurs without an exit barrier and is endothermic by 43.2 kcal mol^{-1}. However, the alternative H loss from the tetrahedral carbon center in **i19** leading to 2-ethynyl-naphthalene is clearly more favorable, as it proceeds via a 24.9 kcal mol^{-1} barrier and is endothermic by only 14.8 kcal mol^{-1}. This area of the PES also illustrates that naphthalene can react with the ethynyl radical in a similar way as benzene, i.e., via the C_2H-for-H exchange mechanism. The C_2H addition to the 2-position in naphthalene is barrierless and exothermic by 43.2 kcal mol^{-1} (42.2 kcal mol^{-1} for benzene) and then H eliminations occurs from the attacked carbon atom via the barrier of 24.9 kcal mol^{-1} (24.4 kcal mol^{-1} in the case of benzene), with the overall C_2H + naphthalene → 2-ethynyl-naphthalene + H reaction being exothermic by 28.4 kcal mol^{-1} (the same as for benzene). Branching ratio calculations for the reaction scheme in Fig. 8 using our RRKM/kinetic equations approach show that **P3** + H should be the nearly exclusive product of the C_2H + **t-PVA** reaction under single-collision conditions when the ethynyl addition takes place to the *ortho* ring carbon.

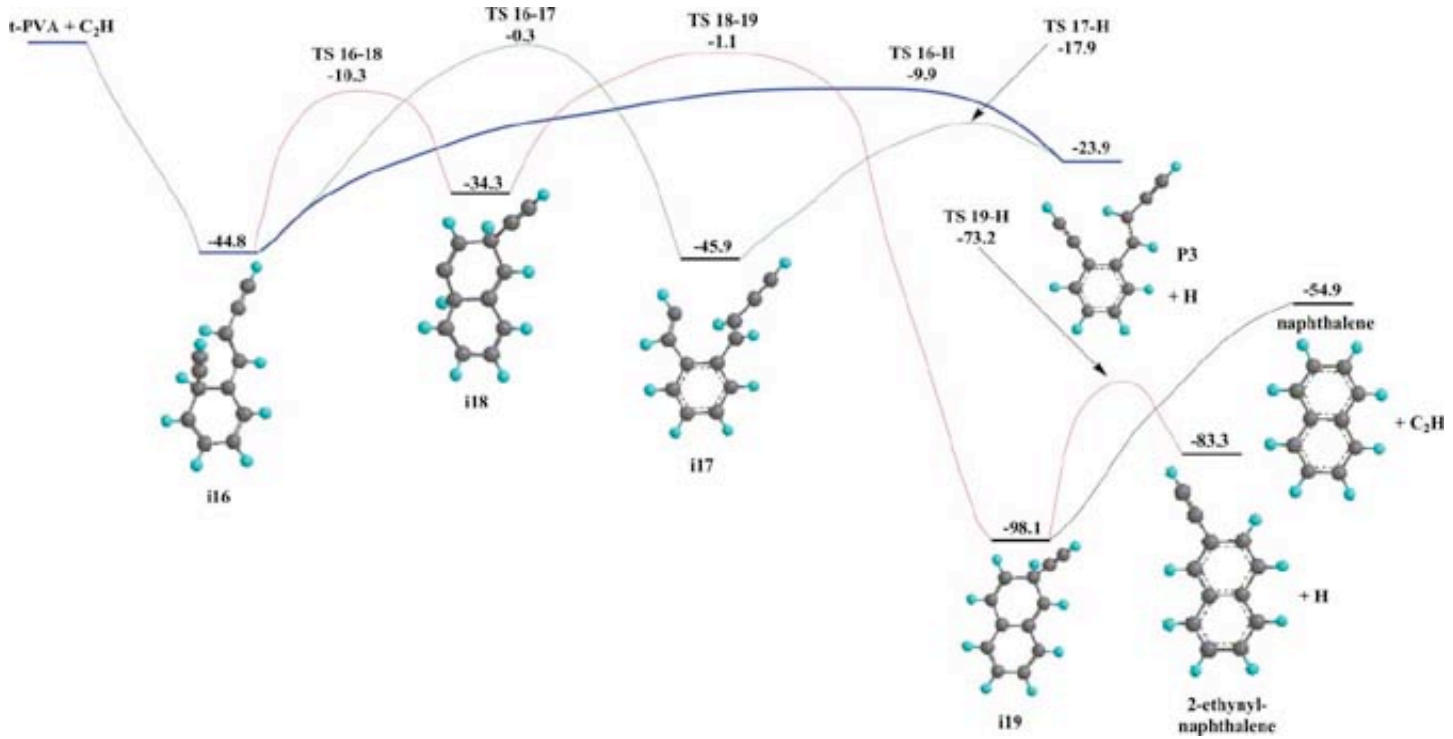

Fig. 8: PES illustrating the addition of C_2H to the ortho position of t-PVA computed at the G3(MP2,CC) level of theory.

Again, in this context, the most favorable mechanism is the one leading to hydrogen loss, leading to the formation of $C_6H_4(C_2H)(CHCHC_2H)$ + H. Barriers on the competitive pathways are still too high (nearly 9 kcal mol^{-1} too high). Clearly our thinking needs to change otherwise, it will take several more additions of C_2H before we see any evidence of PAH formation. The next thought was to attack the carbon on the existing C_2H side chain of **c-PVA** and **t-PVA**. By doing this, we are forcing the radical to be positioned on the terminal carbon of the side chain. This should bring ring cyclization barriers down, as radicals can't be as effectively stabilized when they are centered on the terminal carbon atom.

C_2H addition can also occur to the triple bond carbons of the side chain in **t-PVA**. In particular, the ethynyl attack toward the β-C atom produces the intermediate **i20** with exothermicity of 53.0 kcal mol^{-1} (Figure 9). The further fate of **i20** can be threefold. First, it can dissociate by losing a diacetylene fragment to produce C_6H_5CHCH **P4**. This C_4H_2 loss channel proceeds via a barrier of 47.4 kcal mol^{-1} and the products are exothermic by 21.4 kcal mol^{-1}. Second, two consequent rotations around CC bonds in **i20** featuring barriers of 45.0 and 18.3 kcal mol^{-1} lead to the structure **i22** via **i21**. **i22** lies 51.2 kcal mol^{-1} below the initial reactants. Ring closure in this intermediate is facile, as it occurs via a barrier of 10.8 kcal mol^{-1}, and leads to the bicyclic intermediate **i23**, with a relative energy of -77.6 kcal mol^{-1}. H loss can then occur with a 8.8 kcal mol^{-1} barrier to yield 2-ethynyl-napthalene. The third competing pathway from **i20** features a two-step C_2H migration to the terminal carbon. The barriers for the first and second steps in this process are 18.6 and 7.8 kcal mol^{-1}, respectively, and the C_2H shift leads to the formation of **i25**

via a bicyclic intermediate **i24**. **i25** can decompose by a loss of a hydrogen atom via a 46.6 kcal mol^{-1} barrier producing trans-1-hexene-3,5-diynyl-benzene (**THDB**). The **THDB** + H products reside 30.7 kcal mol^{-1} below the C_2H + **t-PVA** reactants. **i25** can also be formed directly from the reactants by addition of the ethynyl radical to the α-C atom of the side chain. After that, this initial adduct can either dissociate to **THDB** + H or isomerize to **i20** via the C_2H migration described above.

Figure 10 illustrates various pathways of the C_2H + **c-PVA** reaction. For instance, ethynyl radical addition to the β-carbon in **c-PVA**'s side chain can directly lead to **i22**, thus avoiding the difficult steps involving the double bond rotations, which are required for its formation from the initial adduct **i20** in the C_2H + **t-PVA** reaction. As we already know, ring closure in **i22** gives **i23**, which can easily split a hydrogen to form 2-ethynyl-naphthalene. Alternatives to the cyclization process in **i22** include C_4H_2 elimination to produce **P4** and a two-step C_2H shift to form **i27**, analogous to the **i20→i24→i25** pathway. The intermediate **i27** also serves as the initial adduct in the C_2H + **c-PVA** reaction when the ethynyl radical attacks the α-C atom in **c-PVA**. For such α-addition, competing reaction scenarios include direct H loss from **i27** to form a *cis* conformation of HDB (**CHDB**) and isomerization to **i22** followed by either cyclization and H loss yielding 2-ethynyl-naphthalene or C_4H_2 elimination producing **P4**. In our RRKM calculations we therefore considered four different possibilities including α- and β-additions of C_2H to **t-PVA** and **c-PVA**. Based on the branching ratios, one can see that 2-ethynyl-naphthalene can only be formed starting from the cis isomer of **PVA**. The reaction with **t-PVA** appears to be incapable of forming the naphthalene core, because the cyclization process is hindered by the high barrier for the preceding trans-cis isomerization step **i20→i21** involving rotation around a double C=C bond. On the other hand, the initial adduct **i22** in the reaction with **c-PVA** is already in position to cyclize and therefore the double bond rotation can be avoided.

The thought of adding the second C_2H component to the bare carbon on the C_2H side chain proved to work well. Under these circumstances, the barrier to ring closure is only

about 10 kcal mol^{-1}. Comparison with our previous attempts to ring close directly from the initial adduct show that those barriers are on average 33.8 kcal mol^{-1}. However, the addition to **t-PVA** still does not yield PAHs, because of the high barrier involved in the double bond rotation needed to go to the cis conformation. Indeed the attack of the cis conformation by C_2H yields exclusively **2-ethynylnaphthalene + H**.

Now we consider C_2H additions to the ethynyl side chain in c-o-ethynylstyrene. The addition to the α-position occurs through a barrierless entrance channel producing **i28**, with an exothermicity of 65.0 kcal mol^{-1} (Figure 10). A direct H loss from **i28** occurs via a 40.1 kcal mol^{-1} barrier and leads to the formation of 1-buta-1,3-diynyl-2-vinyl-benzene (**BDVB**). **BDVB** lies 30.7 kcal mol^{-1} below the initial reactants. Alternatively, **i28** can isomerize to the most stable **i31** isomer, 107.8 kcal mol^{-1} below the reactants, via two different two-step pathways. Both of them involve ring closure and 1,2-hydrogen migration but these steps occur in different orders. In the first pathway,**i28 →i29 →i31**,the H shift takes place first and is followed by the cyclization, whereas in the second, **i28 →i30 →i31**, the sequence is reversed. In both channels, the highest barrier corresponds to the H migration steps and the respective transition states TS 28-29 and TS 30-31 are located 47.3 and 48.4 kcal mol^{-1} higher in energy than **i28**. **I31** can split a hydrogen atom from the CH_2 group to produce 2-ethynyl-naphthalene via a barrier of 28.8 kcal mol^{-1}. Alternatively, **i31** can be subjected to H migration from CH_2 over a potential barrier of 39.5 kcal mol^{-1} to form **i32** with a C(H)(C_2H) group. **i32** is an enantiomer of **i19** (Fig. 8) and it can either barrierlessly lose the C_2H group to form naphthalene with endothermicity of 44.4 kcal mol^{-1}, or expel the hydrogen atom from the

sp^3 carbon overcoming a lower barrier of 22.1 kcal mol^{-1} to produce 2-ethynyl-napthalene. To complete the description of all possible reaction channels shown in Fig. 6, we should mention decomposition pathways of **i29**, including H loss producing BDVB and C_4H_2 elimination giving rise to the $C_6H_4C_2H_3$**P5** radical. However, both of these dissociation channels feature relatively high barriers of 42.1 and 48.4 kcal mol^{-1}, respectively, and hence they are not expected to compete with **i29→i31** cyclization pathway occurring via a low 2.7 kcal mol^{-1} barrier.

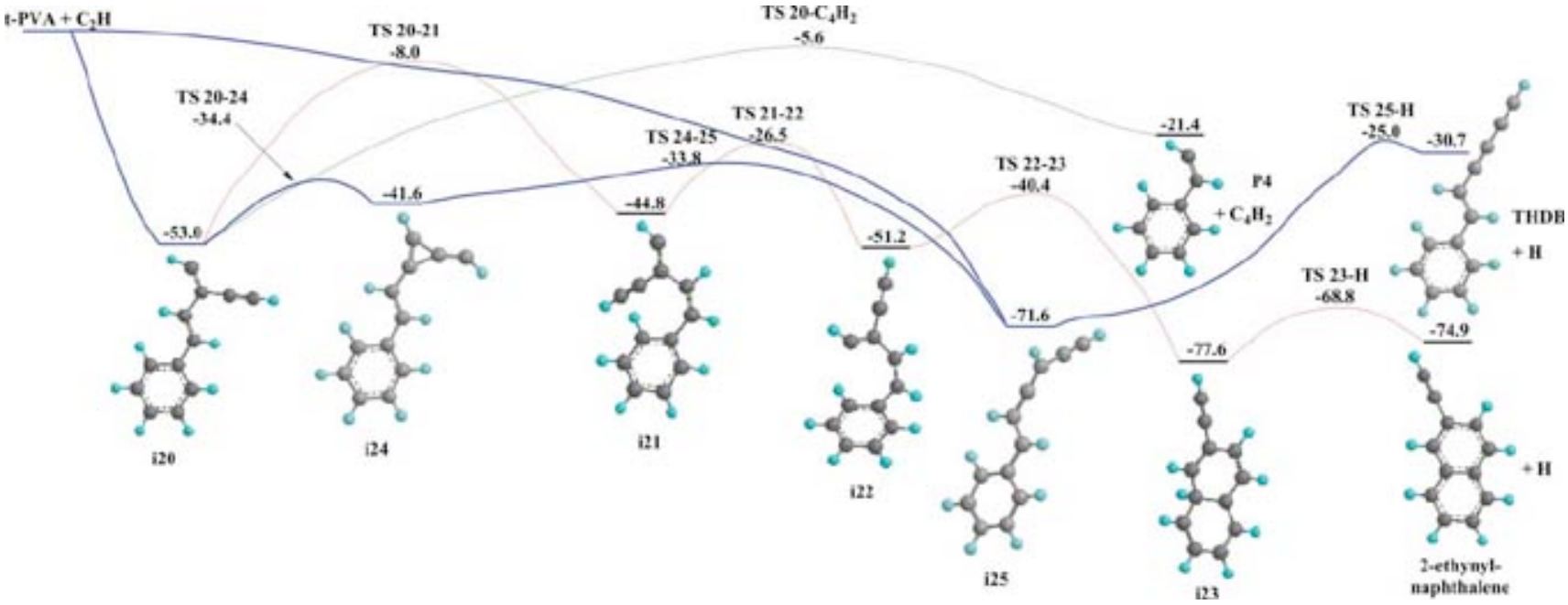

Fig. 9: PES illustrating the addition of C_2H to the bear carbon of t-PVA computed at the G3(MP2,CC) level of theory.

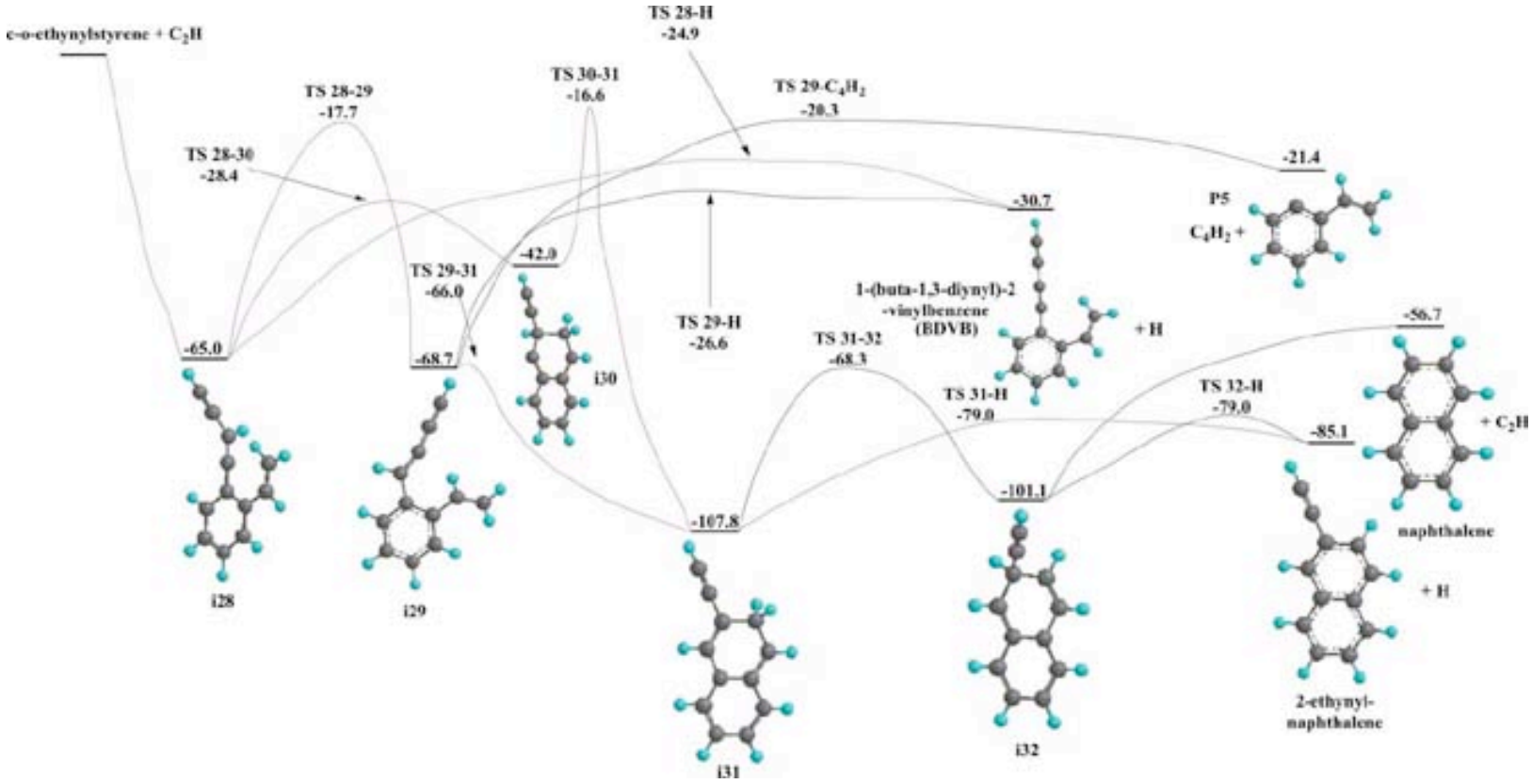

Fig. 10: PES illustrating the addition of C_2H to o-ethynylstyrene computed at the G3(MP2,CC) level of theory.

Finally, C_2H can attack the β-position of the ethynyl side chain in c-o-ethynylstyreneproducing adduct **i33** (see Figure 11) with an energy gain of 54.8 kcal mol^{-1}. Once **i33** is produced, it can easily cyclize via a low 2.1 kcal mol^{-1} barrier forming **i34**. Next, a hydrogen loss from the latter gives 1-ethynyl-naphthaleneas the final product overcoming a barrier of 27.6 kcal mol^{-1}. Alternatively, **i33** may lose diacetylene to form **P5** with an activation energy of 38.2 kcal mol^{-1}. The **i33** adduct can be also accessed from **i28**, which is the initial complex corresponding to the α-addition of C_2H to c-o-ethynylstyrene. **i28** can isomerise to **i33** via a two-step C_2H migration process, occurring via a bicyclic intermediate **i35** and featuring barriers of 29.7 and 7.9 kcal mol^{-1} for the first and second steps, respectively. The **i28 →i35→i33** channel should be competitive to the other isomerization and dissociation pathways of **i28** illustrated in Fig. 10 and, conversely, the **i33 →i35→i28** path followed by further changes of **i28** may in principle compete with the ring closure in **i32**. Therefore, in our kinetic calculations of product branching ratios we treated the two reaction schemes shown in Figs. 10 and 11 together, but took **i28** and **i33** as two different possible initial adducts. The results of RRKM calculations of individual rate constants followed by solving kinetic equations show that indeed the overwhelmingly major product is **1-ethynyl-naphthalene**. Moreover, the branching ratios are fairly insensitive to which of the two entrance channels is pursued.

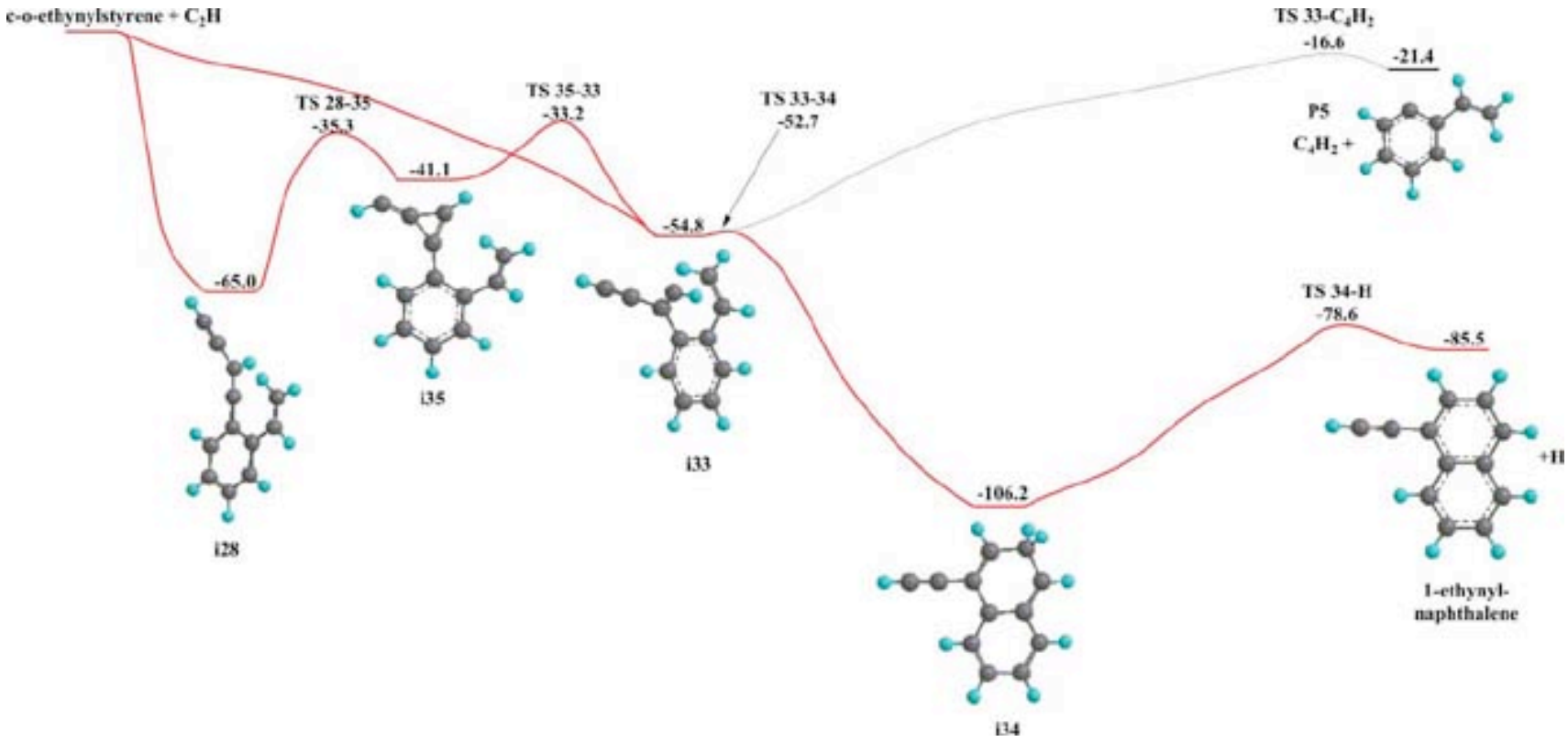

Fig. 11: PES illustrating the addition of C_2H to the β position of the side chain of o-ethynylstyrene computed at the G3(MP2,CC) level of theory.

From this experience, we learned a fair amount about how PAHs might form under the conditions found on Titan. For one thing, if you can place a radical onto a terminal carbon, it will increase the cyclization event. Also, judicious choice of starting reagents is very important. In figures 4-7, the initial adduct could not stabilize itself through loss of a hydrogen. That is to say, loss of a hydrogen did not produce a conjugated system where by electrons could diffuse along the entire length of the molecule. Instead, loss of hydrogen atoms only produced localized radical species, which are unable to stabilize themselves. This, along with the muted cyclization barriers allowed for the effective production of PAHs.

Chapter 5: Nitrogen Insertions into Aromatic Rings: The Role of Pressure Stabilization, Radiative Stabilization and the Destabilizing effect of Nitrogen Insertions

Can nitrogen atoms be inserted into polycyclic aromatics? Given that the atmosphere of Titan is composed of ≈ 95 % nitrogen, this possibility should be considered. Moreover, it can help explain the brownish/orange haze layers that are found there. The studies of tholins, laboratory analogues of Titan's haze, support the hypothesis that neutral PAHs and their cations as well as N-PACs may constitute the fundamental building blocks of aerosol particles in Titan's hazes.[23] N-PACs and PAHs have been detected in tholins by Khare et al.[21] and Sagan et al.[20] More recently, Khare and co-workers measured time-dependent infrared spectra of a simulated Titan's tholin synthesized in their laboratory and found that one of the earliest spectral features to emerge was a very strong absorption band at ~1351 cm^{-1} ascribed to skeletal ring vibrations[17] between members of C and N rings, perhaps arranged in relatively dehydrogenated, positively charged heterocyclic ring structures reminiscent of graphitic structures.[1]

To achieve the formation of a pyridine ring fused with the benzene ring present in 2-ethynylbenzonitrile, C_2H addition may proceed to either the CCH or CN side chains. The PES diagram for the reaction channels involving the additions of ethynyl radical to the CCH group is illustrated in Fig.12. One can see that the reaction of 2-ethynylbenzonitrile with C_2H features two barrierless entrance channels leading to the formation of **i1**, with a relative energy of -48.7 kcal mol^{-1} with respect to the initial reactants (the addition to the β-C atom of CCH), or **i4** residing 64.3 kcal mol^{-1} below the reactants (α-C addition). The

intermediate **i1** can isomerize to **i4** via a two-step C_2H migration to the adjacent carbon center α-C. The first step on this pathway exhibits an energy barrier of 13.7 kcal mol^{-1} relative to **i1** and leads to a transient bicyclic species **i3**, which can then further rearrange to **i4** through a relatively low ≈ 7 kcal mol^{-1} barrier. Alternatively, **i1** may undergo cyclization occurring with a modest 11.7 kcal mol^{-1} energy barrier producing **i2**, 2-aza-4-ethynyl-1-naphthyl radical, which lies 74.1 kcal mol^{-1}lower in energy than the $C_6H_4(CN)(C_2H) + C_2H$ reactants. Another possible pathway from **i1** involves elimination of diacetylene(C_4H_2) leading to the formation of cyano-substituted phenyl radical, 19.5 kcal mol^{-1} below the reactants. However, the barrier for the C_4H_2 loss is relatively high, 32.4 kcal mol^{-1} with respect to **i1**, and hence this reaction channel is not expected to be competitive with either i1→i3→i4 C_2H migration or the ring closure to form an N-PAC radical **i2**. Besides isomerizing to **i1**, intermediate **i4** can be subjected to an H loss from the side chain leading to the formation of 2-buta-1,3-diynyl-benzonitrile. The H-loss occurs via a relatively high barrier of 40.6 kcal mol^{-1} and the $C_6H_4(CN)(C_4H)$ + H products are 29.9 kcal mol^{-1} exothermic as compared with the $C_6H_4(CN)(C_2H) + C_2H$ reactants. Elimination of the hydrogen atom from the pyridine ring of 2-aza-4-ethynyl-1-naphthyl **i2** producing 2-aza-4-ethynyl-1,3-didehydronaphtthalene is highly unfavorable, as the computed strength of breaking the CH bond is 110.1 kcal mol^{-1} and the product resides 35.5 kcal mol^{-1} above the initial reactants. Elimination of hydrogen atoms from the benzene ring in **i2** is also expected to be highly endothermic as this would lead to a diradical product. A loss of the external C_2H group would result in the formation of a nitro-generated p-benzyne ring, in contrast to a nitrogenated m-benzyne ring present in the 2-aza-4-ethynyl-1,3-didehydronaphthalene product of H elimination. Since p-

benzyne is known to be less stable than m-benzyne, we do not consider the C_2H loss channel.

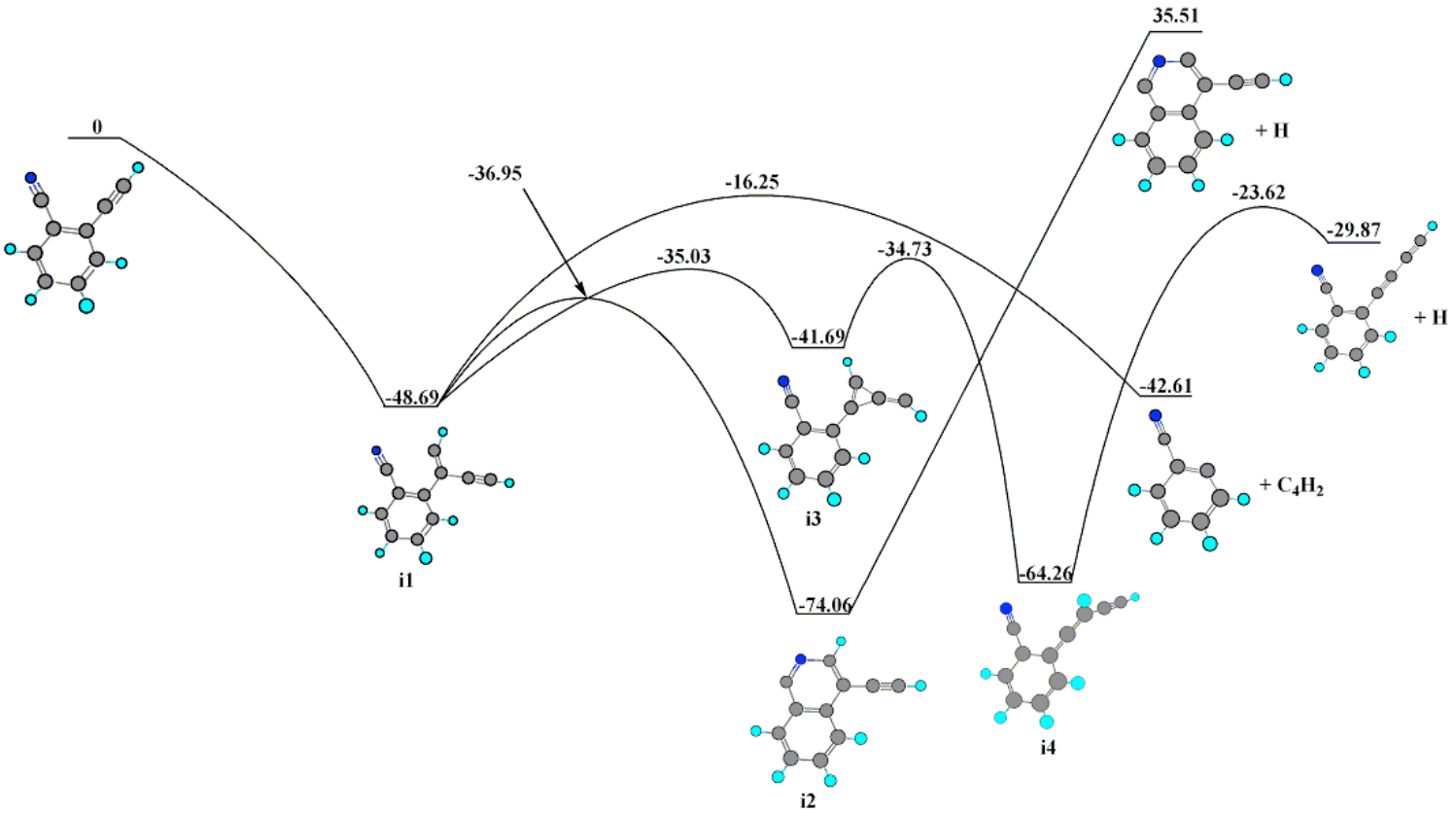

Fig. 12: PES illustrating the addition of C_2H to the β Carbon position of 1-ethynylbenzonitrile computed at the G3(MP2,CC) level of theory.

To analyze this PES, one should first note that the transition from **i1** to **i2** is the preferred pathway. However, as stated before, loss of hydrogen from **i2** to form **2-aza-4-ethynyl-1,3-didehydronaphthalene + H** is to endothermic, and will not occur. This means that under conditions of zero collision (no collisional stabilization), all of the reaction flux moving from **i1** to **i2** will revert back to **i1**, at which point it will move through the C_2H migration pathway leading to **i4**, and ultimately the formation of the **$C_6H_4(CN)(C_4H)$ + H** molecule. Our branching ratios confirm this, and **$C_6H_4(CN)(C_4H)$** turns out to be the nearly exclusive product.

Can pressure stabilize **i2** ? Being that pressures in the PAH forming region of Titan (120 to 300 km above the surface) are between 3 and 0.1 millibars, it seems unlikely. According to work by Woon, studying the collisional stabilization of benzene + C_2H/CN using RRKM-ME (Master Equation), some stabilization of the initial adduct was found [56]. To answer this question (definitively), sophisticated RRKM-ME calculations need to be carried out at the different pressures and temperatures present in the PAH forming region. This however, is outside the scope of our work.

As seen in Fig. 8, an alternative entrance channel for the C_2H + 2-ethynylbenzonitrile reaction is the addition of ethynyl radical to the CN group. This leads to the formation of intermediate **i5**, with a relative energy of -35.2 kcal mol^{-1} with respect to the initial reactants. By overcoming a modest ≈ 10 kcal mol^{-1} energy barrier, **i5** can cyclize to produce a polycylic intermediate **i6**, 2-aza-1-ethynyl-4-naphthyl radical, which lies 64.4 kcal mol^{-1} below the reactants. Elimination of a hydrogen atom from **i6** would lead to the production of 1-ethynyl-3,4-isoquinolinediyl, but this channel is highly unfavorable,

because the product resides 43.5 kcal mol^{-1} above C_2H + 2-ethynylbenzonitrile. Besides the isomerization to **i6**, the adduct **i5** can decompose to ethynylphenyl + HCCCN by elimination of the cynanoacetylene fragment. This process is calculated to have a barrier of 32.7 kcal mol^{-1} relative to **i5**, with the transition state and products lying 2.5 and 7.5 kcal mol^{-1} lower in energy than the initial reactants, respectively. At zero collision, the clear product is $C_6H_4(C_2H)$ + HCCN. Again, if the reaction flux experiences collisions with the bath gas, the possibility of collisional stabilization of 2-aza-1-ethynyl-4-naphthyl radical.

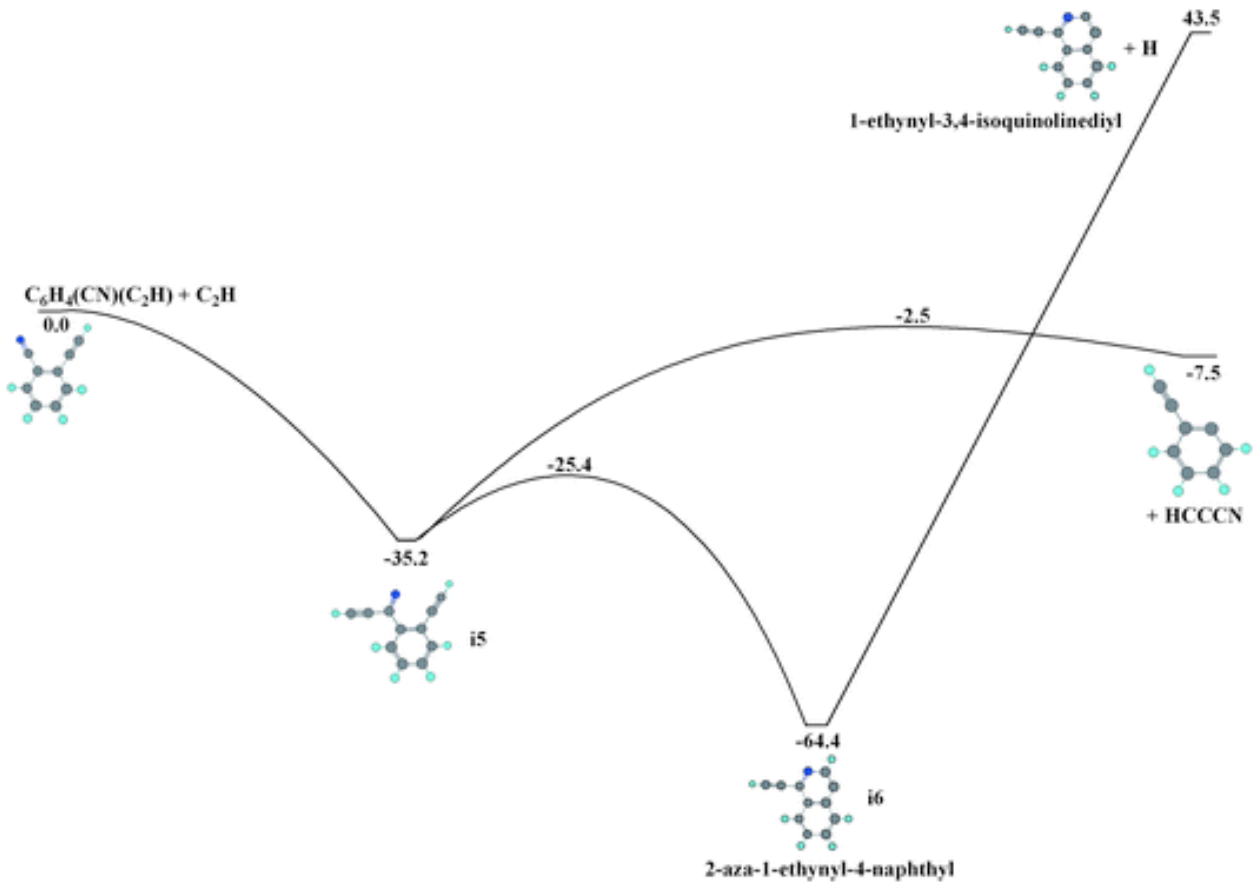

Fig. 13: PES illustrating the addition of C_2H to the CN carbon of 1-ethynylbenzonitrile computed at the G3(MP2,CC) level of theory.

As seen in Fig. 14, an attack of phthalonitrile by C_2H to the C atom of one of the CN groups can produce, via a barrierless entrance channel, intermediate **i7**, residing 37.4 kcal mol^{-1} below the reactants. Next, **i7** may ring-close by overcoming a 29 kcal mol^{-1} barrier and produce a bicyclic structure **i8**, 2,3-diaza-4-ethynyl-1-naphthyl radical. This radical lies only 18.8 kcal mol^{-1} lower in energy than the C_2H +$C_6H_4(CN)_2$ reactants, which is a much shallower well on the PES as compared to those for 2-aza-4-ethynyl-1-naphthyl and 2-aza-1-ethynyl-4-naphthyl, -74.1 and -64.4 kcal mol^{-1} relative to C_2H + $C_6H_4(CN)C_2H$ respectively, and especially that for 4-ethynyl-1-naphthyl, -113.6 kcal mol^{-1} with respect to C_2H + $C_6H_4(C_2H)_2$. As an alternative to **i7**→**i8** cyclization process, a loss of cyanoacetylene from **i7** may produce cyanophenyl radical via a 33 kcal mol^{-1}barrier. Otherwise, **i7** may pursue a C_2H migration route leading to **i9**, but this process proceeds via a 38.8 kcal mol^{-1} activationbarrier with the transition state positioned 1.4 kcal mol^{-1} above the C_2H + phthalonitrile reactants, and hence, this channel is unlikely at low-temperature conditions. The intermediate **i9**, which lies 23.9 kcal mol^{-1} below the reactants, can be formed directly from them by barrierless C_2H addition to one of the nitrogen atoms in phthalonitrile. **i9** represents a dead end on the PES because its isomerization to **i7** requires a higher barrier than the energy needed for the reverse **i9** →C_2H + $C_6H_4(CN)_2$ reaction and the alternative dissociation to cyanophenyl + isocyanoacetylene (28 kcal mol^{-1} less stable than cyanoacetylene) is also unfavorableas it is computed to be endothermic by 36.6 kcal mol^{-1}. Alternatively, the C_2H addition to the C atom of the external cyano group in **i7** may lead to the formation of intermediate **i10** without an entrance barrier and with the energy gain of 34.6 kcal mol^{-1}. From the energized adduct **i10**, the reaction can proceed by cyclization, by elimination of one of

the two external cyanoacetylene groups, or by migration of the added C_2H fragment from C to N of the cyano group. The cyclization occurs through a rather low activation barrier of 2.8 kcal mol^{-1} and leads to intermediate **i11**, a symmetric N-PAC 1,4-diethynylphthalazine (**1,4-DPZ**) molecule. **1,4-DPZ** is 103.3 kcal mol^{-1} more stable than **i7** + C_2H. In the competing pathways, **i10** may lose cyanoacetylene via a 30.9 kcal mol^{-1} activation barrier or migrate the C_2H group from C to N via a higher barrier of 47 kcal mol^{-1} to produce intermediate **i12**. A comparison of the barrier for the considered transformations of the energized adduct **i10**, **i10→i11**, **i10→C_6H_4(HCCN) + HCCN**, and **i10→i12**, clearly shows that the cyclization pathway to **1,4-DPZ**, **i11** should dominate. An alternative C_2H addition to the N atom of the CN group in **i7** may lead, without a barrier, to the other initial adduct **i12** with exothermicity of 22.3 kcal mol^{-1}. Next, **i12** can ring close to a bicyclic structure **i13** via a barrier of 25.4 kcal mol^{-1}, undergo a C to N C_2H shift to form **i14**, **C_6H_4(CNCCH)$_2$**, with a barrier of 30.2 kcal mol^{-1}, lose cyanoacetylene producing C_6H_4(CNCCH) **i15** through a 34.2 kcal mol^{-1} barrier, or isomerize back to **i10** overcoming a barrier of 34.6 kcal mol^{-1}. The bicyclic intermediate **i13**, which is ≈ 7 kcal mol^{-1} less stable than **i12**, can in turn be subjected to C_2H migration from N to C in the nitrogen containing ring to produce the N-PAC **1,4-DPZ** structure **i11** after overcoming a 27.6 kcal mol^{-1} barrier.

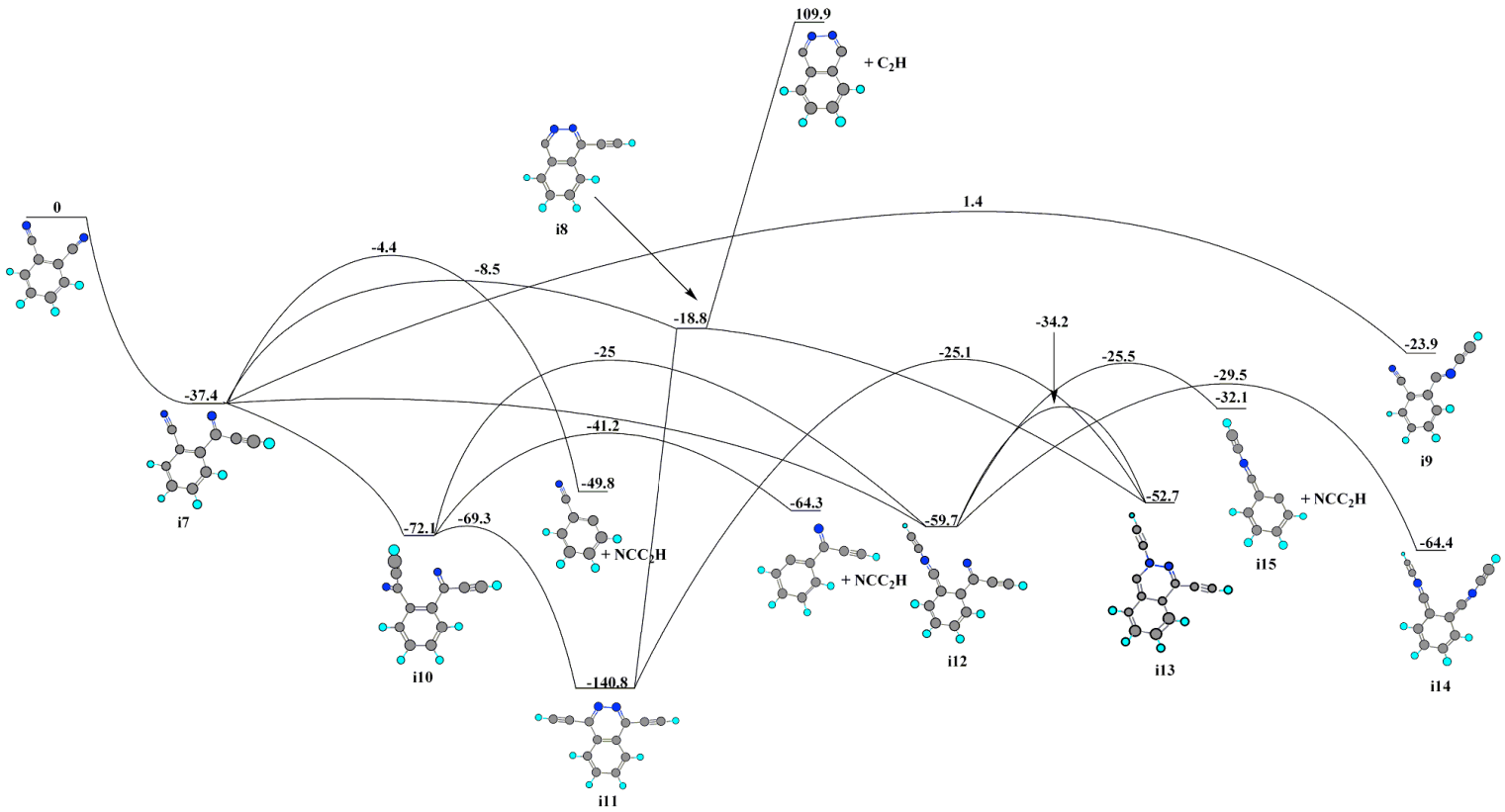

Fig. 14: PES illustrating the addition of C_2H to phthalonitrile computed at the G3(MP2,CC) level of theory.

Okay, so the PES here is somewhat complicated. In actuality, it is two PES in one. The first, is the very first C_2H addition to $C_6H_4(CN)_2$, and the second is the subsequent reaction (again with C_2H). Let's take the first PES first. If only one C_2H addition is allowed, then the only product that can be formed (under zero collision conditions) is $C_6H_4(CN)$ + HCCCN. **i8** represents a dead end molecule, in the sense that it can only lose C_2H, but that product is ridiculously high in energy. If this is the only addition that occurs, then this is the only possible product that can form. However, if **i7** is struck by another C_2H molecule, then this opens up the possibility for several other options. Note that for this to happen, we would need to access the collisional stabilization of **i7**. However, it is worth noting that since the only exothermic process available has a relative barrier close to the energetic limit, the rate constant for this unimolecular step will be very small, therefore, the rate constant for the collisional stabilization of **i7** will have an increased chance of being larger than the decomposition step. In other words, collisional stabilization is not out of the question. At collisionless conditions, the attack of a second C_2H will yield $C_6H_4(NCCCH)$ + cyanoacetylene (if the attack occurs on the carbon side of CN), or $C_6H_4(CNCCH)$ + cyanoacetylene (if the attack occurs on the nitrogen side of CN). At the Faraday meeting, where this work was discussed, one of the attendees suggested we determine if any of the intermediates could be radiatively stabilized [57]. **i11** was found to be radiatively stabilized, having a k_{rad} equal to 92.2 s^{-1}, much greater than the corresponding rate constant going from **i11** to **i10**. This proves that the synthesis of **1,4-DPZ** is possible (assuming a second C_2H attack on **i7**).

Another possible N-PAC precursor is 2-methyleneaminobenzonitrile **i18** (see Fig.15). It can react with C_2H forming the initial adduct **i19** without a barrier and with the energy gain of 44.2 kcal mol^{-1}. The energized **i19** adduct can undergo ring closure to the bicyclic structure **i20** via a relatively low barrier of 14.6 kcal mol^{-1}. This reaction step is exothermic by 14.2 kcal mol^{-1} and the resulting **i20** intermediate lies 58.4 kcal mol^{-1}lower in energy than the **i18** + **C_2H** reactants. The CH bond in the CH_2 group of **i20** is weak and it only takes 18.8 kcal mol^{-1} to break it and to produce the polycyclic aromatic **4-ethynylquinazoline** product. Overall, the 2-methyleneaminobenzonitrile + C_2H → 4-ethynylquinoline + H reaction is calculated to be 39.6 kcal mol^{-1} exothermic. The only feasible competitive channel is elimination of cyanoacetylene from the initial adduct **i19** leading to the formation of the 2-methyleneaminophenyl radical. However, the barrier for HCCCN loss from **i19** is 42.1 kcal mol^{-1}, 27.5 kcal mol^{-1} higher than that for the ring closure. Also the HCCCN elimination transition state resides 37.5 kcal mol^{-1} in energy than the 4-ethynylquinazoline + H products.

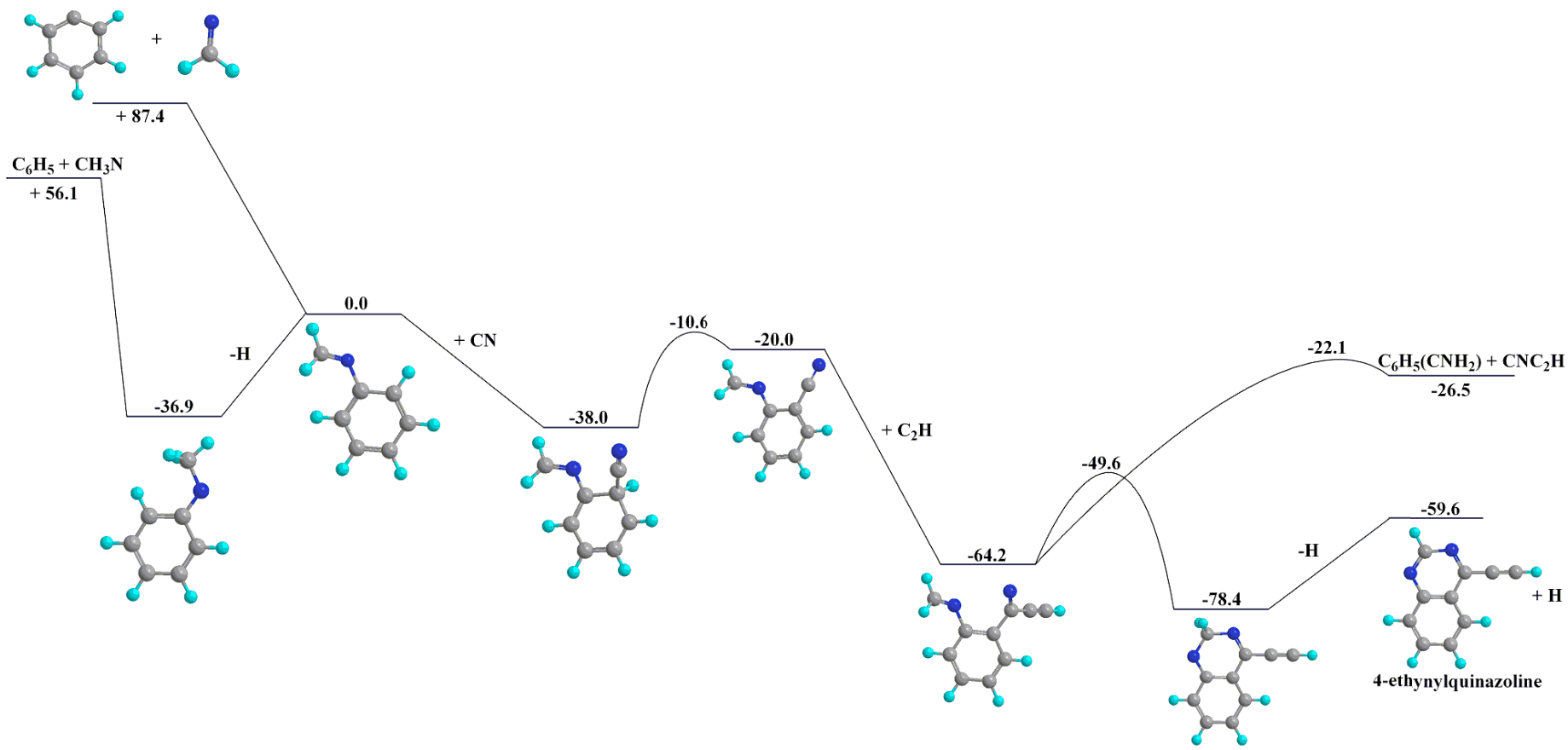

Fig. 15: PES illustrating the various pathways which can lead to 4-ethynyl-quinoline computed at the G3(MP2,CC) level of theory.

It is clear that if the reaction proceeds as outlined in Fig. 15, 4-ethynyl-quinazoline will be formed as the exclusive product. We should also examine the synthesis of **i16**. There are two pathways with barriers, one is the addition of CH_2N (methylene-amidogen) to benzene, and the other is the addition of CH_2NH (methyleneimine) to phenyl radical. These will not contribute to the synthesis of **i16** in the cold temperature environment of Titan. A third process is the addition of the methylene-amidogen to phenyl radical. This process is barrierless, and will produce **i16** as its initial adduct. A fourth possibility is the reaction of CH_3N with phenyl radical. This process is also barrierless and will also produce **i16**. Vuitton et al. have inferred the existence of methyleneimine in the atmosphere of Titan, by the detection of the CH_2NH_2+ charged species. Additionally, they measured the mole fraction to be 10 ppm (with a rather large uncertainty). In crossed molecular beams experiments, CH_2NH was formed through the reaction of $N(^2D)$ + CH_4. If methyleneimine is formed in Titan's atmosphere, then methylene-amidogen can be formed through photodissociation processes.

Chapter 6: The addition of CN to styrene: A plausible route to N-PACs

After some thought, we decided that our next step should be to attempt to study the reaction mechanism of styrene with nitrogen analogs of C_2H, namely CN. If this mechanism is feasible, it will have the potential to produce N-PACs without the requirement of collisional stabilization, an overall improvement of the mechanism described in Chapter 5.

The cyano radical can attack various sites in styrene, including unsaturated carbon atoms in this molecule, two C atoms forming the vinyl group in the side chain and six C atoms in the aromatic ring. Considering that the additions to each of these sites are barrierless and fast, a simplest assumption one can made is that they are equally likely and each of them have a probability of 12.5% to occur. Here, we focus our study only on those CN additions, which may eventually, after a consecutive C_2H addition to a primary product of the CN + styrene reaction, lead to the production of substituted azanaphthalenes. Let us first consider the CN attack toward the terminal CH_2 group in styrene. In this case, the CN addition can yield two conformers **i1** and **i2** with exothermicities of 60.7 and 60.0 kcal mol^{-1}, respectively (Figure 16).

Both entrance channels are found to be barrierless and so they may occur rapidly even at low temperatures. This conclusion is supported by experimentally measured constants for CN addition to carbon double bond sites in different molecules, although the kinetics of the CN + styrene has not yet been studied. For example, most recently, Morales et. al. used the CRESU (Reaction kinetics in Uniform Supersonic flow) technique to determine rate constants for CN addition to the double bond in 1,3-butadiene and obtained the

values of 4.33±0.50 and 4.66±0.64 × 10^{-10} cm^3 $molecule^{-1}$ s^{-1} at 83 and 120 K, respectively. These results indicate that the reaction is fast and occurs without an entrance barrier.[58]Both **i1** and **i2** can eject a hydrogen atom from the attacked carbon atom forming *trans*- and *cis*-cinnamonitriles, respectively. The barriers for the H elimination pathways are 40.6 and 41.1 kcal mol^{-1} relative to **i1** and **i2** and the corresponding transition states reside 20.1 and 18.9 kcal mol^{-1} below the initial reactants, respectively. **i1** and **i2** can easily rearrange to each other by rotation around the CH-CH_2 bond via a low barrier of less than 1 kcal mol^{-1}. Other possible isomerization pathways of **i1** and **i2** might lead to the formation of 1- and 2-azanaphthalenes, but they appeared to be not competitive with the direct H losses.

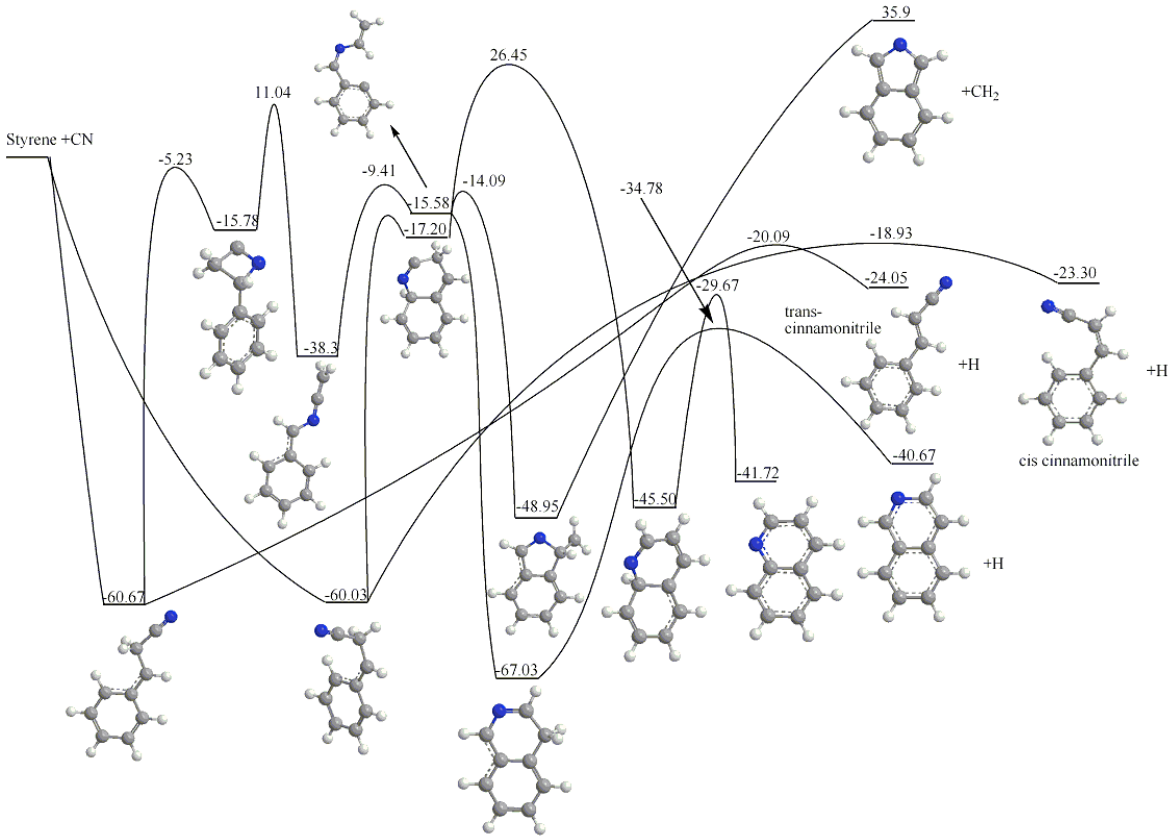

Fig. 16: PES illustrating the addition of CN to the CH_2 position of styrene computed at the G3(MP2,CC) level of theory.

Aside from the addition of CN to the vinyl side chain, CN can also attack the *ortho* carbon position in the phenyl ring. This addition occurs without a barrier and is 43.1 kcal mol^{-1} exothermic (see Figure 12). Again, the finding that the CN addition to the aromatic ring in styrene is barrierless is in line with the previous experimental and theoretical studies of the reaction of cyano radicals with benzene[54,59,53] and toluene.[59] Once the adduct **i10** forms, it may lose the H atom from the attacked *ortho* carbon yielding 2-vinylbenzonitrile. A barrier of 29.2 kcal mol^{-1} must be surmounted in order for the hydrogen loss to proceed. The process alternative to the H loss is a six-member ring formation leading to **i11**, which requires a barrier of 38.5 kcal mol^{-1}. Once the ring is formed, 1,2-H migration may occur from a carbon atom common for the two rings to its neighbor in the N-containing ring forming **i12**. However, this process is unlikely to be competitive under low temperature conditions because the associated transition state resides 23.1 kcal mol^{-1} above the reactants. Theoretically, if **i12** is formed, it can undergo an H loss from the CH_2 carbon producing 2-azanaphthalene.

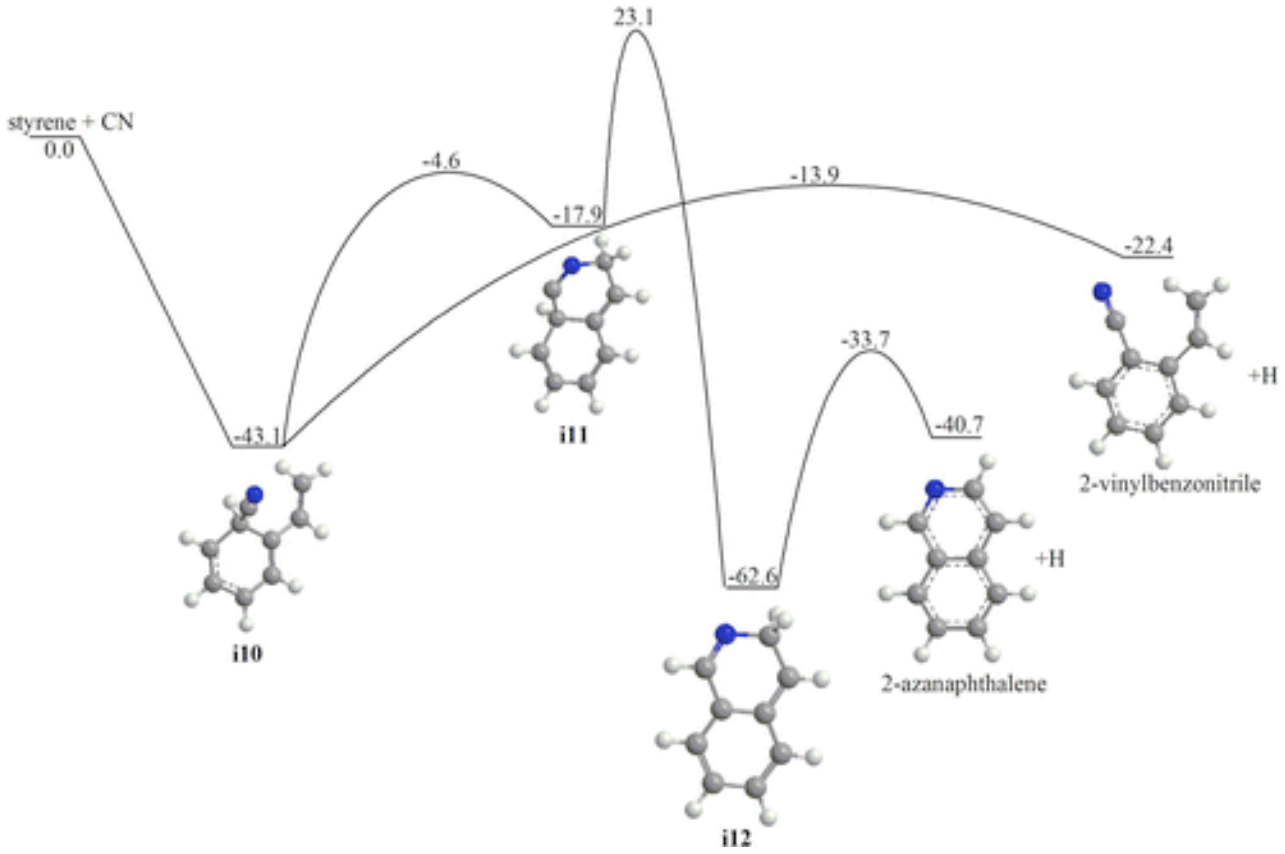

Fig. 17: PES illustrating the addition of CN to the ortho position of styrene computed at the G3(MP2,CC) level of theory.

With PESs in hand, energy-dependent rate constants were calculated for individual reaction steps starting from the initial adducts using RRKM theory under collision-free conditions, in the collision energy range of 0 to 5 kcal mol^{-1}.

The branching ratio of *trans*- versus *cis*-cinnamonitrileis is found to be ~3:1 in favor of the *trans* isomer. This value is insensitive to the collision energy regardless whether **i1** or **i2** is formed as the initial adduct because the two can rearrange to one another much faster than dissociate via the H loss. The branching ratios of *trans*- and *cis*-cinnamonitriles are controlled by the relative energies of the H elimination transition states leading to the formation of the *trans* and *cis* isomer; the former resides 1.2 kcal mol^{-1} lower than the latter. The results also show that 2-vinylbenzonitrile is an exclusive product of CN addition to the *ortho* carbon of styrene under single-collision conditions.

Can the primary products of the CN + styrene reaction potentially lead to the formation of azanaphthalene through some other processes? Recently, Sebree et al. used ultraviolet photoexcitation to probe the isomerization channels of benzylallene.[60] Their results supplemented with DFT calculations revealed isomerization pathways from benzylallene which yield naphthalene. In particular, one of the mechanisms identified in their work involved photoisomerization of benzylallene to 1-phenyl-1,3-butadiene and then to 1,2-dihydronaphthalene, which loses two hydrogen atoms to ultimately produce naphthalene. Alternatively, naphthalene was also formed by H loss from benzylallene leading to benzylallenylradical, which then undergoes a ring closure and a second H elimination. E- and Z-phenylvinylacetylenes (PVAs), which are isoelectronic analogs of *trans*- and *cis*-cinnamonitriles predicted to be formed in the CN + styrene reaction, were also produced.

Though no similar experiments have been yet performed on the nitrogen-containing analogs like cinnamonitriles, it seems plausible that their isomerization (or that of 2-vinylbenzonitrile) promoted by ultraviolet photoexcitation and/or by encounters with radicals may lead to azanaphthalene production.

It may be possible that the initial adducts of the CN + styrene reaction, **i1**, **i2**, or **i10**, could be collisionally stabilized. While the pressure on the surface of Titan is about 1.4 bar, the PAH forming region of the atmosphere has been determined to exist between the altitudes of 140 to 300 km above the surface.[61] The pressures at these altitudes range from 3 to 0.1 millibar[62] with T being approximately 160-180 K and the average time between collisions is in the 20-600 ns range at these conditions. According to the calculated rate constants, the lifetimes of **i1**/**i2** and **i10** are 52 and 7 μs, respectively, at zero collision energy and decrease with E_{col}, meaning that collisional stabilization may play a significant role. To verify this, we carried out more sophisticated RRKM-ME simulations at pertinent temperatures (90-200 K) and pressures (3-10^{-6} mbar). The results are illustrated in Figure 3. It appears that at 160-180 K and 3 mbar **i1** and **i2** are almost completely collisionallystabilized (98-99%) and do not fragment. However, the relative yield of the stabilized intermediates decreases to ~80% and 24-29% at 0.1 and 0.01 mbar, respectively. The collisional stabilization is more significant at lower temperatures at the same pressure. For **i10** which has a lower dissociation barrier (~30 kcal/mol vs. ~40 kcal/mol for **i1**/**i2**), the collisional stabilization in the same temperature interval is less significant and decreases from about 90% at 3 mbar to ~80% at 1 mbar, 25-30%at 0.1mbar, and ~1% at 0.01 mbar. At 10^{-3} mbar and lower pressures, the collisional

stabilization of **i1**/**i2** and **i10** becomes negligible. These results show that at higher altitudes, where the pressure is in the range of 0.1 mbar, the fragmentation products of **i1**/**i2** (*trans*- and *cis*-cinnamonitriles) and **i10** (2-vinylbenzonitrile) will constitute ~20% and 70-75% of the total product yield for the CN addition to the CH_2 group and *ortho*carbon in styrene, respectively. Taking into account the assumed equal probabilities of CN additions to each unsaturated carbon atom in styrene and the computed branching ratios, we estimate relative yields of *trans*- and *cis*-cinnamonitriles and 2-vinylbenzonitrile in the CN + styrene reaction at 0.1 mbar and 160-180 K as 1.9%, 0.6%, and 18-19%, respectively.

Meanwhile, infrared radiative stabilization of the intermediates under these conditions can be ruled out. The radiative stabilization rate constants k_{rad} were computed using the approach by Klippenstein et al.[63] at average temperatures corresponding to the available internal energies of the intermediates, if they were produced in the corresponding bimolecular reactions at zero collision energy, and utilizing B3LYP/6-311G** vibrational frequencies and IR intensities. The radiative stabilization rate constants, 21.2 and 11.5 s^{-1} for **i1** and **i10**, respectively, are 3-4 orders of magnitude lower that the decomposition rate constants of these intermediates (Table 1) and thus infrared radiative stabilization is not competitive with dissociation. If the radical adducts **i1**, **i2**, and **i10** are collisionally stabilized, they may react with other species or be processed photochemically. However, since the formation of azanaphthalenes directly from these radicals is not favorable, here we do not pursue their fate further. Meanwhile, this analysis indicates that significant amounts of *trans*- and *cis*-cinnamonitriles and 2-

vinylbenzonitrile can be produced at the pressure of 0.1 mbar and lower in the temperature range of 160-180 K, i.e. at the conditions relevant to the PAH forming region of Titan's atmosphere.

With the result being that neither of the considered mechanisms of the CN + styrene reaction offer viable pathways towards the immediate formation of N-PACs, we move to investigate consequent reaction of the CN + styrene primary products. In particular, we study addition of the ethynyl radical, C_2H, to *trans*- and *cis*-cinnamonitrile, along with 2-vinylbenzonitrile, to see whether it can lead to the formation of substituted N-PACs. Earlier, our group demonstrated that C_2H addition to $C_{10}H_8$ products of the C_2H + styrene reaction may yield considerable amounts of substituted naphthalene,[64] with the reaction proceeding by ring closure, following the initial C_2H attack on various carbon centers, and finally by hydrogen loss to form PAH molecules. The PAH growth is attainable in these reactions because the cyclization process becomes more favorable than the direct hydrogen loss mechanism. One can expect that the analogous C_2H reactions with cinnamonitrile and 2-vinylbenzonitrile may lead to the formation of substituted azanaphthalenes and hence we consider them here.

C_9H_6N + C_2H, the $C_{11}H_8N$ PES

Addition of the ethynyl radical to the *ortho* positioned carbon in *trans*- or *cis*-cinnamonitriles eventually results in the formation of (*E*)- and (*Z*)-3-(2-ethynylphenyl) acrylonitriles by direct H losses from the initial adducts **i13** and **i13**_cis, respectively. C_2H addition may alternatively occur to the CN carbon of *trans*- or *cis*-cinnamonitriles (Figure 18). The addition to *cis*-cinnamonitrile leads to two rotational isomers, **i17** and

i18, with exothermicities of 40.6 and 38.8 kcal mol^{-1}, respectively, which can easily rearrange to one another via a very low barrier. **i17** can undergo a ring closure via a barrier of 22.0 kcal mol^{-1} forming **i19** in the process. Next, elimination of the hydrogen from C common for the two fused six-member rings in **i19** leads to the formation of 2-ethynyl-1-azanaphthalene via a 15.9 kcal mol^{-1} barrier. The ring closure in **i18**, also to form **i19**, is even more facile than that in **i17**, as this process requires a barrier of only 11.2 kcal mol^{-1}. The only competitive alternative to the ring closure in **i18** is elimination of cyanoacetylene, NCCCH, leading to the formation of the C_6H_5CHCH radical **p2**, but the associated barrier of 29.7 kcal mol^{-1} is almost a factor of 3 higher than that for the **i18** →**i19** cyclization process. One can clearly see that the C_2H + *cis*-cinnamonitrile reaction provides a favorable path to synthesize ethynyl-substituted 1-aza-naphthalene if C_2H adds to the carbon atom of the cyano group. This however is not the case for the similar reaction involving *trans*-cinnamonitrile because isomerization of the initial adduct **i17**_trans to **i17** involves a rotation around a double C=C bond andis not expected to compete with the loss of cyanoacetylene due to a high, ~42 kcal mol^{-1}, barrier. The wavefunction of the transition state associated with this rotation was found to have a strong multireference character and hence its energy was evaluated by multireference perturbation theory CASPT2(5,5)/6-311G** single-point calculations at the optimized B3LYP geometry, relative to the reference **i17** energy calculated at the same level.

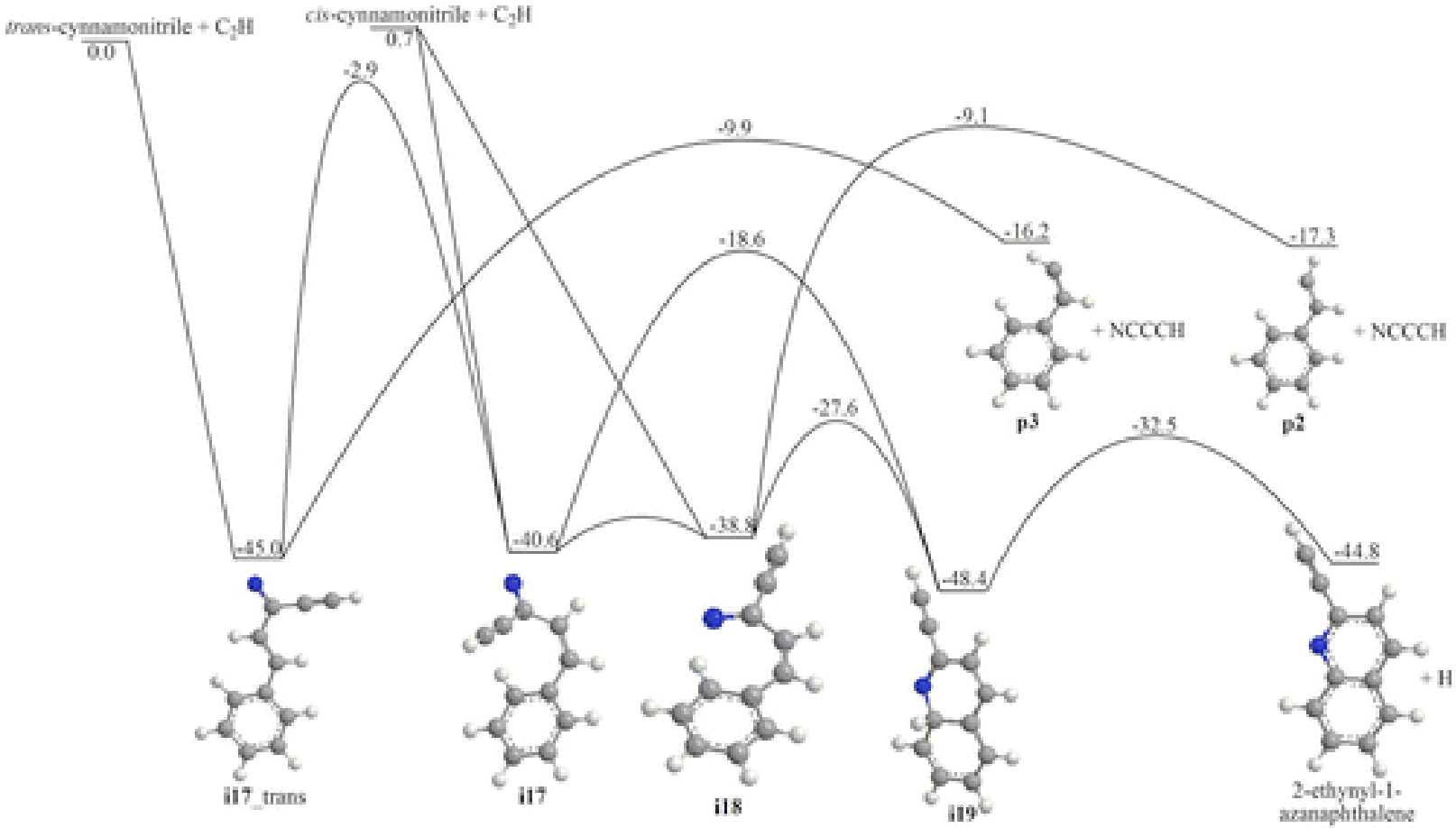

Fig. 18: PES illustrating the addition of C_2H to trans-cynammonitrile computed at the G3(MP2,CC) level of theory.

Finally, C_2H can also add to the carbon atom of the CN group in 2-vinylbenzonitrile

This occurs with an exothermicity of 43.1 kcal mol^{-1} and leads to **i20**. This adduct can feature a spontaneous ring closure to form a bicyclic structure **i21.** A very low barrier for this process was found at the B3LYP level where **i20** is a local minimum. However, the transition state energy at the G3(MP2,CC)/B3LYP/6-311G** level is computed to be lower than that of **i20** indicating a metastable character of this intermediate. Hydrogen elimination can then occur from **i21** via a barrier of 28.2 kcal mol^{-1} leading to the formation of an N-PAC molecule, 1-ethynyl-2-azanaphthalene. Alternatively, NCCCH can be lost from the initial adduct **i20** leading to the $C_6H_4CHCH_2$ radical **p4** via a barrier of 30.3 kcal mol^{-1}. Clearly, the cyanoacetylene elimination is less preferable than the ring closure followed by an H loss.

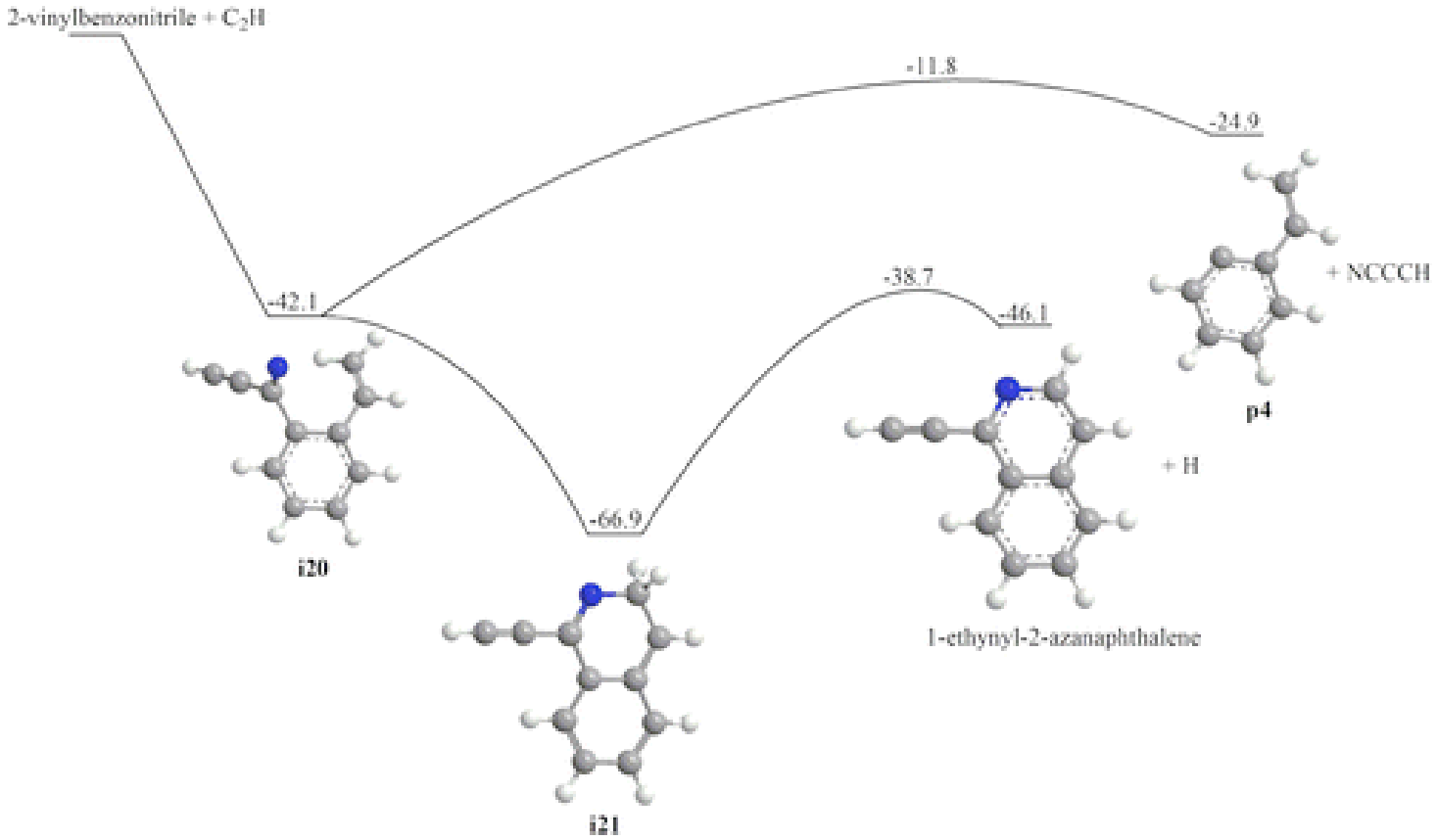

Fig. 19: PES illustrating the addition of C_2H to 2-vinylbenzonitrile computed at the G3(MP2,CC) level of theory.

One can see, based on rate constants, that the monocyclic 3-(2-ethynylphenyl)-acrylonitrile molecule (in two *E* and *Z* conformers) is the sole product of the C_2H + *trans/cis*-cinnamonitrile reactions when C_2H attacks the *ortho* carbon in the ring. The branching ratio of the *E* and *Z* conformers, 94-92/6-8, is insensitive to whether C_2H reacts with *trans*- or *cis*-cinnamonitrile because isomerization between **i13** and **i13**_cis is much faster than their dissociation via the H loss. The reactions do not lead to the formation of bicyclic substituted azanaphthalenes for the same reasons as those for the CN + styrene reaction channels, and 2: the initial cyclization steps appear to be nearly competitive to the direct hydrogen loss, but the subsequent 1,2-H migration impedes the progress toward the formation of N-PAC molecules. In contrast, N-PACs can be achieved through processes involving incorporation of CN into the second ring (Figs. 18 and 19). In particular, 2-ethynyl-1-azanaphthalene is calculated to be the exclusive product of the C_2H + *cis*-cinnamonitrilereaction if the ethynyl radical adds to the CN carbon, as the **i17** and **i18** adducts preferably undergo a ring closure and H elimination to produce N-PACs instead of losing cyanoacetylene. The unpaired electron in **i17** and **i18** is mostly localized on the hydrogen-less nitrogen atom and no viable pathway exists of losing hydrogen. For the reaction channels shown in Figs. 1-3, an H loss is favored because it results in the formation of a closed shell stable species, but that cannot happen for **i17** and **i18**. The formation of a stable closed shell molecule through an H loss can only occur after the cyclization process completes. Once the second ring is closed, the radical center redistributes to carbon atoms in the C_6 ring, allowing for a closed shell species to form through hydrogen elimination. Fig. 5 shows that 1-ethynyl-2-azanaphthalene can also be formed, again as the exclusive product, in the C_2H + 2-vinylbenzonitrile reaction if the

ethynyl radical adds to the C atom of the cyano moiety. Here too, the reason for the success of the N-PAC formation is the inability of the initial adduct**i20** to lose a hydrogen atom. This illustrates an important general mechanistic aspect of the PAH (or N-PAC) synthesis. Hydrogen elimination from an initial adduct almost always outcompetes any cyclization event. Therefore, successful routes to PAHs (N-PACs) should have such adducts formed in an entrance channel, for which a direct hydrogen loss cannot occur or is not competitive as compared to a ring closure.

RRKM-ME calculations at p = 3-10^{-6} mbar and T = 90-200 K do not show any collisional stabilization of the initial adduct **i17** and other intermediates **i18** and **i19** in Fig. 18, which is explained by rather low barriers on the pathway to the dissociation products, where the highest in energy transition state (**i18 →i19**) resides only 13.0 kcal/mol above **i17**. The calculated radiative stabilization rate constant of **i17** at zero collision energy, 16.9 s^{-1}, is several orders of magnitude lower than the rate constants for its isomerization and for the H loss from **i19**. Thus, under the conditions of Titan's atmosphere, **i17** formed in the C_2H + *cis*-cinnamonitrilereactionis expected to decompose to 2-ethynyl-1-azanaphthalene + H rather than to be collisionally or radiatively stabilized. On the other hand, **i17**_trans, the initial adduct of the C_2H + *trans*-cinnamonitrileseparated from the fragmentation products by a much higher barrier of 35.1 kcal/mol, is expected to be largely collisionally stabilized or otherwise form the **p3** + cyanoacetylene products. No collisional stabilization was found also for intermediate **i21** in Fig. 19 and its radiative stabilization rate constant, 51.2 s^{-1}, is much lower than that for the loss from **i21**, 3.30×10^7 s^{-1} at zero collision energy. Although the barrier for the H elimination reaction involving **i21** is

relatively high, 28.2 kcal/mol, the transition state resides 38.7 kcal/mol below the reactants making the collisional stabilization of **i21** unlikely, as verified by RRKM-ME calculations. Thus, the C_2H + 2-vinylbenzonitrile reaction may produce 1-ethynyl-2-azanaphthalene not only under single-collision conditions but also in the PAH forming region of Titan's atmosphere if C_2H attacks the C atom of the CN group. Assuming equal probabilities of C_2H additions to each unsaturated C atom in *cis*-cinnamonitrile and 2-vinylbenzonitrile (11.1%), up to ~2% of styrene molecules can be converted to ethynyl substituted azanaphthalenes under Titan's atmospheric conditions by consecutive reactions with CN and C_2H, predominantly to 1-ethynyl-2-azanaphthalene via 2-vinylbenzonitrile.

N-methylene-benzenamine + $2C_2H$

In our previous work,[54] we found that 4-ethynyl-quinazoline, an N-PAC molecule with two N atoms in an aromatic ring, can be produced from *N*-methylene-benzenamine via two consecutive additions of C_2H and CN: $C_6H_5(NCH_2)$ + CN → $C_6H_4(NCH_2)(CN)$ + H and $C_6H_4(NCH_2)(CN)$ + C_2H → 4-ethynyl-quinazoline + H. Here, we investigate a similar mechanism starting from *N*-methylene-benzenamine, but involving two C_2H additions with an expectation that this process can produce an ethynyl substituted quinolone molecule with one N atom in a ring. The computed potential energy profile is illustrated in Figure 6. The addition of C_2H to an *ortho*carbon in *N*-methylene-benzenamine occurs barrierlessly with an exothermicity of 44.6 kcal mol^{-1}. Next, a direct loss of the hydrogen from the attacked carbon leads to the formation of 2-ethynyl-*N*-methylene-benzenamine, which lies 27.5 kcal mol^{-1} below the initial reactants, via a

barrier of 26.1 kcal/mol. Addition of another C_2H unit then forms the **i23** adduct with an exothermicity of 48.9 kcal mol^{-1}. **i23**can undergo a fast ring closure through a very low barrier of 2.1 kcal mol^{-1} leading to intermediate **i24**, which can then lose hydrogen to form 4-ethynyl-1-azanaphthalene (4-ethynyl-quinoline) via a barrier of 26.3 kcal mol^{-1}. 4-ethynyl-quinoline lies 76.8 kcal mol^{-1} below the initial reactants 2-ethynyl-*N*-methylenebenzenamine + C_2H. The only alternative fate of **i23** could be elimination of the C_4H_2 (diacetylene) side-chain group. However, this process requires a relatively high barrier of 42.2 kcal $mol^{-1}$and thus is not competitive with the ring closure followed by the H loss leading to 4-ethynyl-quinoline.

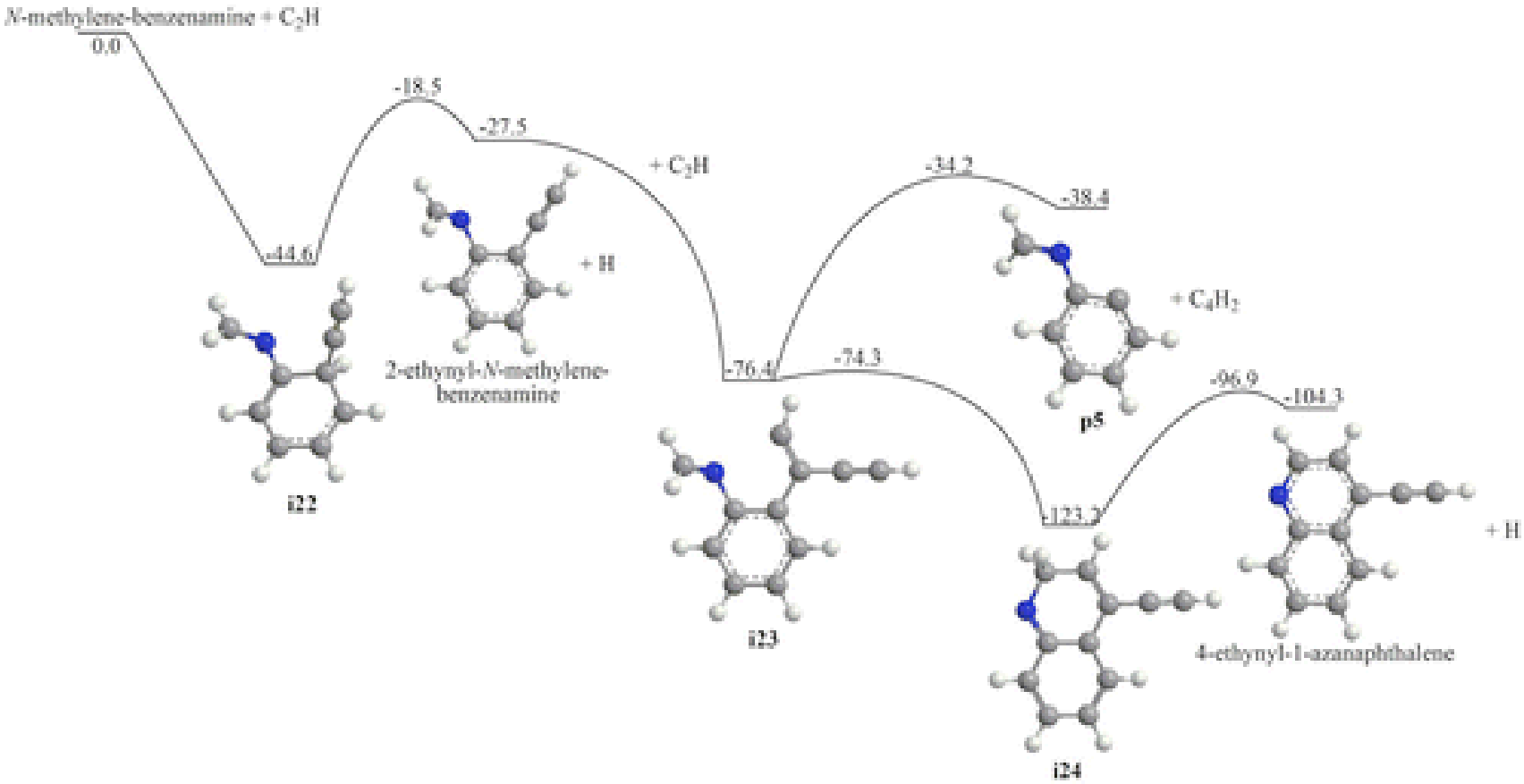

Fig. 20: PES illustrating the various pathways leading to 4-ethynyl-1-azanaphthalene computed at the G3(MP2,CC) level of theory.

According to RRKM calculations at the zero-pressure limit, 4-ethynyl-quinoline is the dominant product of the 2-ethynyl-*N*-methylenebenzenamine + C_2H reaction in the range of collision energies of 0-5 kcal mol^{-1} if C_2H adds to the α carbon of the ethynyl side chain. RRKM-ME calculations at pressures in the $3\text{-}10^{-6}$ mbar range and temperatures of 90-200 K show little collisional stabilization of **i22** in the first C_2H addition reaction for pressures up to 1 mbar and no collisional stabilization of **i23** and **i24** in the second reaction. Also, the computed radiative stabilization rate constants, 19.6, 21.9, and 60.3 s^{-1}, are too low for this process to compete with dissociation of these intermediates.

Thus, if *N*-methylene-benzenamine and C_2H radicals are available, two consecutive reactions described above can lead to the production of substituted quinoline under low-temperature and low-pressure conditions. Assuming equal probabilities of C_2H additions to each carbon of N-methylene-benzenamine (14.3%) and 2-ethynyl-N-methylene-benzenamine (11.1%), ~3% of the former can converted to 4-ethynyl-quinoline at pressures up to 0.1 mbar. Earlier,[54] we discussed that *N*-methylene-benzenamine itself can be formed in various reactions under different conditions, including recombination of phenyl and methylene-amidogen radicals followed by collisional stabilization of the product (low temperature and high pressure), the barrierless $C_6H_5 + CH_3N \rightarrow C_6H_5(NCH_3) \rightarrow C_6H_5(NCH_2) + H$ reaction (low temperature and low pressure), and the reaction of phenyl with methyleneimine, $C_6H_5 + CH_2NH \rightarrow C_6H_5(NHCH_3) \rightarrow C_6H_5(NCH_2) + H$ featuring 3-5 kcal mol^{-1} barriers (elevated/high temperature and low pressure).

Chapter 7: Finally, a Route to Naphthalene ? : An Unexpected Pathway offers the way

Although the creation of the naphthalene core could now be achieved without any problems, we still had failed to make naphthalene itself. Our best attempts, up to now, had been producing substituted naphthalene or azanaphthalene molecules. However, from our previous works, we had learned quite a lot. Firstly, we had realized that careful consideration of the reacting species is of utmost importance. If the initial adduct can lose hydrogen cleanly, it will do so, and this process will overwhelm any ring formation process. Through this process, we also learned that producing a terminal radical as quickly and as efficiently as possible would allow ring closure to occur through a muted barrier allowing the ring forming process to occur faster. Lastly, we could no longer rely on pressure stabilization as a suitable source for producing PAHs or N-PACs. This is difficult to predict, and is often not the most direct route for forming PAHs.

At about the same time, our collaborator, (the Kaiser group based out of Manoa, Hawaii) had asked us to study the reaction of phenyl radical (C_6H_5) with vinylacetylene (C_4H_4) as a suitable source of naphthalene in combustion flame. Although, this was for combustion flame, and whether it is barrierless or not is not as important as it is in astrochemistry, I decided to run a PES scan of the addition process to the CH_2 carbon of vinylacetylene. The scan, which was conducted at the B3LYP/6-311G** level of theory, and revealed that there was either a very small barrier to the reaction, or none at all. Single point calculations along the reaction path, such as G3(MP2), MP2, and even CCSD(T) proved to contradict each other, with some predicting a small barrier, and others predicting the

formation of a small complex, with no barrier to reaction. It cannot be adequately stressed, the importance of whether there is a barrier or not. Even a small barrier, will render the reaction, at the low temperature conditions of Titan mute therefore, more sophisticated, and advanced methods were sought. For this, we decided to use the CASPT2(7,7)/6-311G**//CASSCF(9,9)/6-311G** method, in which geometry optimizations along the reaction channel are performed using CASSCF(9,9)/6-311G**, and subsequent single point energy calculations using CASPT2(7,7)/6-311G** are obtained. The results, descriobed below show that a van der Waals complex is initially formed, which then goes on to climb a small submerged barrier leading to the formation of the initial adduct. Further, at 100 K, thermal rate constants for the entrance channel were calculated to be $2.5x10^{-10}$ $cm^3molecule^{-1}s^{-1}$, proving that the reaction indeed occurs fast even at the low temperature conditions of Titan.

Why is this reaction barrierless? Frenklach and others, have studied this same reaction, at higher temperatures, using the G2(MP2) method, and found a small barrier of 1.7 kcal mol^{-1} for this reaction[65]. Using the same method, we were able to reproduce their work, however, it is only when we go to higher levels of theory that our transition state becomes lower in energy than the infinitely separated reactants. So, what is at play here? One thing that can be at work here, is the polarizability of vinylacetylene (measured as 7.70 A^3). Compared to reactions of phenyl radical with acetylene or ethylene, which show small, about 3.6 and 2.4 kcal mol^{-1}, barriers respectively, their polarizabilites have been shown to be 3.48 and 4.15 A^3 respectively[66]. The greater polarizability of vinylacetylene means that at larger separation, there is an attractive polarizability, which

could contribute to the formation of the van der Waals complex. Also, semi-empirical work by Smith and coworkers has shown that for the addition of a closed shell species on to an open shell species, the reaction proceeds barrierlessly if the difference in the ionization energy of the closed shell species and the electron affinity of the open shell reactant is below 8.75 eV, and the rate constant at 298 K is greater than $5x10^{-12}$ cm^3 $molecule^{-1}$ s^{-1}.[67] For the addition to the CH_2 group of vinylacetylene, this difference turns out to be 8.48 eV, and $k_{298} = 1.5x10^{-11}$ cm^3 $molecule^{-1}$ s^{-1}, thus satisfying both criteria developed my Smith et. al.

The rest of the surface involving this entrance channel is fairly straight forward. Once the initial adduct is formed, internal 1-5 hydrogen shift occurs through a barrier of 36.9 kcal mol^{-1}. The hydrogen migration intermediate than undergoes single bond rotation and cyclization over a very small barrier of 2.20 kcal mol^{-1}, leading to a very exothermic cyclized intermediate. Because hydrogen loss at this stage is unfeasible, 1-2 hydrogen shift over a large, but still manageable barrier followed by hydrogen loss finishes off the synthesis of naphthalene. From the initial adduct, there is still one more possibility. Hydrogen loss from the CH_2 group can yield **cis-PVA**, through a barrier of 39.9 kcal mol^{-1}. This PES is shown pictorially in Fig. 20 Since the rest of the PES is only relevant to combustion conditions, those results and discussions will be withheld until we reach those chapters dealing with our combustion flame studies. At collisionless conditions, this route gives naphthalene + H as the nearly exclusive (≈ 99.99%) product.

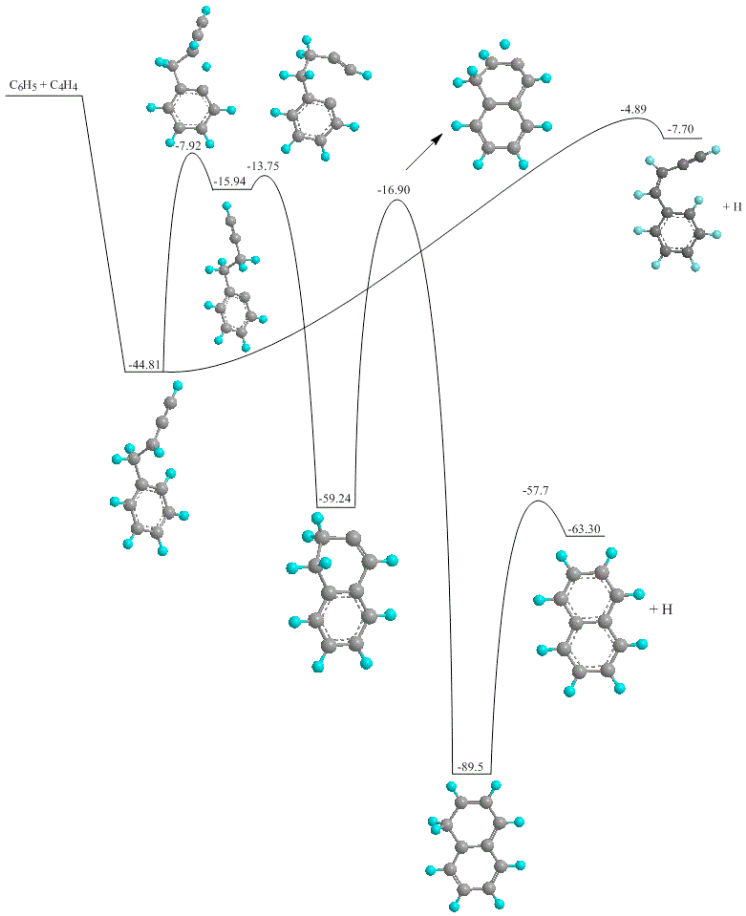

Fig. 20: PES illustrating the barrierless pathway leading to naphthalene computed at the G3(MP2,CC) level of theory.

The next set of chapters are devoted to the analysis of combustion reactions in the quest to find methods suitable towards the synthesis of PAHs. As with the previous astrochemistry chapters, we will outline our results, and most importantly, when reactions fail to produce PAHs, we will explain what we learned from it, and what we did to overcome these obstacles.

Chapter 8: Vinylacetylene addition to Phenyl radical: A Combustion Study

Previously, in chapter 7, I had begun talking about the reaction of vinylacetylene (C_4H_4) with phenyl radical (C_6H_5). In that chapter, I had only described one of the possible four addition sites on vinylacetylene, because that was the only one which was shown to be barrierless. In this chapter, we begin by describing the remaining three surfaces.

Addition to the internal carbon of the C_2H link in vinylacetylene occurs through a 4.03 kcal mol^{-1} barrier (see Fig. 21), and produces an initial adduct which is exothermic by 36.74 kcal mol^{-1}. CH insertion into the adjacent bond occurs through a two step process requiring barriers of 19.22 and 6.38 kcal mol^{-1} (for step one and two respectively) to be overcome. From here, 1-4 H shift from the terminal carbon of the side chain can occur requiring 32.92 kcal mol^{-1} to pass through the transition state. Four membered ring formation followed by ring opening to obtain the correct cis stereochemistry occurs in a two step process requiring 25.07 and 19.31 kcal mol^{-1} of energy respectively to overcome these barriers. At this point, ring closure followed by hydrogen loss occur easily and finish off the synthesis of naphthalene + H.

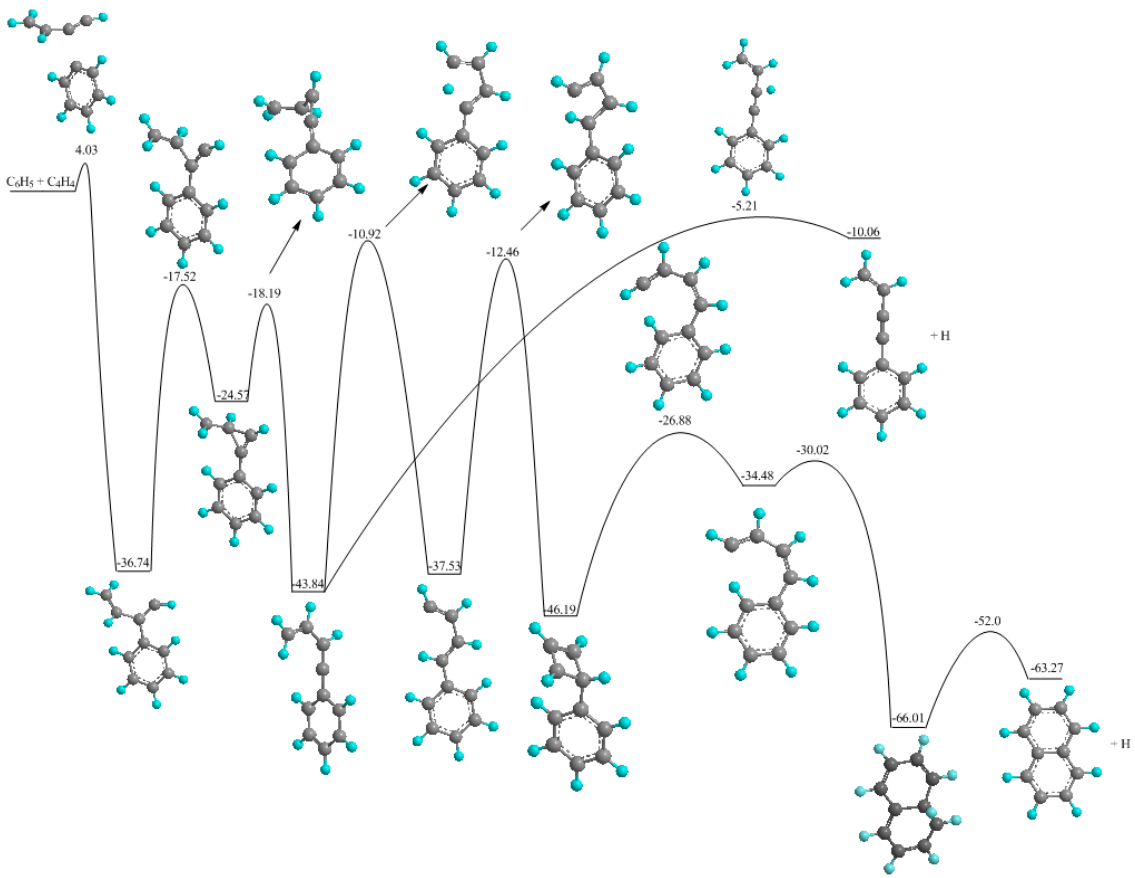

Fig. 21: PES illustrating the addition of vinylacetylene through the internal carbon of the C_2H side chain to phenyl radical computed at the G3(MP2,CC) level of theory.

An alternative hydrogen loss channel exists starting from the CH insertion step. This hydrogen loss occurs with a barrier of 38.63 kcal mol^{-1}, and forms $C_6H_5(CCCHCH_2)$ + H.

Addition to the terminal CH group in vinylacetylene occurs through a barrier of 1.2 kcal mol^{-1}, and produces an adduct which is exothermic by 49.7 kcal mol^{-1} (see Fig. 22). 1-4 H shift from an adjacent carbon on the ring can occur through an energetic barrier of 34.98 kcal mol^{-1}. Single bond rotation and ring closure occur in a concerted manner through a 7.37 kcal mol^{-1} barrier, and finally loss of an hydrogen atom from the ring core produces naphthalene. A competing pathway can occur if hydrogen is lost from the initial adduct. The process requires 47.62 kcal mol^{-1} in order to go over the transition state, and the product has an overall exothermicity of 5 kcal mol^{-1}.

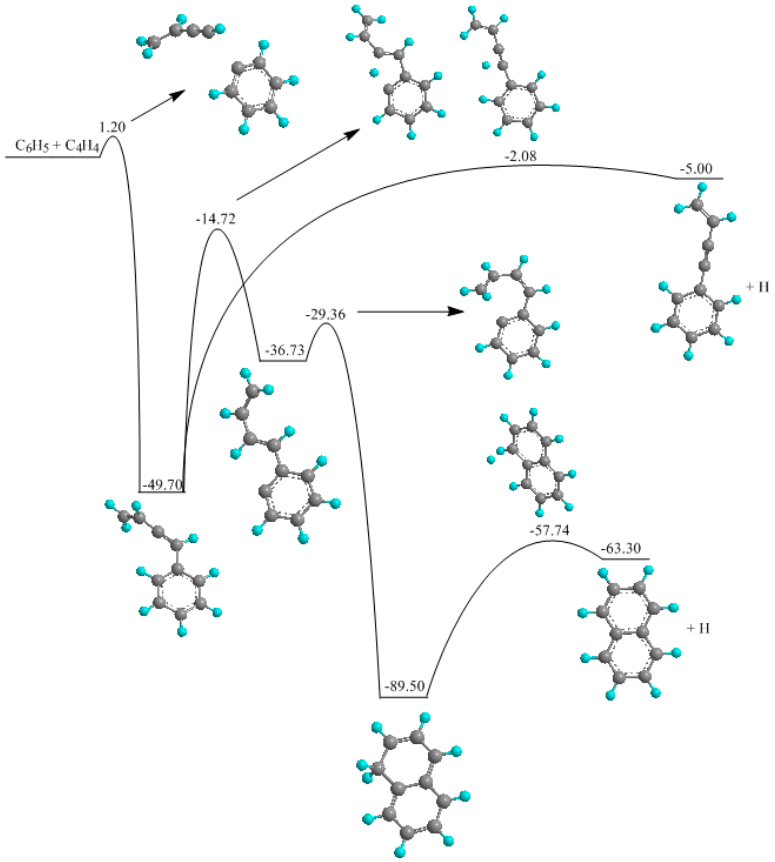

Fig. 22: PES illustrating the addition of vinylacetylene through the terminal carbon to phenyl radical computed at the G3(MP2,CC) level of theory.

Lastly, addition can also occur to the internal CH of vinylacetylene (see Fig. 23). This requires overcoming a barrier of 2.63 kcal mol^{-1}, and the initial adduct is exothermic by 33.01 kcal mol^{-1}. CH_2 insertion into the adjacent bond requires two steps, and the energetic barriers are 17.7 and 3.59 kcal $mol_{.1}$ respectively. At this point, the intermediate that is formed is the direct precursor of **t-PVA**. From previous chapters, it has already been shown that the most likely step is hydrogen loss to produce **t-PVA + H**.

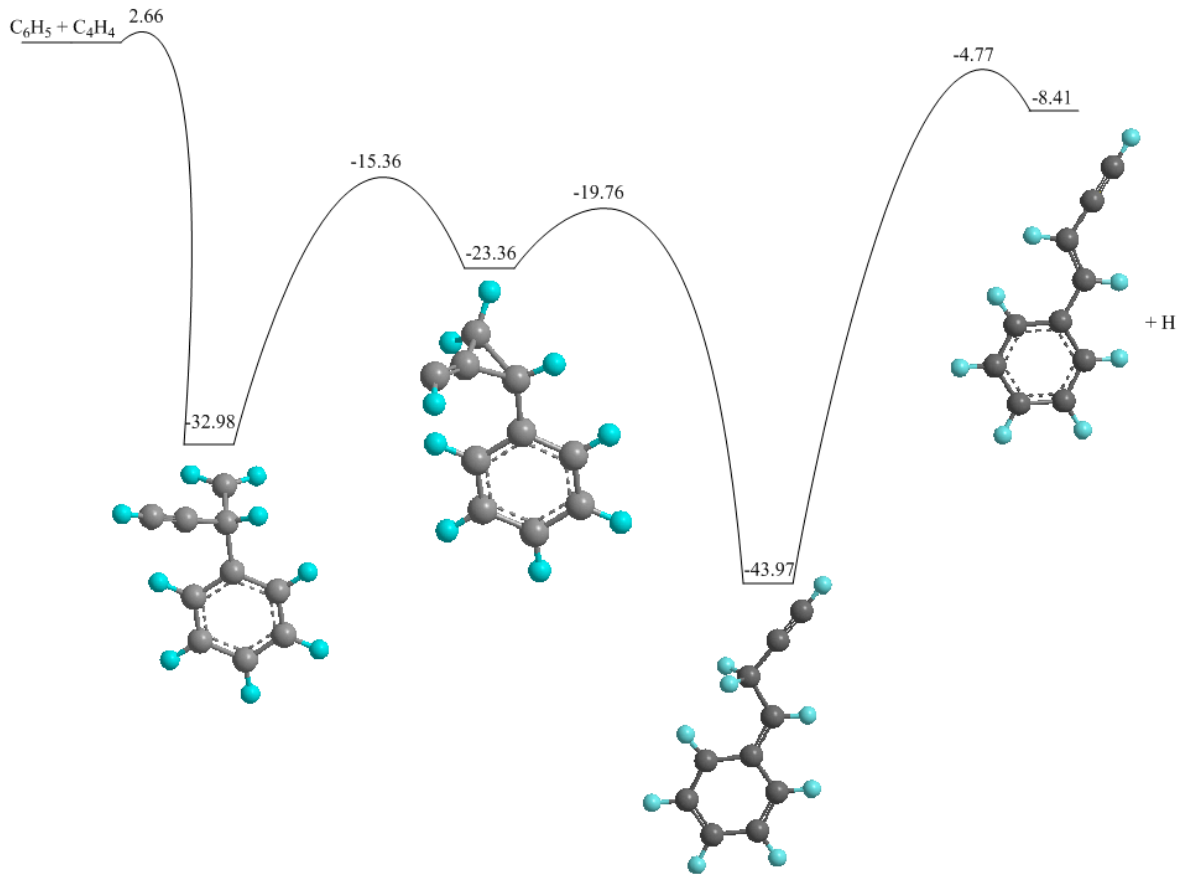

Fig. 23: PES illustrating the addition of vinylacetylene through the internal CH to phenyl radical computed at the G3(MP2,CC) level of theory.

Due to the fact that we were interested in these reactions and how they relate to combustion, we decided it would be better to use a Master Equation (ME) approach to RRKM (RRKM-ME). In this method, pressure is brought into the equation, and when struck by a bath gas, can either move up in energy or down in energy. As collisions continue, molecules will surmount barriers until the number of total collisions has been reached. Afterwards, statistical analysis can reveal the proper branching ratios.

For Figure 20, RRKM-ME revealed that at 7.6 Torr, production of naphthalene decreased from 18.7 % at 1000K to 6.5 % at 3000 K. As pressure is increased to 76 Torr, naphthalene production decreases from 15 % at 1000 K to just over 3 % at 3000K. Finally, increasing the pressure to 760 Torr further decreased the percentage of naphthalene obtained to 10.6 % at 1000 K to just over 2 % at 3000 K. There is no possibility of forming naphthalene from Figure 23. Moving on, Figure 21 shows that at 7.6 Torr, 46.5 % of naphthalene is synthesized at 1000 K, which at 3000 K drops to 24 %. When the pressure is raised to 76 Torr, naphthalene production starts at 36.4 % and drops to 15.9 %. Lastly, at 760 Torr, 29.7 % of the product is naphthalene, and at 3000 K this drops to just above 10 %. For Figure 22, naphthalene production starts out at 37.9 % at 1000K and 7 bar, and decreases to 36.2 % at 3000 K and 7.6 Torr. Raising the pressure to 76 Torr and keeping the temperature at 1000 K yields 39.4 % naphthalene, and decreases to 34.6 % when the temperature is increased to 3000 K. Finally, increasing the pressure from 76 Torr to 760 Torr while keeping the temperature at1000 K gives 43.5 % naphthalene , and decreases to 29.3 % when the temperature is increased to 3000 K. When including processes like hydrogen abstractions by phenyl radical on

vinylacetylene, which is a pressure independent process, we obtain some production of benzene. The global production of various species in all of the PES presented in this chapter are shown in Fig. 24. From viewing these graphs, one should see that regardless of the pressure, naphthalene production is fairly temperature insensitive yielding about 20 % of the product mixture regardless of temperature. On the other hand, benzene production increases, starting at almost no production at 500K, and maxing out at about 20 % at temperatures of 3000 K.

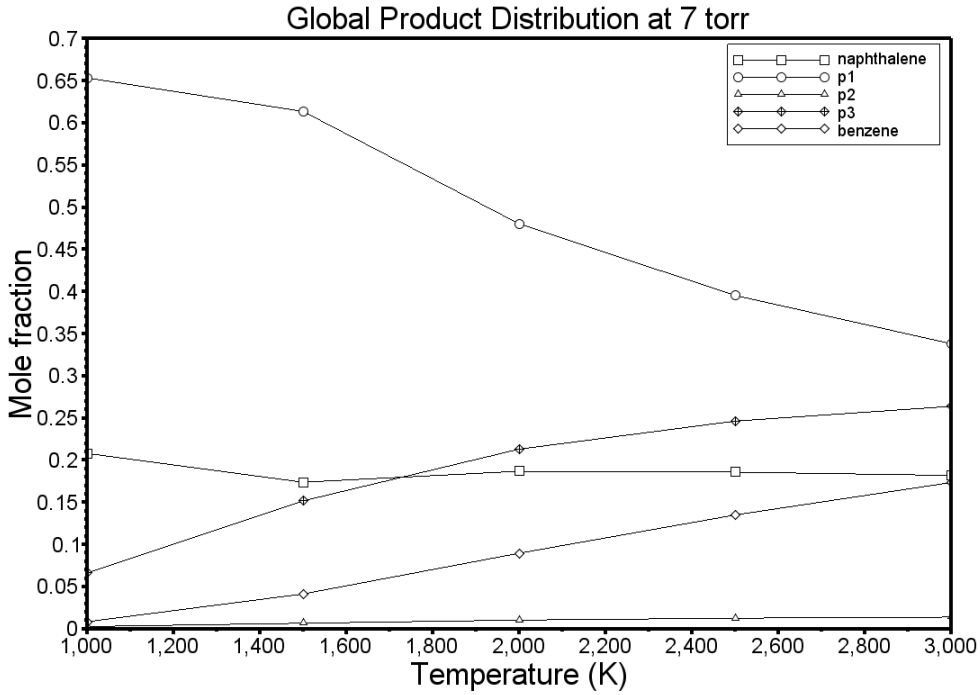

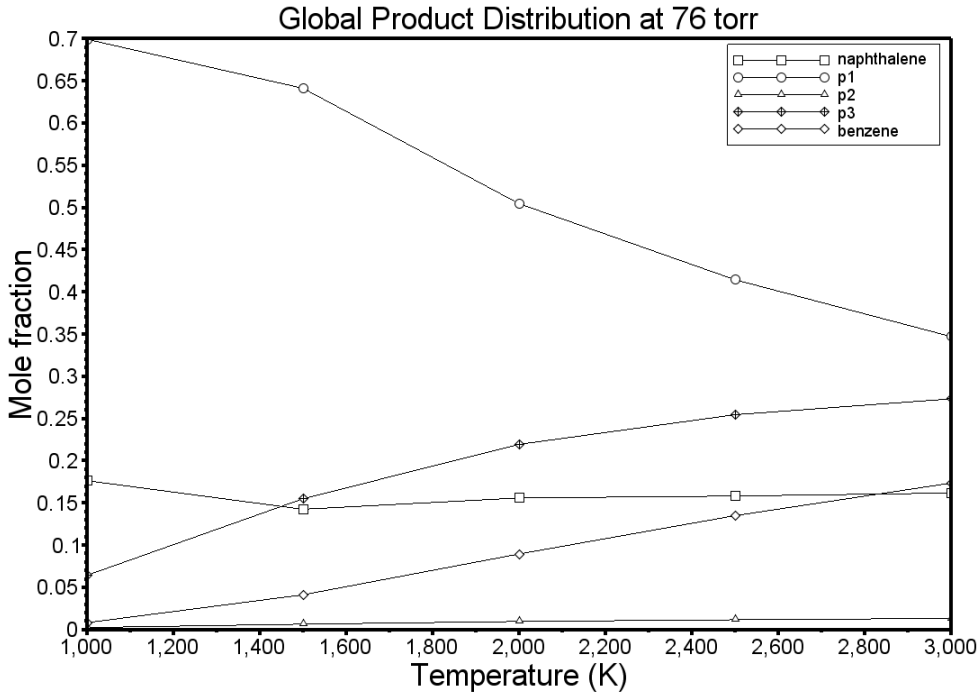
Global Product Distribution at 76 torr
naphthalene
p1
p2
p3
benzene
Mole fraction
0.7
0.65
0.6
0.55
0.5
0.45
0.4
0.35
0.3
0.25
0.2
0.15
0.1
0.05
0
1,000
1,200
1,400
1,600
1,800
2,000
2,200
2,400
2,600
2,800
3,000
Temperature (K)

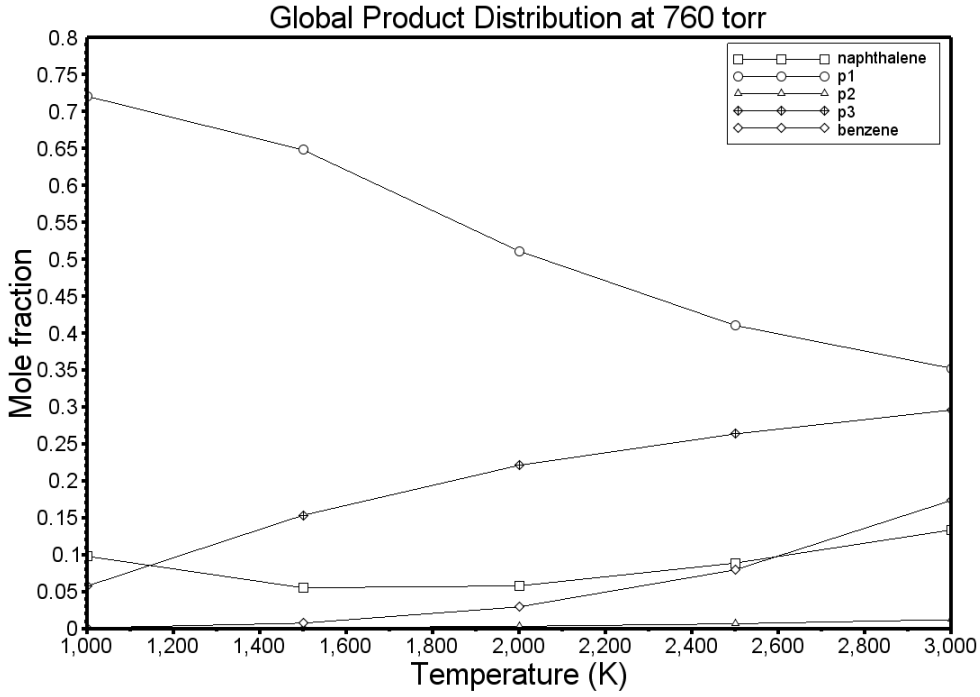
Global Product Distribution at 760 torr
naphthalene
p1
p2
p3
benzene
Mole fraction
0.8
0.75
0.7
0.65
0.6
0.55
0.5
0.45
0.4
0.35
0.3
0.25
0.2
0.15
0.1
0.05
0
1,000
1,200
1,400
1,600
1,800
2,000
2,200
2,400
2,600
2,800
3,000
Temperature (K)

Figure 24: Global product distribution of various products on the vinylacetylene + phenyl radical surface

In this chapter, we have shown a valuable mechanism for obtaining naphthalene. The production of naphthalene appears to be temperature independent, and is fairly constant at consisting of about 20 % of the reaction product mixture. The method also yields benzene, although that should not be too exciting, as one of the reactants, phenyl radical, was most likely formed from the dissociation of a hydrogen atom from benzene. In other words, it forms a benzene/phenyl radical cycle by which one can convert vinylacetylene into naphthalene + H.

Chapter 9: Formation of Dehydronaphthalene

The first reaction we thought about was the addition of diacetylene (C_4H_2) to phenyl radical (C_6H_5) (see Fig. 25). Due to the symmetry of diacetylene, there are only two attacks possible. The first, and the one with the lowest entrance barrier, is addition to the terminal carbon of diacetylene, overcoming a barrier of 1 kcal mol^{-1}, and exhibiting an exothermicity of 48.5 kcal mol^{-1}. Ring cyclization can occur through an energetic barrier of 49.1 kcal mol^{-1}, leading to **i2**. **i2** can then lose a bridging (fused) hydrogen forming **di-dehydronaphthalene + H**. The barrier for the hydrogen loss is computed to be 12.2 kcal mol^{-1}, and the final product lies 12.9 kcal mol^{-1} below the infinitely separated reactants. Other possible pathways include loss of hydrogen directly from the initial adduct. This leads to **phenyldiacetylene + H**, lying 10.6 kcal mol^{-1} below the energy of the reactants, and exhibiting a barrier of 43.1 kcal mol^{-1}. One last possibility for this entrance channel exists, and requires a 1-2 H shift, overcoming a barrier of 52.1 kcal mol^{-1}. H elimination from this isomer leads to **phenyldiacetylene + H** with a reverse barrier of 4.8 kcal mol^{-1}.

The second entrance channel involves addition to the interior carbon of diacetylene. The entrance barrier is 4.9 kcal mol^{-1}, and the resulting adduct lies 37.2 kcal mol^{-1} exothermic (relative to the energies of the fully separated reactants). CH migration to the terminal carbon occurs in two steps, with barriers of 23.1 and 7.3 kcal mol^{-1} respectively. The resulting intermediate is interconnected with the first entrance channel, and as previously stated, can lose hydrogen to form **phenyldiacetylene + H**.

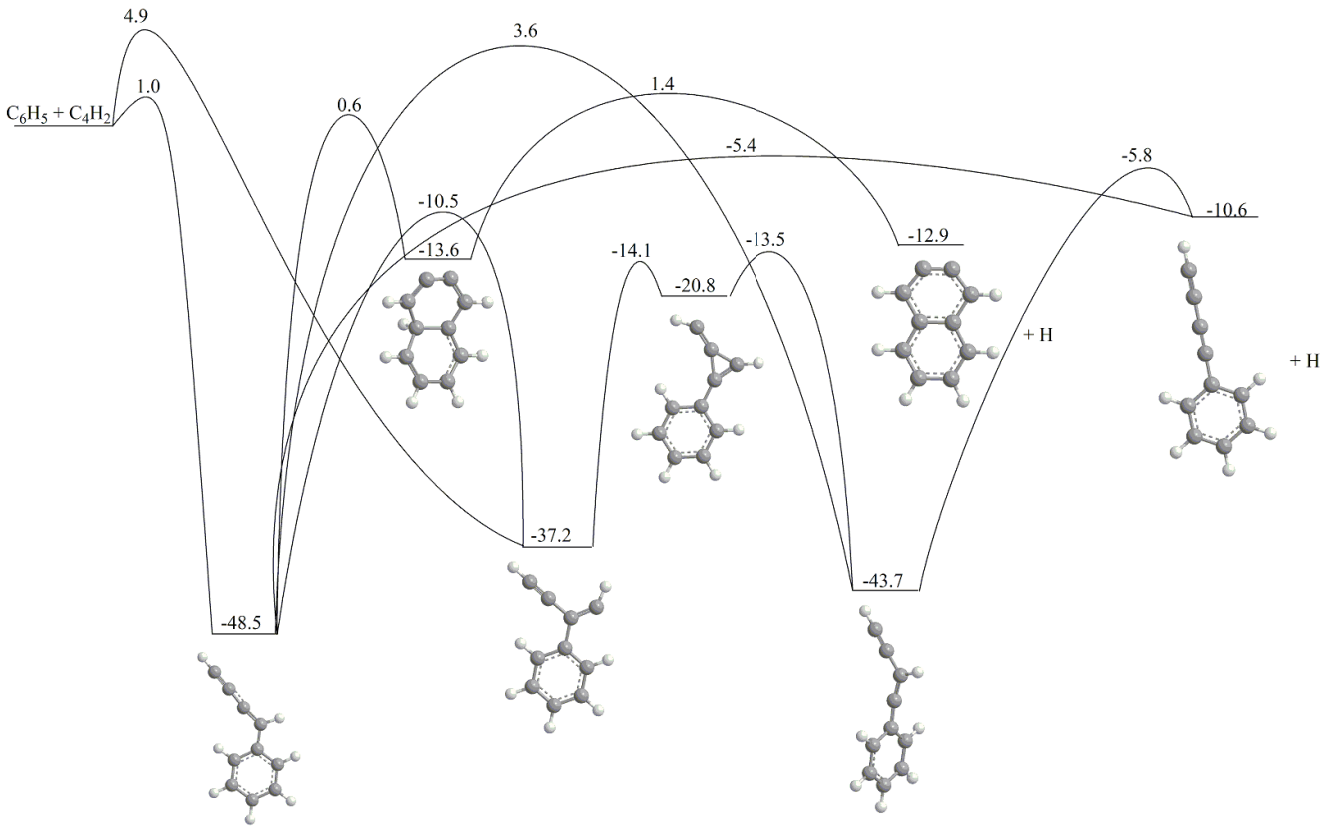

Fig. 25: PES illustrating the addition of $C_6H_5 + C_4H_2$ computed at the G3(MP2,CC) level of theory.

Using computed rate constants, branching ratios were computed between 0 and 5 kcal mol^{-1}, and the near exclusive product was found to be **phenyldiacetylene + H**. By now, these results should not be too surprising. Based on our astrochemical results, the fact that a simple and facile hydrogen loss pathway exists, any attempts to cyclize and form the naphthalene core are futile. Another problem involves the relative inflexibility of the side chain. Long side chains with double and triple bonds (unless conjugated), are relatively stiff. This hinders their cyclization pathways.

Chapter 10: Pyrolysis of o-benzyne: A possible pathway towards dehydrogenated naphthalenes

Our next thought was to go one step backwards and revisit ways the first ring can be formed in combustion flames. One way to do this is to start with the compound of interest, and look at its pyrolysis mechanism (ie. how does it degrade in combustion flames). If we know this pathway, we can infer that the formation route can be easily explained by simply reversing the pyrolysis pathway. One molecule we decided to try this on was o-benzyne. The reason for this is that it is reasonably found in combustion flames, and our work, can solve one of the more fundamental questions about its synthesis in combustion flame. Additionally, due to its relative instability, o-benzyne is a difficult molecule to work with experimentally.

It is well known that when a sample of benzene is combusted at low temperatures, the dominant products are acetylene (H-CC-H) and diacetylene (H-CCCC-H), in 1:1 molar ratios. The following set of reactions are often invoked to explain this:[68-69].

$$C_6H_6 \rightarrow C_6H_5 + H \quad (1)$$

$$C_6H_5 \rightarrow o\text{-}C_6H4 + H \quad (2)$$

$$o\text{-}C_6H_4 \rightarrow H\text{-}CC\text{-}H + H\text{-}CCCC\text{-}H \quad (3)$$

The phenyl radical has yet to be observed experimentally, however, through theoretical quantum mechanical and RRKM statistical methods, it seems almost certain that phenyl radical forms as the first step in benzene combustion1. Experimental and theoretical calculations also verify that once phenyl radical forms, rapid H-loss occurs, to form the

relatively unstable o-benzyne[69]. Although much work has centered on elucidating equation (3), many questions still remain. A thorough combined experimental/theoretical analysis by Zhang and coworkers explored the combustion of o-benzyne by using time-of-flight photoionization mass spectrometry (TOF-PIMS), matrix-isolation Fourier transform infrared absorption spectroscopy and chemical ionization mass spctrometry (CIMS), and showed that the products of (3) form fast and dominate at temperatures below 1800K[70], the maximum temperature recorded in their apparatus. This was supplemented with high level quantum mechanical (QM) calculations of several stationary points on the PES[70], which showed the possibility of the bond rupture process occurring in either a concerted or step-wise fashion. Another paper on the pyrolysis of o-benzyne from M. C. Lin's group used the G2M(rcc,MP2) method to determine accurate energies of several stationary points on the o-benzyne combustion surface[71]. They followed this with an implementation of RRKM theory to determine accurate branching ratios. Their results showed that isomerizations leading to m-benzyne and p-benzyne are important at temperatures below 2000K[71], and that the dominant reaction species is diacetylene and acetylene. Recently, using Atomic Resonance Absorption Spectroscopy (ARAS), and modeling, Xu and coworkers determined that the combustion of o-benzyne could not be governed solely by equation (3). They adequately explain that rupture of a CH bond from o-benzyne may also occur, leading to either 1,2,3-tridehydrobenzene or 1,3,4-tridehydrobenzene, estimating the ΔHrxn as 108 and 110 kcal mol^{-1} respectively[72]. M.C.Lin's paper did not include possible hydrogen losses in their PES however, based on a difference of only 18.4 kcal mol^{-1}, and the possibility that these H-loss mechanisms

occur through rather loose transition states, at higher temperatures there can be some competition.

O-benzyne can decompose through many different routes (see fig. 28). Concerted reactions, involving the rupture of a C-H bond, can lead to two separate C_6H_3 aromatic species, 1,2,3 and 1,2,4-tridehydrobenzene. 1,2,3-tridehydrobenzene is observed to be ≈ 1.91 kcal $mole^{-1}$ more stable than its 1,2,4 counterpart. The exothermicity of 108.6 and 110.5 kcal $mole^{-1}$ respectively are consistent with previous research[72]. Additionally, one other concerted reaction leading to the retro-diels alder adduct diacetylene (C_6H_4) and acetylene (C_2H_2) occurs through a C_2V symmetric transition state, and an energetic barrier of 90.2 kcal $mole^{-1}$. Previous research from M. C. Lin's group has suggested that isomerizations from o-benzyne to the corresponding meta and para isomers may be important in combustion processes4. To this end, our work suggests that the ortho to meta; and meta to para transitions require a barrier of 71.3 and 61.7 kcal $mole^{-1}$. H loss channels originating from either the meta and para isomer also exist. From symmetric considerations, the meta isomer has the possibility of forming all three tri-dehydrobenzene derivatives, while the para isomer can only form the 1,2,4 tridehydrobenzene isomer. All of these hydrogen loss channels are observed to be loose, and are endothermic by over 100 kcal $mole^{-1}$, with respect to the energy of o-benzyne.

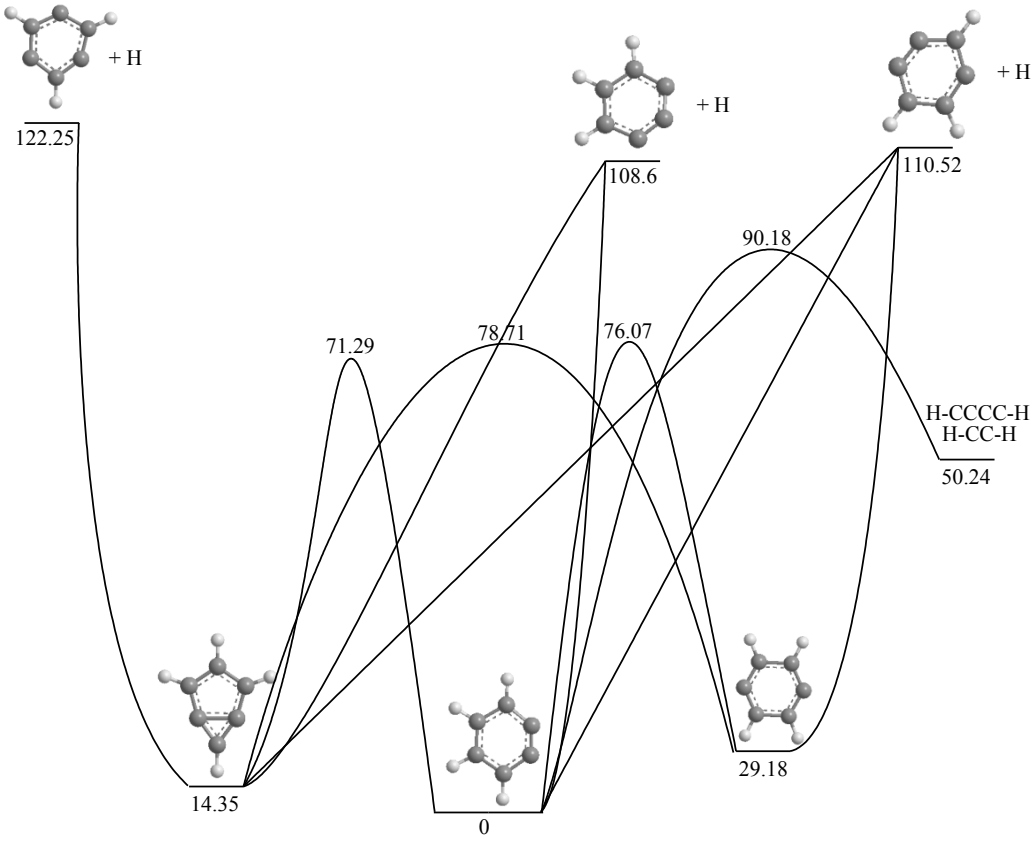

Fig. 28: PES illustrating the pyrolysis of o-benzyne computed at the G3(MP2,CC) level of theory.

Thermal high pressure rate constants were obtained for each unimolecular reaction, and branching ratios were obtained every 500K from 500K to 2500K. The results were startling, in that the only set of products predicted to form was the retro diels alder set. To explain these results, let us look at a more familiar form of the thermal high pressure rate constant equation.

$$k(T) = \frac{kT}{h}\exp\left(\frac{-\Delta G}{RT}\right)\frac{Q^{\neq}}{Q}$$

This equation is exactly equivalent to that shown in equation ?. One thing to note is that it is dependent on the change in Gibbs free energy, and the ratio of partition functions. For a reaction where the barrier is smaller, ΔG will also be small. Now, let us turn our attention to the partition function. To analyze the partition function ratio, let us look at the lowest frequencies for the retro diels alder reaction versus the most stable H loss product. The lowest frequency for the retro diels alder transition state is 175 cm^{-1}, compared to 372 cm^{-1} for the H loss transition state. In light of these findings, it makes sense that the retro diels alder reaction should be the major product observed. The fact that it requires overcoming a smaller reaction energy, coupled with an increase in the contribution from the vibrational partition function, acetylene and diacetylene should be the major products observed. Are these branching ratios likely to change as a result of relaxing the high pressure limit constraint, and using more sophisticated RRKM-ME kinetics formulations? The answer to this question is likely no. The reason is that at the high pressure limit, all of your reactant (o-benzyne) is already in an excited state. This excited state confers the greatest possible chance of fractionating in such a way as to

favor higher energy pathways. Using the high pressure limit rate constants only reveals to us what the upper limit is to contributions from hydrogen loss pathways, and this upper limit was established as being zero (or really close to it).

It should be noted that some experimental papers on this topic contradict our results. While we are in line with M. C. Lin and Zhang, our work is contradicted by the study of Xu et. al. It is important to note that we are not suggesting that any of these previous works are wrong (or right). To us, our results are reasonable, and can be fully explained by simple molecular properties however, more work needs to be performed before a definitive answer can be arrived at.

Can a diels alder reaction be used to synthesize PAH's ? To test this theory, we decided to react o-benzyne with diacetylene. The reaction is illustrated below, and one can see that the calculated transition state lies only 2 kcal mol^{-1} above the reactants. In combustion conditions, this barrier is readily overcome, and thus this reaction can serve as a simple one step synthesis to further extend cyclic systems.

Chapter 11: C_2 addition to vinylacetylene

Having determined the pyrolysis mechanism for o-benzyne, we believed the logical route was to investigate its formation from molecules present in flame chemistry, such as vinylacetylene (C_4H_4) and dicarbon (C_2) The ground triplet state of C_2 ($C_2(a^3\Pi_u)$) and the ground singlet state of C_2 ($C_2(X^1\Sigma_g^+)$) are separated by 1.74 kcal mol^{-1}. As such, both states need to be considered along with their additions to vinylacetylene (C_4H_4).

The singlet surface begins by three possible initial entrance channels (see fig. 26). The first, and most energetically favorable leads to isomer si2, with exothermicity of 79.6 kcal mol^{-1}. This entrance channel is attack of dicarbon via the CH_2-CH bond forming a three membered ring. The second most favorable channel leads to isomer si1, residing 72.2 kcal mol^{-1} more stable than the initial adducts. This second entrance channel is associated with attack of the triple bond of vinylacetylene, also forming a three membered ring. Finally, the last entrance channel leads to isomer si3, with an exothermicity of 40.7 kcal mol^{-1}, representing attack of the CH_2 group by dicarbon. Isomers si2 and si3 are coupled to each other by a transition state which lies 40.0 kcal mol^{-1} below the reactant energies. Ring cyclization from si3 leads to si10 can occur through a barrier of 4.1 kcal mol^{-1}. At this stage, si10 has three possible fates. The first is hydrogen loss, yielding **1,2,4-tridehydrobenzene** and hydrogen, residing 44.3 kcal mol^{-1} below the energy of the reactants, and exhibiting an energetic barrier of 41.1 kcal mol^{-1}. A second possible fate is hydrogen migration from the CH_2 group on the ring to the adjacent bare carbon. This requires a small barrier of 14.3 kcal mol^{-1}, and leads to m-benzyne. M-benzyne has a relative energy of 140.4 kcal mol^{-1}. Lastly, the third possible

fate of si10 is ring opening to yield $CH_2CCCHCCH$. The barrier associated with this is 7.9 kcal mol^{-1}, and $CH_2CCCHCCH$ has a relative energy of 129.7 kcal mol^{-1}. At this point, $CH_2CCCHCCH$ can lose an hydrogen atom from the middle CH group, yielding the resonantly stabilized product **$H_2CCCCCCH$ + H**. This path is barrierless, and the product is exothermic by 44.7 kcal mol^{-1} relative to the reactants. Immediate loss of a hydrogen from m-benzyne leads to the formation of **1,3,5-tridehydrobenzene + H**. The computed reaction energy for this hydrogen loss step is 107.9 kcal mol^{-1}, and occurs through a loose transition state. A second hydrogen loss channel is also possible from m-benzyne, leading to the formation of **1,2,4-tridehydrobenzene + H**, with a computed reaction energy of 96.2 kcal mol^{-1}. Lastly, due to symmetry requirements, there exists a third hydrogen atom loss channel leading to **1,2,3-tridehydrobenzene + H**, with computed reaction energy of 94.0 kcal mol^{-1}. It too is also barrierless. Hydrogen migration from m-benzyne can either lead to o-benzyne or p-benzyne, with barriers of 56.9 and 61.7 kcal mol^{-1} respectively. If it forms o-benzyne then, due to the symmetry of o-benzyne, two hydrogen elimination mechanisms may proceed, giving rise to either **1,2,4-tridehydrobenzene + H**, or **1,2,3-tridehydrobenzene + H**. Each of these hydrogen elimination processes are barrierless. From o-benzyne, there also exists a retro-diels alder pathway leading to the fragmentation pathway yielding **acetylene + diacetylene**. This pathway exhibits a barrier of 90.2 kcal mol^{-1}, and the resulting products are produced with a relative energy of -104.5 kcal mol^{-1}. If p-benzyne is produced, then by symmetry arguments, only one hydrogen loss path is allowed. This hydrogen loss path yields **1,2,4-tridehydrobenzene + H**, with a reaction energy of 81.3 kcal mol^{-1}.

Going back to isomer si1, the three membered ring can be transformed into a four membered ring via a barrier of 16.5 kcal mol^{-1}. The resulting four membered ring is nearly iso-energetic with si1. Insertion of the dicarbon fragment, leading to a linear structure (CHCCCCHCH2), which can then lose hydrogen to form **$H_2CCCCCCH$ + H**.

The lowest energy pathway along this surface is **si2 => si3 => si10 => si4 => $CH_2CCCCCH$ + H**. If we start from si1 instead, then there is only one pathway possible, and that is the one leading to **$CH_2CCCCCH$ + H**. Computed rate constants, and subsequent calculated branching ratios are in agreement with this.

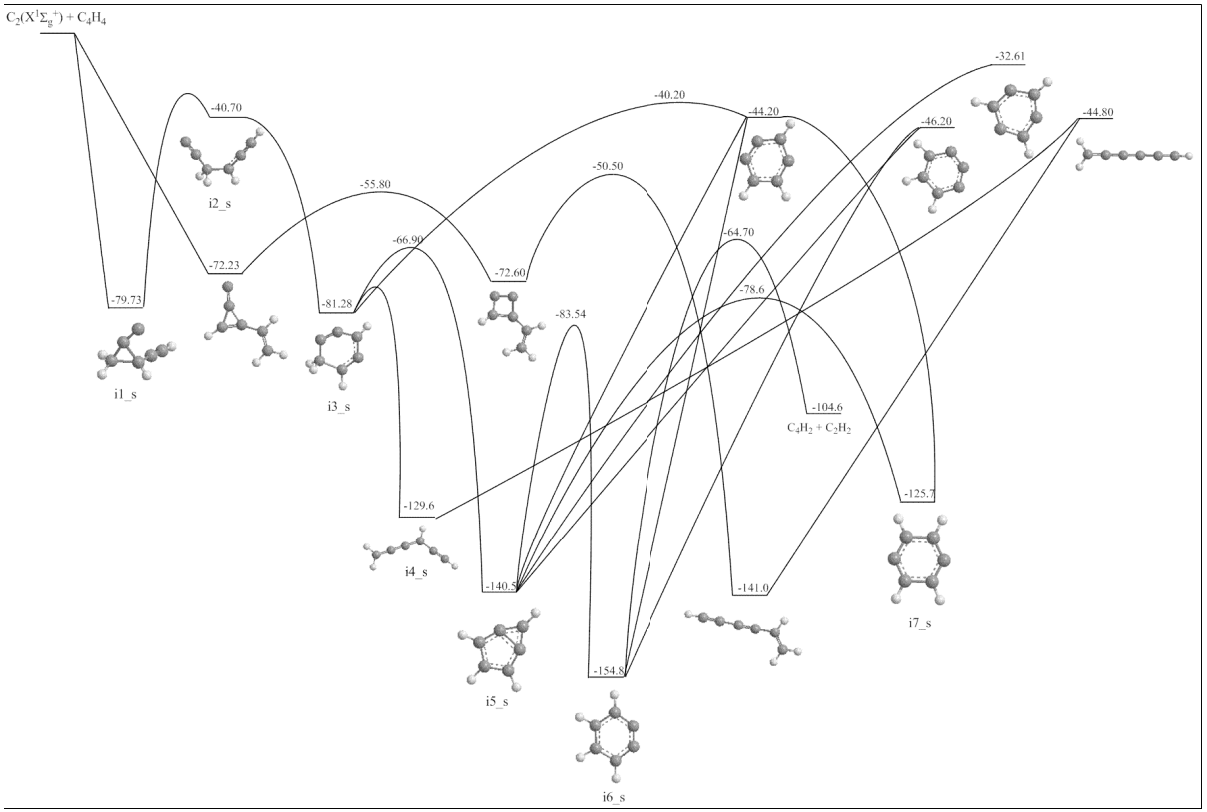

Fig. 26: PES illustrating the addition of $C_2(X^1\Sigma_g^+)$ + C_4H_4 computed at the CCSD(T)/CBS level of theory.

Switching our focus to the triplet surface, we see again that there are three entrance channels, leading to ti1, ti2 and ti3 (see fig. 27). These three are exothermic by 53.6, 44.0 and 44.7 kcal mol^{-1}. Ti3 and ti2 are coupled together by a transition state residing at a relative energy of -23.9 kcal mol^{-1}. Aside from this, ti3 can also ring condense to form CH_2 CCCHCCH. This step requires 17.2 kcal mol^{-1} to surmount the resulting transition state. Direct hydrogen loss from this linear structure requires 56.5 kcal mol^{-1} of energy, and results in the formation of **$CH_2CCCCCH$ + H**. The ring condensed structure, $CH_2CCCHCCH$ can also cyclize to form ti5. This step has a barrier of 44.5 kcal mol^{-1}. An energy barrier of 34.4 kcal mol^{-1} is then needed to hydrogen migrate from the CH_2 position to the adjacent bare carbon, forming m-benzyne. M-benzyne has three hydrogen loss pathways leading to **1,3,5-tridehydrobenzene + H**, **1,2,3-tridehydrobenzene + H** and **1,2,4-tridehydrobenzene + H**. The first two are barrierless, and exhibit reaction energies of 92.8 and 78.9 kcal mol^{-1}. The one leading to 1,2,4-tridehydrobenzene has a barrier of 82.1 kcal mol^{-1}. M-benzyne can also migrate a hydrogen forming either o-benzyne or p-benzyne. The barriers associated with these reactions are 63.4 and 67.5 kcal mol^{-1} respectively. O-benzyne can form **1,2,3- tridehydrobenzene + H** and **1,2,4-tridehydrobenzene + H** through hydrogen atom loss. Both have barriers of 73.7 and 80.1 kcal mol^{-1}. P-benzyne can lose hydrogen to form **1,2,4-tridehydrobenzene + H**. The reaction is barrierless, with a reaction energy of 82.3 kcal mol^{-1}. If ti2 is formed, it may lose hydrogen to form **CCCHCHCCH + H**, with a barrier of 36.1 kcal mol^{-1}. It is unlikely to do this however, because a lower energy cyclization reaction can also occur leading to ti5, and exhibiting a barrier of only 9.1 kcal mol^{-1}. If ti1 is formed, then the only option is to ring cyclize to form ti5. The barrier for this process is 16.0 kcal mol^{-1}.

The lowest energy pathway on this surface is **ti2 => ti5 => ti4 => CH2CCCCCH + H.** Since all other pathways connect to ti5, this is the only pathway we need to consider, and it suggests that the resonantly stabilized product **$CH_2CCCCCH$ + H** is the most likely product. RRKM and branching rations confirm this.

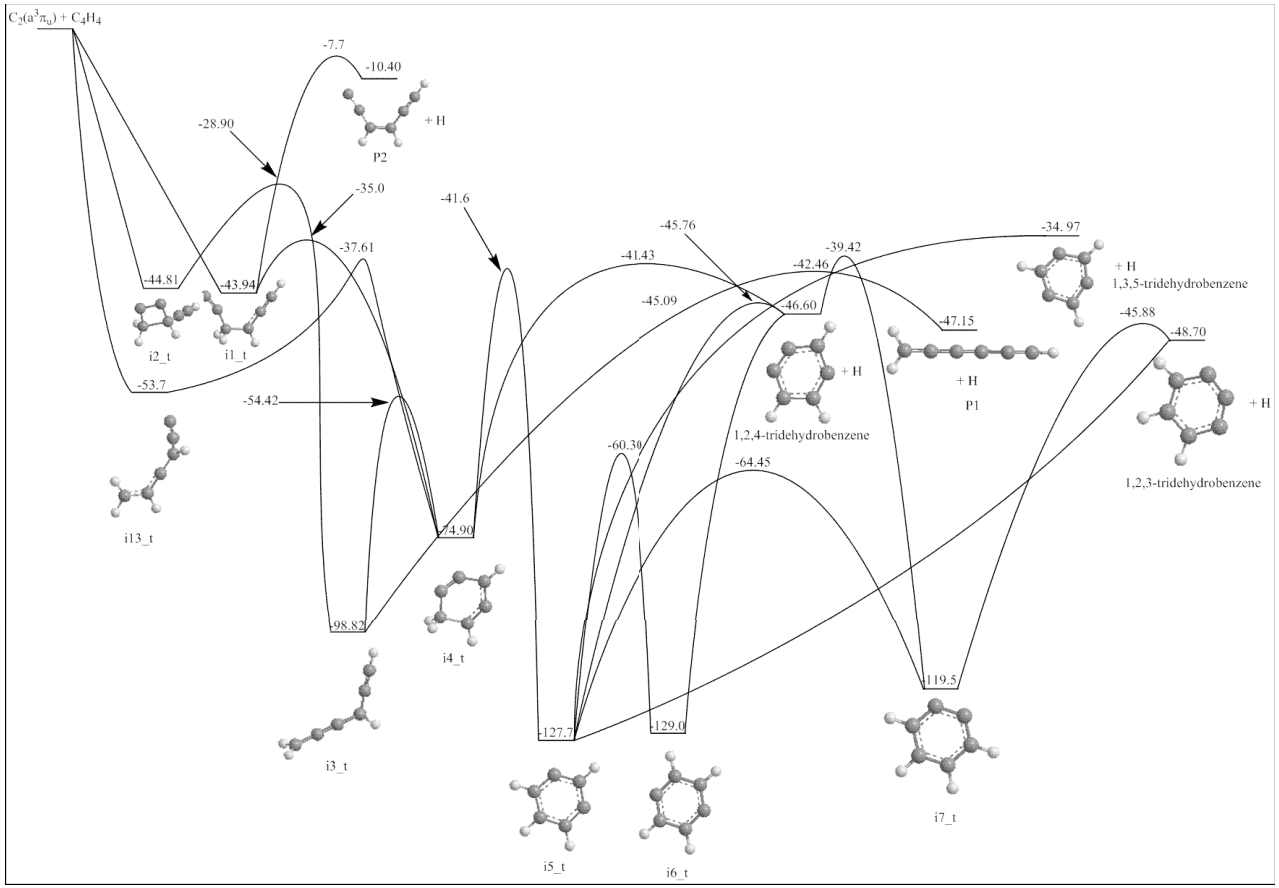

Fig. 27: PES illustrating the addition of $C_2(a^3\Pi_u) + C_4H_4$ computed at the G3(MP2,CC) level of theory.

Chapter 12: Concluding remarks

The contents of this dissertation have shown several novel synthetic routes towards the formation of polycyclic aromatics. Some of these mechanisms offer the flexibility of being able to incorporate atomic nitrogen into an aromatic ring, while others afford the opportunity for preparing polycyclic aromatics without the need of invoking pressure stabilization to aid in their formation. Many of these mechanisms work in the cold temperatures of Titan, and the low pressure conditions of the Interstellar Medium. Further, some of these mechanisms also work well in combustion conditions, where pressure stabilization of intermediate species may be important.

This work will benefit the astrochemistry community, by suggesting several pathways for polycyclic aromatic formation. It may also aid in the assignment of molecules from complex spectra, and un-identified radiation emitting from nearby galaxies. Moreover, it gives an idea for how these complex molecules can be formed as part of the Titan haze layers. Additionally, it may help researchers identify how derivatives of these polycyclic aromatics, many of which are biologically relevant, may form in oxygen containing atmospheres.

On the combustion side, this work helps to identify which temperatures and pressure polycyclic aromatics form. These aromatic species are the result of incomplete fuel combustion and, once released into the atmosphere can pose as dangerous carcinogens. Combustion engine designs which operate at other temperature and pressure regimes will minimize the formation of these toxic aromatic compounds, which may also aid in a cleaner and more efficient designs.

Prospects for third ring formation are promising. Research has already begun in our lab which suggests that the mechanisms involving phenyl radical and vinylacetylene may have natural extensions for the formation of the third ring. If these reactions occur barrierlessly, they may have the benefit of forming phenanthrene or anthracene, the two aromatic isomers of $C_{13}H_{10}$.

References:

1. Imanaka, H., Khare, B. N., Elsila, J. E., Bakes, E. L. O., McKay, C. P., Sugita, C. S., Matsui, T., Zare, R. N., Icarus, 168, **2**, 344 (2004).

2. E. Peeters, A. L. Mattioda, D. M. Hudgins, and L. J. Allamandola, Astrophys. J. **617**, L65 (2004).

3. T. H. Jarrett, M. Polletta, I. P. Fournon, G. Stacey, K. Xu, B. Siana, D. Farrah, S. Berta, E. Hatziminaoglou, G. Rodighiero, J. Surace, D. Dominigue, D. Shupe, F. Fang, C. Lonsdale, S. Oliver, M. Rowan-Robinson, G. Smith, T. Babbedge, E. Gonzalez-Solares, F. Masci, A. Franceschini, and D. Padgett, Astronom. J. **131**, 261 (2006).

4. R. I. Kaiser, A. M. Mebel, Chem. Phys. Lett. **465**, 1 (2008).
5. M. M. Mumitaz, J. D. George, K. W. Gold, W. Cibulas, C. T. Derosa, Toxicology and Industrial Health, **12**, 6 (1996).

6. Mastral, A. M., Callen, M., Murillo, R., Fuel, **75**,13,1533 (1996).

7. Suits, G. A., *J. Phys.Chem.A*, **113**, 42, 11097-11098 (2009).

8. Peters, N., Progress in Energy and Combustion Science, **10**, 3, 319 (1984).

9. Friedman, C. L., Selin, N. E., Environmental Science and Technology, **46**,17 (2012).

10. Thyssen, J., Althoff, J. K. G., Mohr, U. J. Natl. Cancer Inst., **66**,575 (1981).

11. Gupta, P., Banerjee, D. K., Bhargave, S. K., Indoor Environ., **2**, 26 (1993).

12. Szczeklik, A., Szczeklik, J., Galuszka, Z., Environ Health Perspect., **102**, 3, 302 (1994).

13. Melton, T. R., Inal, F., Senkan, S. M., The Combustion Inst., **121**, 671 (2000).

14. Bagley, S. P., Wornat, M. J., Energy Fuels, **27**, 1321 (2013).

15. Mimura, K., Madono, T., Toyama, S., Sugitani, K., Sugisaki, R., Iwamatsu, S., Murata S., J. Anal. Appl. Pyrolysis, **72**, 273 (2004).

16. D. J. Cook, S. Schlemmer, N. Balucani, D. R. Wagner, B. Steiner, and R. J. Saykally, Nature (London) **380**, 227 (1996).

17. L. J. Allamandola, A. G. G. M. Tielens, and J. R. Barker, Astrophys. J. Suppl. Ser. **71**, 733 (1989).

18. E. Peeters, A. L. Mattioda, D. M. Hudgins, and L. J. Allamandola, Astrophys. J. **617**, L65 (2004).

19. T. H. Jarrett, M. Polletta, I. P. Fournon, G. Stacey, K. Xu, B. Siana, D. Farrah, S. Berta, E. Hatziminaoglou, G. Rodighiero, J. Surace, D. Dominigue, D. Shupe, F. Fang, C. Lonsdale, S. Oliver, M. Rowan-Robinson, G. Smith, T. Babbedge, E. Gonzalez-Solares, F. Masci, A. Franceschini, and D. Padgett, Astronom. J. **131**, 261 (2006).

20. C. Sagan, B. N. Khare, W. R. Thompson, G. D. McDonald, M. R. Wing, and J. L. Bada, Astrophys. J. **414**, 399 (1993).

21. B. N. Khare, C. Sagan, W. R. Thompson, E. T. Arakawa, F. Suits, T. A. Callcott, M. W. Williams, S. Shrader, H. Ogino, T. O. Willingham, and B. Nagy, Adv. Space Res. **4**, 59 (1984).

22. C. Sagan, B. N. Khare, W. R. Thompson, G. D. McDonald, M. R. Wing, J. L. Bada, T. Vo-Dinh, and E. T. Arakawa, Astrophys. J. **414**, 399 (1993).

23. B. N. Khare, N. Bishun,E. L. O. Bakes,H. Imanaka, C. P. McKay,D. P. Cruikshank, and E. T. Arakawa, Icarus **160,** 172 (2002).

24. A. Coustenis, A. Salama, B. Schulz, S. Ott, E. Lellouch, Th. Encrenaz, D. Gautier, and H. Feuchtgruber, Icarus**161**, 383 (2003).

25. A. Coustenis, R. K. Achterberg, B. J. Conrath, D. E. Jennings, A. Marten, D. Gautier, C. A. Nixon, F. M. Flasar, N. A. Teanby, B. Bezard, R. E. Samuelson, R. C. Carlson, E. Lellouch, G. L. Bjoraker, P. N. Romani, F. W. Taylor, P. G. J. Irwin, T. Fouchet, A. Hubert, G. S. Orton, V. G. Kunde, S. Vinatier, J. Mondllini, M. M. Abvas, and R. Courtin, Icarus **189**, 35 (2007).

26. M. McGuigan, J. H. Waite, H. Imanaka, and R. D. Sacks, J. Chromat. A**1132**, 280 (2006).

27. M. Frencklach, Phys. Chem. Chem. Phys.**4**, 2028 (2002).

28. J. D. Bittner and J. B. Howard, Symp. (Int.) Combust.**18**, 1105 (1981).

29. H. Wang and M. Frenklach, Combust. Flame, **110**, 173 (1997).

30. E. H. Wilson and S. K. Atreya, Planet. Space Sci., **51**, 1017 (2003).

31. E. H. Wilson, S. K. Atreya, and A. Coustenis, J. Geophys. Res.**108**, 5014 (2003).

32. E. H. Wilson and S. K. Atreya, Bull. Amer. Astron. Soc., **33**, 1139 (2001).

33. A. M. Mebel, V.V. Kislov, and R. I. Kaiser, J. Am. Chem. Soc., **130**, 13618 (2008).

34. D. Carty, V. Le Page, I. R. Sims, I. W. M. Smith, Chem. Phys. Lett., **344**, 310 (2001).

35. E. Hebard, M. Dobrijevic, P. Pernot, N. Carrasco, A. Bergeat, K. M. Hickson, A. Canosa, S. D. Le Picard and I. R. Sims, J. Phys. Chem. A **113**, 11227 (2009) and references therein.

36. C. Berteloite, S. D. Le Picard, N. Balucani, A. Canosa, and I. R. Sims, Phys. Chem. Chem. Phys. **12**, 3666 (2010) ; *ibid.* **12**, 3677 (2010).

37. A. Landera, S. P. Krishtal, V. V. Kislov, A. M. Mebel, and R. I. Kaiser, J. Chem. Phys. **128**, 214301 (2008).

38. X. Gu, Y. S. Kim, R. I. Kaiser, A. M. Mebel, M. C. Liang, and Y. L. Yung, Proc. Natl. Acad. Sci. **106**, 16078 (2009).

39. W. M. Jackson and A. Scodinu, Astrophys. Space Sci. Lab.**31**,1 85 (2004).

40. K. Seki and H. Okabe, J. Phys. Chem.**97** 5284 (1993).

41. B. A. Balko,J. Zhang, and Y. T. Lee,J. Chem. Phys.**94**, 7958 (1991).

42. A. Läuter, K. S. Lee, K. H. Jung, R. K. Vatsa, J. P. Mittal, and H. -R. Volpp, Chem. Phys. Lett., **358**, 314 (2002).

43. Gilbert, R. G., Smith, S. C., Theory of Unimolecular and Recombination Reactions, Blackwell Scientific Publications, 1990.

44. Atkins, P., De Paula, J., Physical Chemistry 7th ed., W. H. Freeman and Company, New York, 2002.

45. Wilson, E. B., Decius, J. C., Cross, P. C., Molecular Vibrations: The Theory of Infrared and Raman Vibrational Spectra, McGraw-Hill Book Company, New York, 1955.

46. Ochterski, J., October 29, 1999, Vibrational Analysis in Gaussian, http://www.gaussian.com/g_whitepap/vib.htm, accessed July 25, 2013.

47. A. G. Baboul, L. A. Curtiss, P. C. Redfern, and K. Raghavachari, J. Chem. Phys. **110**, 7650 (1999); L. A .Curtiss, K. Raghavachari, P. C. Redfern, A. G. Baboul, and J. A. Pople, Chem. Phys, Lett. **314**, 101 (1999).

48. L. A. Curtiss, K. Raghavachari, P. C. Redfern, V. Rassolov, and J. A. Pople, J. Chem. Phys. **109**, 7764 (1998).

49. Gaussian 98, Revision A.11, M. J. Frisch, G. W. Trucks, H. B. Schlegel, G. E. Scuseria, M. A. Robb, J. R. Cheeseman, V. G. Zakrzewski, J. A. Montgomery, Jr., R. E. Stratmann, J. C. Burant, S. Dapprich, J. M. Millam, A. D. Daniels, K. N. Kudin, M. C. Strain, O. Farkas, J. Tomasi, V. Barone, M. Cossi, R. Cammi, B. Mennucci, C. Pomelli, C. Adamo, S. Clifford, J. Ochterski, G. A. Petersson, P. Y. Ayala, Q. Cui, K. Morokuma, D. K. Malick, A. D. Rabuck, K. Raghavachari, J. B. Foresman, J. Cioslowski, J. V. Ortiz, B. B. Stefanov, G. Liu, A. Liashenko, P. Piskorz, I. Komaromi, R. Gomperts, R. L. Martin, D. J. Fox, T. Keith, M. A. Al-Laham, C. Y. Peng, A. Nanayakkara, C. Gonzalez, M. Challacombe, P. M. W. Gill, B. Johnson, W. Chen, M. W. Wong, J. L. Andres, C. Gonzalez, M. Head-Gordon, E. S. Replogle, and J. A. Pople, Gaussian, Inc., Pittsburgh PA, 1998.

50. R. D. Amos, A. Bernhardsson, A. Berning, P. Celani, D. L. Cooper, M. J. O. Deegan, A. J. Dobbyn, F. Eckert, C. Hampel, B. Hetzer, P. J. Knowles, T. Korona, R. Lindh, A. W. Lloyd, S. J. McNicholas, F. R. Manby, W. Meyer, M. E. Mura, A. Nicklab, P. Palmieri, R. Pitzer, G. Rauhut, M. Schutz, U. Schumann, H. Stoll, A. J. Stone, R. Tarroni, T. Thorsteinsson and H.-J. Werner, *MOLPRO* version 2002.6, University of Birmingham, Birmingham, UK, 2003.

51. Gaussian 09, Revision A.1, M. J. Frisch, G. W. Trucks, H. B. Schlegel, G. E. Scuseria, M. A. Robb, J. R. Cheeseman, G. Scalmani, V. Barone, B. Mennucci, G. A. Petersson, H. Nakatsuji, M. Caricato, X. Li, H. P. Hratchian, A. F. Izmaylov, J. Bloino, G. Zheng, J. L. Sonnenberg, M. Hada, M. Ehara, K. Toyota, R. Fukuda, J. Hasegawa, M. Ishida, T. Nakajima, Y. Honda, O. Kitao, H. Nakai, T. Vreven, J. A. Montgomery, Jr., J. E. Peralta, F. Ogliaro, M. Bearpark, J. J. Heyd, E. Brothers, K. N. Kudin, V. N. Staroverov, R. Kobayashi, J. Normand, K. Raghavachari, A. Rendell, J. C. Burant, S. S. Iyengar, J. Tomasi, M. Cossi, N. Rega, J. M. Millam, M. Klene, J. E. Knox, J. B. Cross, V. Bakken, C. Adamo, J. Jaramillo, R. Gomperts, R. E. Stratmann, O. Yazyev, A. J. Austin, R. Cammi, C. Pomelli, J. W. Ochterski, R. L. Martin, K. Morokuma, V. G. Zakrzewski, G. A. Voth, P. Salvador, J. J. Dannenberg, S. Dapprich, A. D. Daniels, Ö. Farkas, J. B. Foresman, J. V. Ortiz, J. Cioslowski, and D. J. Fox, Gaussian, Inc., Wallingford CT, 2009.

52. M. Valiev, E.J. Bylaska, N. Govind, K. Kowalski, T.P. Straatsma, H.J.J. van Dam, D. Wang, J. Nieplocha, E. Apra, T.L. Windus, W.A. de Jong, "NWChem: a comprehensive and scalable open-source solution for large scale molecular simulations" Comput. Phys. Commun. **181**, 1477 (2010)

53. T. M. Selby, J. R. Clarkson, D. Mitchell, J. A. J. Fitzpatrick, H. D. Lee, D. W. Pratt, T. S. Zwier, J. Phys. Chem. A. **109**, 4484 (2005).

54. M. Prall, A. Kruger, P. R. Schreiner, H. Hopf, Chem. Eur. J. **7**, 4386 (2001).

55. K. Schulz, J. Hofmann, G. Zimmermann, Liebigs Annalen/Recueil **12**, 2535 (1997).

56. D. E. Woon, Chem. Phys., **331**, 67 (2006).

57. A. Landera, A. M. Mebel, Faraday Discuss., **147**, 479 (2010).

58. Morales, S. B.; Bennett, C. J.; Le Picard, S. D.; Canosa, A.; Sims, I. R.; Sun, B. J.; Chen, P. H.; Chang, A. H. H.; Kislov, V. V.; Mebel, A. M.; Gu, X.; Zhang, F.; Maksyutenko, P.; Kaiser, R. I. *Astrophys. J.***, 742**, 26/1-26/10 (2011).

59. Trevitt, A. J.; Goulay, F.; Taatjes, C. A.; Osborn, D. L.; Leone, S. R. *J. Phys. Chem. A*, **114**, 1749-1755 (2010).

60. Sebree, J. A.; Kidwell, N. M.; Selby, T. M.; Amberger, B. K.; McMahon, R. J.; Zwier, T. S. *J. Am. Chem. Soc.*, **134**, 1153-1163 (2012).

61. Liang, M. C. ;Yung, Y. L.; Shemansky, D. E. Astrophys. J. Lett., **661**, L199-L202 (2007).

62. Flasar, F. M.; Achterberg, R. K. *Philosoph. Trans. Royal Soc.* A, **367**, 649-664 (2009).

63. Klippenstein, S. J.; Yang, Y.-C.; Ryzhov, V.; Dunbar, R. C. *J. Chem. Phys.*, **104**, 4502-4516 (1996).

64. Landera, A.; Mebel, A. M.; Kaiser, R. I. *J. Chem. Phys.*, **134**, 024302/1-024302/13 (2011).

65. Moriarty, N . W., Frenklach, M. Proceedings of the Combustion Institute, **28**, 2563 (2000).

66. Tokmakov, I. V., Lin, M. C., J. Phys. Chem. A., **108**, 9697 (2004).

67. Smith, I. M. W, Sage, A. M, Donahue, N. M., Herbst, E., Quan, D., Faraday Discuss 2006, 133.

68. Cioslowski, J., Liu, G., Martinov, M., Piskorz, P., Moncrieff, D. *J. Am. Chem. Soc.*, **118**, 5261-5264 (1996).

69. Madden, L. K., Moskaleva, L. V., Kristyan, S., Lin, M. C. *J. Phys. Chem. A.*, **101**, 6790-6797 (1997).

70. Zhang, X., Maccarone, A. T., Nimlos, M. R., Kato, S., Bierbaum, V. M., Ellison, G. B., Ruscic, B., Simmonett, A. C., Allen, W. D., Schaefer III, H. F. *J.Chem.Phys.*, **126**, 044312 (2007).

71. Moskaleva, L. V., Madden, L. K., Lin, M. C. *Phys. Chem. Chem. Phys.*, **1**, 3967-3972 (1999).

72. Xu, C., Braun-Unkhoff, M., Naumann, C., Frank, P. *Proceedings of the Combustion Institute*, **31**, 231-239 (2007).

VITA

ALEXANDER LANDERA

EDUCATION

Florida International University, Florida

Research: PES relevant to formation of aromatic compounds on Titan and combustion
Ph.D. in Chemistry **Expected 2013**

Duke University, NC
2007-2009
Research: "Synthesis and Characterization of Porphyrin Arrays"

Florida International University, Miami, Florida
B.S. Chemistry **2002-2007**
Areas of Concentration: Physical chemistry / Electronic structure calculations
Minor: Biology

POSTER PRESENTATIONS

Faraday Discussions #147, Saint Jacut de la Mer, France
Addition of One and Two Units of C2H to Styrene: A Theoretical Study of the C10H9 and C12H9 Systems and Implications Towards Titan's Atmosphere **June 2010**

V Titan conference, Popui Hawaii
A Theoretical Study of the Potential Energy Surfaces for the $C_2 + C_4H_4 \rightarrow C_6H_3 + H$ Reaction **April 2011**

242nd American Chemical Society (ACS) National Meeting and Exposition, Denver Colorado **August 2011**
Addition of vinylacetylene (C4H4) to phenyl radical (C6H5): A theoretical and kinetic investigation towards the formation of naphthalene in combustion flames

244nd American Chemical Society (ACS) National Meeting and Exposition, Philadelphia, Pennsylvania **August 2012**
A combined theoretical study of the dissociation mechanism or ortho-benzyne in photodissociation and pyrolysis

PUBLICATIONS AND PAPERS

- Winkle, Stephen; Arango, Dillon; Landera, Alex; Pulido, Jesse; Shaqra, Ala; Wedderburn, Lamar; Sheardy, Richard D. **RNA polymerase binds to specific nonpromoter DNA sequences.** Abstracts of Papers, 235th ACS National Meeting, New Orleans, LA, United States, April 6-10, 2008 (2008),
- Landera, Alexander; Krishtal, Sergey P.; Kislov, Vadim V.; Mebel, Alexander M.; Kaiser, Ralf I. **Theoretical study of the C6H3 potential energy surface and rate constants and product branching ratios of the C2H(2Σ +)+C4H2(1Σ g+) and C4H(2Σ +)+C2H2(1Σ g+) reactions.** *J. Chem. Phys.* (2008), 128(21), 214301/1-214301/12. CODEN: JCPSA6 ISSN:0021-9606. CAN 149:175803 AN 2008:690673 CAPLUS
- Landera, Alexander; Mebel, Alexander M.; Kaiser, Ralf I. **Theoretical study of the reaction mechanism of ethynyl radical with benzene and**

related reactions on the C8H7 potential energy surface. *Chem. Phys. Lett.* (2008), 459(1-6), 54-59. CODEN: CHPLBC ISSN:0009-2614. CAN 149:200461 AN 2008:768164 CAPLUS

- Silva, R.; Gichuhi, W. K.; Kislov, V. V.; Landera, A.; Mebel, A. M.; Suits, A. G. **UV Photodissociation of Cyanoacetylene: A Combined Ion Imaging and Theoretical Investigation.** *J. Phys. Chem. A.* (2009), 113(42), 11182-11186. CODEN: JPCAFH ISSN:1089-5639. CAN 151:392420 AN 2009:819732 CAPLUS
- Zhou, Li; Zheng, Weijun; Kaiser, Ralf I.; Landera, Alexander; Mebel, Alexander M.; Liang, Mao-Chang; Yung, Yuk L. **Cosmic-ray-mediated formation of benzene on the surface of Saturn's moon Titan.** Astrophysical Journal (2010), 718(2, Pt. 1), 1243-1251. CODEN: ASJOAB ISSN:0004-637X. AN 2010:1086969 CAPLUS
- Landera, Alexander; Mebel, Alexander M. **Mechanisms of formation of nitrogen-containing polycyclic aromatic compounds in low-temperature environments of planetary atmospheres: A theoretical study.** Faraday Discussions (2010), 147(Chemistry of the Planets), 479-494. CODEN: FDISE6 ISSN:1359-6640. AN 2010:1478156 CAPLUS
- Landera, Alexander; Kaiser, Ralf I.; Mebel, Alexander M. **Addition of one and two units of C2H to styrene: A theoretical study of the $C_{10}H_9$ and $C_{12}H_9$ systems and implications toward growth of polycyclic aromatic hydrocarbons at low temperatures.** *J. Chem. Phys.* (2011), 134(2), 024302/1-024302/13. CODEN: JCPSA6 ISSN:0021-9606. CAN 154:135936 AN 2011:41167 CAPLUS
- Kaiser, R. I.; Goswami, M.; Maksyutenko, P.; Zhang, F.; Kim, Y. S.; Landera, Alexander; Mebel, Alexander M. **A crossed molecular bemas and ab initio study on the formation of C6H3 Radicals. An interface between resonantly stabilized and aromatic radicals**. *J. Chem. Phys. A*(2011), 115(37), 10251-10258.
- Parker, Dorian S. N.; Zhang, Fangtong; Kim, Y. Seol; Kaiser, Ralf I.; Landera, Alexander; Kislov, Vadim V.; Mebel, Alexander M.; Tielens, A. G. G. M**. Low temperature formation of naphthalene and its role in the synthesis of PAH's (Polycyclic Aromatic Hydrocarbons) in the interstellar medium**. *Proc. Natl. Acad. Sci.* (USA), (2011),(Dec. 22 2011), 1-6.
- Parker, Dorian.; Zhang, Fangtong; Kim, Y. Seol; Kaiser, Ralf I.; Landera, Alexander; Mebel, Alexander M.**On the Formation of Phenyldiacetylene (C6H5CCCCH) and D5-phenyldiacetylene(C5D5CCCCH) studied under single collision conditions**, *Phys. Chem. Chem. Phys*., (2012), 14, 2997-3003.
- Kaiser, R. I.; Parker, D. S. N.; Zhang, F.; Landera, A.; Kislov, V. V.; Mebel, A. M. **PAH Formation under Single Collision Conditions: Reaction of Phenyl Radical and 1,3-Butadiene to Form 1,4-Dihydronaphthalene**, *J. Chem. Phys. A* (2012), 116(17), 4248-4258.
- Mebel, Alexander M.; Landera, Alexander. **Product branching ratios in photodissociation of phenyl radical: A theoretical ab initio/Rice-Ramsperger-Kassel-Marcus study.** *J. Chem. Phys*(2012), 136(23), 234305/1-234305/9.
- Landera, Alexander, Mebel, A. M. Low Temperature Mechanisms for the formation of Substituted Azanaphthalenes Through Consecutive CN and C2H Addition to Styrene and N-methynelenebenzenamine: A Theoretical Study, *J. Am. Chem. Soc.*(2013), 135(19), 7251-7263.